Characterising the novel efflux pump, EefABC, of *Escherichia coli*.

By

Leah Burgess

A thesis submitted to the University of Birmingham for the degree of MSc by Research

Institute of Microbiology and Infection

College of Medical and Dental Sciences

University of Birmingham

2024

ABSTRACT

Gram-negative bacteria, such as *Escherichia coli*, contain RND efflux pumps that form tripartite efflux pumps which span the inner and outer membrane. A seventh RND pump, EefB, was identified prior to this study by the Blair lab at the University of Birmingham, in addition to the six known RND pumps of *E. coli*; AcrB, AcrD, AcrF, MdtBC, MdtF and CusA.

The gene for the seventh RND pump is located on a five-gene locus, *eefRABCD*, which encodes a TetR regulator (EefR), a periplasmic adaptor protein (EefA), an inner membrane RND pump (EefB), an outer membrane protein (EefC) and a major facilitator superfamily transporter (EefD). EefB forms a tripartite efflux pump, EefABC, which is highly conserved across *E. coli* phylogroups commonly associated with infection.

Experimental techniques utilising loss and gain of EefABC function strains show that the pump is functional and able to transport toxic dyes ethidium bromide and rhodamine-6G, and that overexpression increases fatality of infected *Galleria mellonella*. Unlike common RND efflux pump complexes, such as AcrAB-TolC, there is no evidence to suggest that EefABC confers antimicrobial resistance in *E. coli*.

Metabolomic analysis of the exometabolome reveals the mass of three potential substrates of EefABC, though further work is necessary for the assignment of these to known molecules.

Overall, my findings present EefABC as a functional RND efflux complex which can increase the infection potential of *E. coli*.

ACKNOWLEDGEMENTS

I owe my success to my amazing supervisor, Professor Jessica Blair. Thank you for guiding my research and always making yourself available whenever I needed the extra help. You really have been exceptional.

I would also like to thank Lizzy and Pauline of the Blair lab for taking your time to train me to work effectively in the lab and for welcoming me as part of the team. The same goes for Ilyas who was always there to assist me if the others were not there, and for making me laugh even on a bad day.

Thank you to the student loans company, who made it possible for people like me to attend University without financial burden.

I am extremely appreciative of my parents, for providing me with emotional and financial stability to support me to continue my studies, and to my sister who has been proud of me throughout.

CLARIFICATION OF RESULTS PRODUCED IN COLLABORATION

Chapter 5

Metabolomics analysis was carried out by Dr Gerald Larrouy-Maumus at Imperial College London.

CONTENTS

LIST OF FIGURES

LIST OF TABLES

LIST OF ABBREVIATIONS

ABC ATP-binding cassette

AbgT p-aminobenzoyl-glutamate transporter

AMR antimicrobial resistance

APEC avian pathogenic *E. coli*

CMR chloramphenicol resistant

DAEC diffusely adherent *E. coli*

EAEC enteroaggregative *E. coli*

EHEC enterohaemorrhagic *E. coli*

EIEC enteroinvasive *E. coli*

EPEC enteropathogenic *E. coli*

EPI efflux pump inhibitor

EPS extracellular polymeric substances

EtBr ethidium bromide

ETEC enterotoxigenic *E. coli*

ExPEC extraintestinal pathogenic *E. coli*

FAO food agriculture organisation

IPC infection prevention and control

LB Luria Bertani

LC-MS liquid-chromatography mass-spectrometry

LOS lipooligosaccharides

LPS lipopolysaccharides

MATE multidrug and toxic compound extrusion

MDR multidrug resistant

MFS major facilitator family

MIC minimum inhibitory concentration

MNEC meningitis-associated *E. coli*

MS/MS tandem mass spectrometry

NMR nuclear magnetic resonance

OD optical density

OIE world organisation for animal health

PACE proteobacterial antimicrobial compound efflux

PAP periplasmic adaptor protein

PPB potassium phosphate buffer

QQ quorum quenching

QS quorum sensing

R6G rhodamine-6G

RND resistance-nodulation division

SMR small multidrug resistant

ST sequence type

UPEC uropathogenic *E. coli*

UTI urinary tract infection

WHO World Health Organisation

1. INTRODUCTION

1.1 Gram-positive and Gram-negative bacterial cell walls

Gram-positive bacterial cell walls include a single phospholipid bilayer membrane which surrounds the cytoplasm and have a thick layer of peptidoglycan, which surrounds the cytoplasmic membrane and protects the cell from lysis due to osmotic swelling. Hydrophilic molecules such as sugars and amino acids are unable to pass through the cytoplasmic membrane, however, small uncharged hydrophobic molecules such as O_2, H_2O and CO_2 can (Henderson *et al.*, 2021).

Bacteria species from Enterobacteriaceae, and non-fermenter groups are Gram-negative, and bacteria from these groups are responsible for most infections, many of which are derived from patients in the intensive care unit of hospitals. These isolates tend to have high antimicrobial resistance and are significant cause for concern (Oliveira and Reygaert, 2023).

Gram-negative cell walls have an “inner membrane” which is a cytoplasmic membrane composed of phospholipids – like that of Gram-positive cells walls – however the peptidoglycan layer surrounding this is thinner in Gram-negative cells. Gram-negative cell walls also consist of a second “outer membrane” which is composed mainly of lipid-carbohydrates such as lipopolysaccharides (LPS) or lipooligosaccharides (LOS) (figure 1), which pack tightly together on the cell surface. The presence of polysaccharides makes the outer membrane less permeable to small molecules and ions than the inner membrane (Henderson *et al.*, 2021).

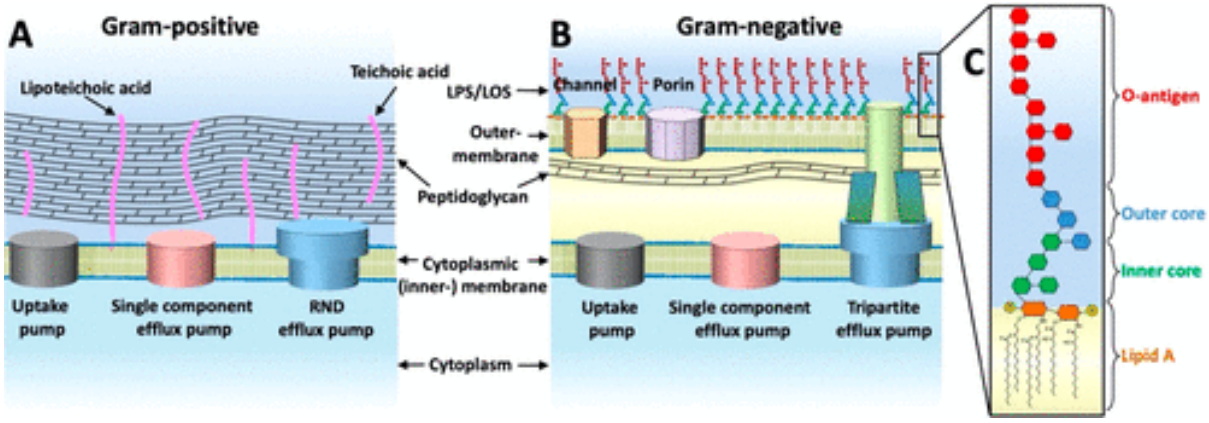

Figure 1. Diagram of Gram-positive and Gram-negative cell walls. Panel A is a typical Gram-positive cell wall. Panel B is a typical Gram-negative cell wall. Figure from Henderson *et al*., 2021.

The Gram-negative cell wall is composed of two membranes which create a space called the periplasm. Both Gram-positive and Gram-negative cell walls have efflux pumps embedded into the cytoplasmic membrane; however, Gram-negative cell walls need a pump that will span the inner and outer membrane to allow transportation of substrates from the periplasm (Henderson *et al*., 2021).

1.2 *Escherichia coli* as an opportunistic pathogen

Escherichia coli is a motile Gram-negative bacillus from the *Enterobacteriaceae* family (Nataro and Kaper, 1998). *E. coli* colonizes the gastrointestinal tract of humans within hours after birth; from the mother or via food or water or direct transmission from individuals handling the infant. Commensal strains adhere to the mucosal layer of the mammalian colon and can coexist with humans for months to years (Kaper, 2002). *E. coli* can become pathogenic in immunocompromised hosts or if gastrointestinal barriers are breached and can cause intestinal diseases such as diarrhoea, as well as extra-intestinal diseases such as urinary tract infections (UTIs)

and sepsis/meningitis (Kaper, 2002). *E. coli* is one of the most common causes of healthcare-associated infections (HAIs) (Haque *et al.*, 2018) which include central line-associated bloodstream infections, catheter-associated UTIs and surgical site infections (Kaper, 2002).

E. coli strains can acquire virulence factors which allow them to cause a wide range of diseases in healthy mammals, and clones which use a specific set of virulence factors to cause similar diseases are split into different pathotypes. The six pathotypes of intestinal *E. coli* pathogens are: enteropathogenic *E. coli* (EPEC), enterohaemorrhagic *E. coli* (EHEC), enterotoxigenic *E. coli* (ETEC), enteroaggregative *E. coli* (EAEC), enteroinvasive *E. coli* (EIEC) and diffusely adherent *E. coli* (DAEC). Several extraintestinal *E. coli* pathotypes have been described, including: uropathogenic *E. coli* (UPEC) which causes urinary tract infections (UTIs), meningitis-associated *E. coli* (MNEC) which is responsible for meningitis and sepsis and extraintestinal pathogenic *E. coli* (ExPEC) which is a general term for pathotypes involved in extraintestinal infections. Animal pathotypes responsible for extraintestinal infections consist of EPEC, EHEC, ETEC and avian pathogenic *E. coli* (APEC) (Kaper, 2002).

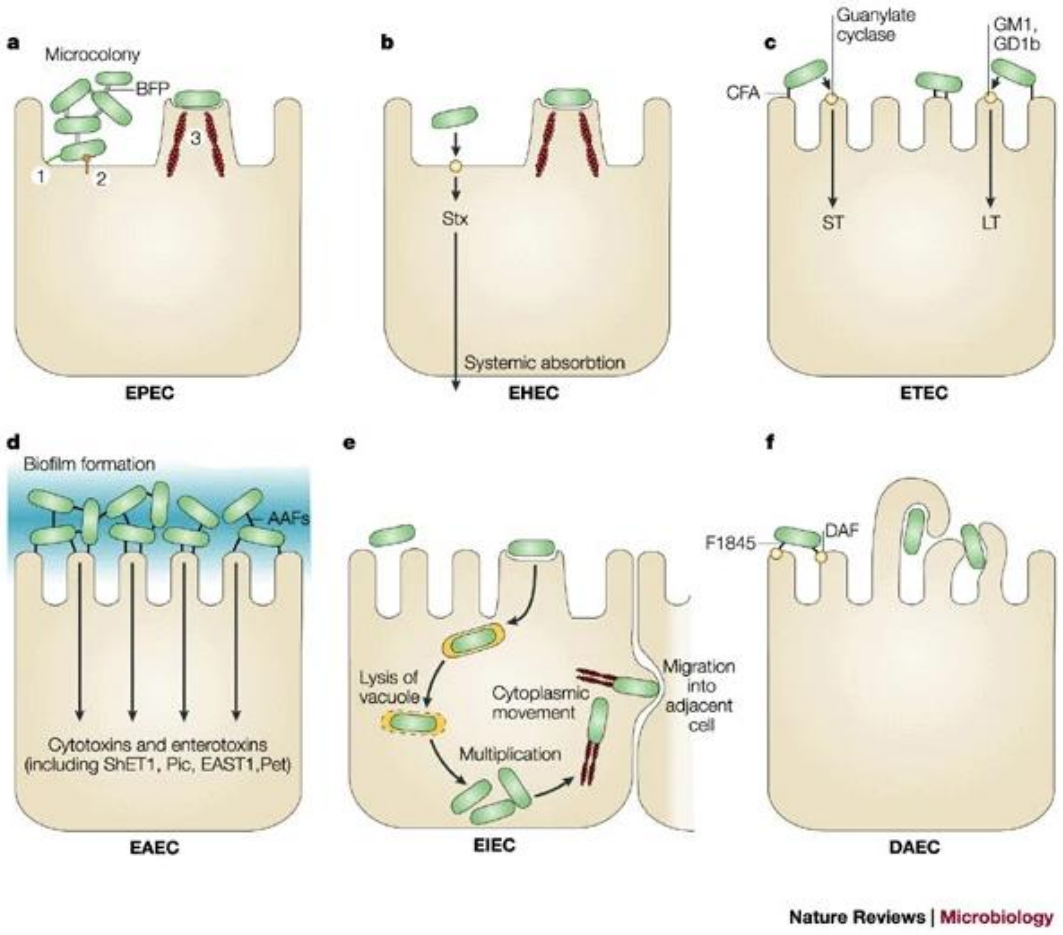

Figure 2. Pathogenic schema of diarrhoeagenic *E. Coli*. Figure from Kaper, 2002. This figure schematically represents the interaction of each category of *E. coli* with a specific target cell. **A)** EPEC adhere to bowel enterocytes and destroy the microvillar architecture, inducing the attaching and effacing lesion. This is accompanied by an inflammatory response and diarrhoea. 1. Adhesion, 2. Protein translocation by type III secretion, 3. Pedestal formation. **B)** EHEC induce the attaching and effacing lesion in the colon. EHEC and Shiga toxin (Stx) cause systemic absorption which can be life-threatening. **C)** ETEC adhere to bowel enterocytes and induce diarrhoea by secretion of heat-labile (LT) or heat-stable (ST) enterotoxins. **D)** EAEC adheres to bowel epithelia in a thick biofilm and elaborates secretory enterotoxins and cytotoxins. **E)** EIEC invades colonic epithelial cells, lyses the phagosome, and moves through the cell by nucleating actin-microfilaments. **F)** DAEC elicits signal transduction in bowel enterocytes that manifests as the growth of long cellular projections, which wrap around the bacteria (Kaper, 2002).

1.2.1 Phylogeny of *E. coli*

E. coli is separated into six major phylogenetic groups – A, B1, B2, C, D and E (Chaudhuri and Henderson, 2012). Since then, whole genome sequencing has helped to separate the phylogroups into two clusters, based on whether the phylogroups consisted mostly of commensal or opportunistic *E. coli* strains: phylogroups B2, G, F and D; and phylogroups A, B1, C and E, along with an additional group, H (Denamur *et al.*, 2021).

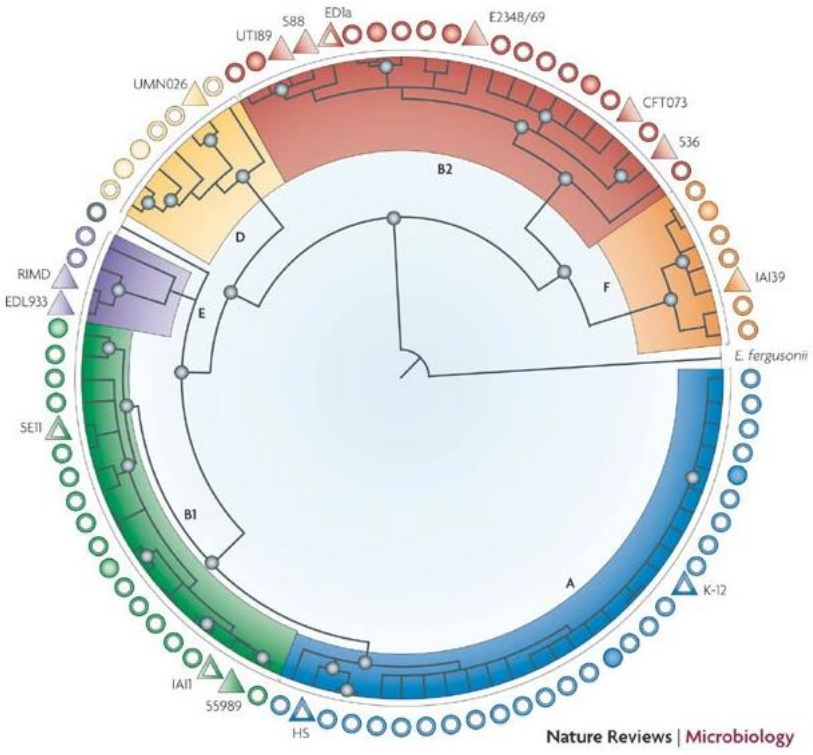

Figure 3. Phylogenetic tree of *E. coli,* from Tenaillon *et al*., 2010. The above shows a ClonalFrame analysis based on the sequences of 8 housekeeping genes, 72 strains from the ECOR (outer circles) and 15 genome reference strains (outer triangles), rooted on *Escherichia fergusonii*. Open symbols represent commensal strains, full symbols represent pathogenic strains. Colours refer to the 6 main phylogenetic groups. Blue dots on nodes indicate that the corresponding clade is monophyletic (Tenaillon *et al*., 2010).

A triplex PCR was used to determine phylogenetic groups of *E. coli* present in 1889 commensal isolates taken from the faeces of healthy adult humans from across the globe. It was found that group A (32.0% of the total) and group B2 (29.4%) were the most abundant in human faeces, whilst B1 (17.9%) and D (20.7%) were less. Whilst

geographical differences were present, this pattern was true for most countries (Bailey *et al.*, 2010).

E. coli can acquire new virulence genes/functions through horizontal gene transfer and lose virulence genes before undergoing point mutations, leading to a change of function. This results in strains from some phylogroups being more virulent/pathogenic than others and also leads to the emergence of pathotypes, which are groups of pathogens from the same species (not necessarily from the same phylogroup) which have acquired virulence factors through horizontal gene transfer (Jesser and Levy, 2020; Denamur *et al.*, 2021). Strains from group B2 are typically more pathogenic than other groups. Some strains from pathotypes ExPEC, UPEC, APEC, EPEC, EAEC DAEC belong to the typically pathogenic phylogroup B2, but pathogenic strains can also belong to other groups (Denamur *et al.*, 2021). A study found that out of 407 human extraintestinal pathogenic *E. coli* strains (ExPEC) isolated from skin, respiratory and intra-abdominal infections as well as from genital smears, 52.6% belonged to the phylogenetic group B2 (Micenková *et al.*, 2016). ExPEC strains sometimes come from phylogroup D (previously known as clonal group A) as strains belonging to this group were identified in urine obtained from women suffering from trimethoprim-sulfamethoxazole-resistant UTIs across the United States in the late 1990s (Denamur *et al.*, 2021).

Whole genome sequencing and de novo assembly that was performed on 312 ExPEC isolates derived from blood or urine obtained from patients found that ExPEC *E. coli* is highly genomically heterogeneous and were found to belong to multiple phylogroups. The most represented phylogroups were B2 (65.7% of the population) and D (16.3%), supporting evidence that these phylogroups typically accommodate the most pathotypes of *E. coli* (Salipante *et al.*, 2015).

Overall, research supports that whilst there are 9 phylogroups of *E. coli* strains, some are more prevalent than others (Phylogroups A and B2), depending on the environment from which the strains were characterised, and some are more pathogenic than others (phylogroups B2 and D).

1.3 Antimicrobial Resistance (AMR)

Antimicrobial resistance has been considered “one of the greatest threats to human health worldwide” (Spellberg, B., 2011) with an estimate of 4.95 million deaths across the globe associated with bacterial AMR in 2019 (Murray *et al.*, 2022). Infection with AMR pathogens leads to serious illnesses, extended hospital admissions and increases in healthcare costs (Dadgostar, 2019). The World Health Organisation (WHO) priority list of antibiotic-resistant bacteria classifies third-generation cephalosporin-resistant *E. coli* as part of the critical-priority tier (Tacconelli *et al.*, 2018).

Multi-drug resistant (MDR) pathogens are becoming an increasing threat. In a study conducted in Khartoum, Sudan, 232 *E. coli* specimens were isolated from patients in hospitals and tested for their susceptibility to antimicrobial drugs. 92.2% of isolates tested were MDR *E. coli*, with high resistance being noted against amoxicillin (97.7%), cefuroxime (92.5%), trimethoprimsulfatemethoxazole (88.3%), tetracycline (77.1%), nalidixic acid (72%) and ceftriaxone (64%). A total of 53.3% of MDR isolates were resistant to more than 7 drugs, raising MDR *E. coli* as a cause for concern (Ibrahim, Bilal and Hamid, 2012).

AMR in *E. coli* is now considered to be a One Health problem (a widespread issue between people, animals, plants and their shared environment), and has been referred to as *E. coli* resistant to extended spectrum cephalosporins (ESC-EC), in animal, human, and environmental sources. The DiSCoVeR ("discovering the sources of *Salmonella, Campylobacter*, VTEC and antimicrobial resistance) ESC-EC (*Escherichia coli* resistant to extended spectrum cephalosporins) database, a One Health European Joint Programme funded by DiSCoVeR, combines data from ESC-EC isolates from animal, human and environmental samples globally. Minimum inhibitory concentration (MIC) data from a total of 10,763 isolates identified that the majority of isolates had a confirmed extended spectrum beta-lactamase (ESBL) phenotype, ESBL and AmpC phenotype, or AmpC phenotype (Perestrelo *et al.*, 2023).

In a bid to combat AMR, following guidance from the WHO, Food and Agriculture Organization (FAO) and World Organisation for Animal Health (OIE), an attempt to create an effective AMR strategy is required. Key components of this strategy include: increasing awareness of AMR, strengthening surveillance and monitoring, strengthening antimicrobial stewardship in human health, strengthening infection prevention and control (IPC) in human health, strengthening IPC and reducing inappropriate antibiotic use in animals, limiting exposure of AMR pathogens to the environment and fostering research and development of new antimicrobial therapies, diagnostics and vaccines (Anderson *et al.*, 2019).

1.3.1 Mechanisms of resistance

There are multiple mechanisms of resistance in pathogens, which are represented in figure 4 (Darby *et al.*, 2022).

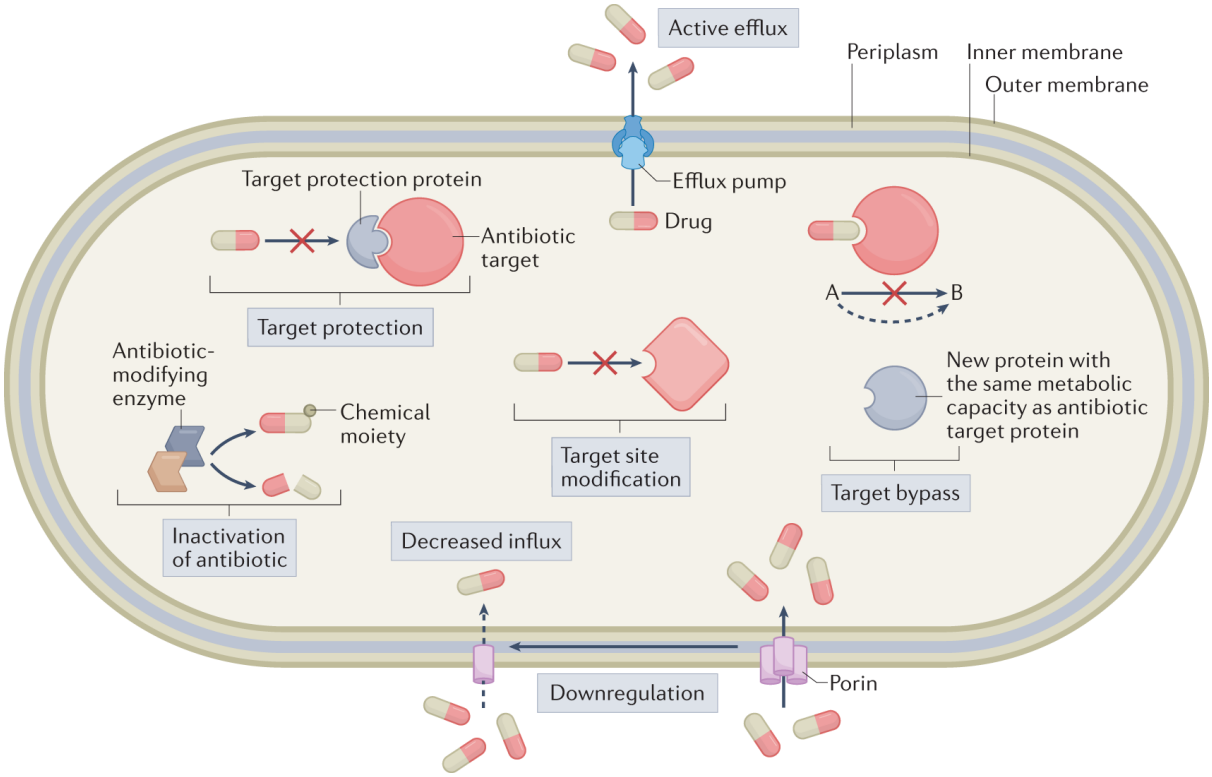

Figure 4. Overview of the molecular mechanisms of antibiotic resistance, take from the review, Darby *et al.*, 2022.

1. Target site modification via enzymatic action or genetic mutation prevents antibiotic binding (Schaenzer and Wright, 2020). For example, in vancomycin-resistant enterococci, there is an amino acid modification on the pentapeptide stem of Lipid II (the protein responsible for blocking peptidoglycan synthesis). This prevents a hydrogen bond occurring between the glycopeptide antibiotic and the peptide stem, reducing vancomycin's affinity for the peptide target (Schaenzer and Wright, 2020).

2. Active efflux – Efflux pumps transport toxic substrates (including antibiotics) out of bacterial cells to reduce the level of intracellular concentration (Blair and Piddock, 2009). There are seven classes of bacterial efflux pumps: the major facilitator superfamily (MFS), the ATP-binding cassette (ABC) family, the resistance-

nodulation-division (RND) family, the small multidrug resistance (SMR) family, the multidrug and toxic compound extrusion (MATE) family, the proteobacterial antimicrobial compound efflux (PACE) family and the p-aminobenzoyl-glutamate transporter (AbgT) family (Chitsaz and Brown, 2017).

3. Target bypass – An alternative target (which is antibiotic resistant) is produced by bacteria along with the native target (not resistant). The alternative target adopts the role of the native target, rendering the native target useless/ unnecessary. This makes the original target redundant and therefore makes the antibiotic ineffective (Giedraitienė *et al.*, 2011). This mechanism is responsible for conferring resistance to trimethoprim and sulphonamides because there is a lower affinity of the altered targets (dihydropteroate synthetase (DHPS) and dihydropteroate reductase (DHFR)) to the drugs (Giedraitienė *et al.*, 2011).

4. Decreased influx by downregulating the expression of porins or other channels into the cell so that less antibiotic enters the cell (Fernández and Hancock, 2012). In *E. coli*, porin proteins OmpF and OmpC facilitate entry of various β-lactams via the cell membrane, so downregulation of these proteins leads to resistance to β-lactams (Jaffe, Chabbert and Semonin, 1982).

5. Inactivation of antibiotic by enzymes - the antibiotic is modified or degraded by enzymes to disrupt a key function of the molecule or disable interaction with its target (De Pascale and Wright, 2010). Some *E. coli* and *Klebsiella* strains in India have acquired the New Delhi metallo-β-lactamase 1 (NDM1) antibiotic resistance mechanism (Spellberg, B., 2011), in which metallo-β-lactamases (MBLs) hydrolyse most β-lactam antibiotics (Zhang and Hao, 2011), rendering them useless.

6. Target protection – A target protection protein becomes physically associated with the antibiotic target to prevent inhibition of the target. This is only a temporary change in the nature of the target (Wilson *et al.*, 2020). This mechanism is observed in Gram-negative bacteria where the quinolone resistance family of pentapeptide repeat proteins protect the antibiotic target of type II topoisomerases, reducing susceptibility to quinolones and fluoroquinolones (Wilson *et al.*, 2020).

1.4 Resistance nodulation division (RND) efflux pumps

RND pumps exist within the inner membrane of Gram-negative bacteria and work to transport toxic substrates out of the cell (Blair and Piddock, 2009) using power from proton motive force (Murakami, 2008). Efflux complexes which span the inner and outer membranes of Gram-negative bacteria are referred to “trans-envelope efflux complexes” (Zgurskaya *et al.*, 2018). The inner membrane transporter (RND efflux pump) can cooperate with an adaptor – or a periplasmic adaptor protein (PAP) – and an outer membrane exit duct to make up a tripartite efflux pump (Zgurskaya *et al.*, 2018) (Symmons *et al.*, 2009). The complex connects the inner and outer membrane across the periplasmic space to create a pathway for toxic compounds to be transported from the periplasm or the outer leaflet of the inner membrane out of the

cell (Hernando-Amado *et al.*, 2016).

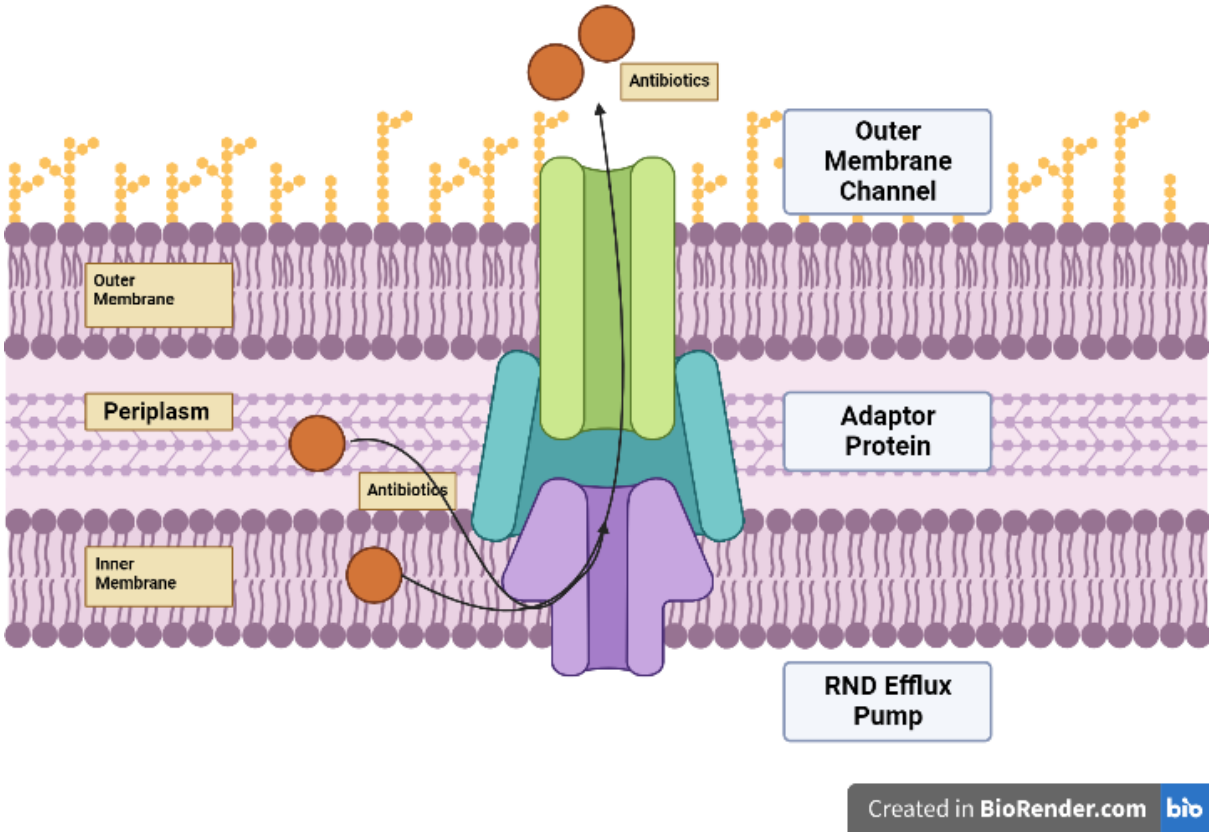

Figure 5. General structure of an RND tripartite efflux pump complex which spans the inner and outer membrane of Gram-negative bacteria. Diagram created in BioRender.com. A periplasmic adaptor protein connects the RND pump in the inner membrane to the outer membrane channel to allow efflux of substrates (sometimes antibiotics) from the periplasm.

AcrB is the major RND transporter in Gram-negative bacteria, including *E. coli,* and creates a tripartite efflux pump along with the AcrA adaptor and the TolC outer membrane exit duct (Murakami, 2008). AcrB transports substances out of the cell using a three-step functionally rotating mechanism (see figure 6 for a schematic), where monomers of AcrB cycle through three conformational states termed access, binding and extrusion (Murakami, 2008). In the resting state, when there is no antibiotic present, AcrB adopts an open conformation (called access), allowing for drug molecules to enter from the periplasm. The pump contracts (binding) to move

the drug up through AcrA and out through the TolC exit duct (extrusion) (Shi *et al.*, 2019).

The *acrAB* operon encodes AcrA and AcrB. A member of the TetR family of repressors, AcrR, is a local repressor of *acrAB* and is encoded for by *acrR* which is upstream of *acrA.* The repressor binds the *acrA* promoter region and is thought to block RNA polymerase, inhibiting *acrAB* expression. MarA, SoxS and Rob, from the XylS/AcraC family of regulators, are global regulators that upregulate *acrAB* expression (Bhandol *et al.*, 2020).

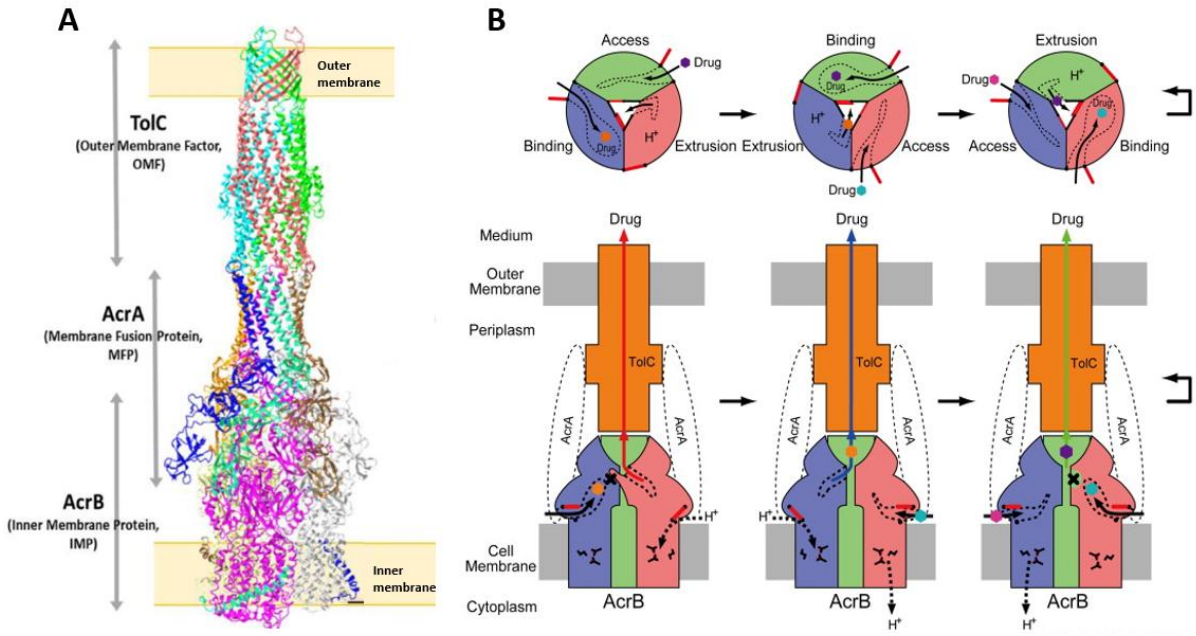

Figure 6. CryoEM structure of the fully assembled AcrAB-TolC complex with schematic. Panel A adapted from Jang, 2023 and panel B adapted from Murakami, 2008. Panel A shows the cryoEM structure of the fully assembled AcrAB-TolC complex with an open TolC (PDI ID: 5NG5) and an AcrB trimer (PDI ID: 6BAJ) (Jang, 2023). Panel B represents a schematic illustration of the functionally rotating ordered multidrug binding change mechanism.

The RND pump alternates between the access, binding, and extrusion conformations. Drugs can enter when the pump is in an open conformation or the

“access” state. Further conformational changes pump the drug up through the adaptor protein and out through the exit duct (Murakami, 2008).

1.5 Roles of efflux pumps

1.5.1 Drug transport

Some RND pumps can transport antibiotics out of the cell, thus reducing the internal concentration of drug and therefore, the susceptibility of the bacteria to such compounds, resulting in AMR (Anes *et al.*, 2015). For example, the AcrAB-TolC efflux system is known to be responsible for efflux of antibiotics, including fluoroquinolones, cephalosporins, and tetracyclines (Anes *et al.*, 2015). Also, multidrug transport (Mdt) systems such as MdtABC-TolC are able to transport novobiocin, quinolones, fosfomycin, myricetin, etc (Anes *et al.*, 2015).

Many RND pumps do not only transport antibiotics, but also other compounds including dyes, detergents, disinfectants and fatty acids (Fernando and Kumar, 2013), suggesting that the pumps can have roles other than AMR.

1.5.2 Biofilm formation

Efflux pumps are important in colonization of bacteria. In *E. coli* responsible for causing UTIs, inhibition of the pumps led to a decrease in biofilm formation (Kvist, Hancock and Klemm, 2008).

First identified in tooth plaque, biofilms are aggregated bacteria cells surrounded by a self-produced polymer matrix (consisting of polysaccharides, proteins, nucleic acids and lipids) which allows them to adhere to surfaces and tissues (Flemming and Wingender, 2010; Høiby, 2017). A total of 206 UPEC *E. coli* isolates associated with

recurrent and persistent UTIs in children were tested for biofilm formation using crystal violet solution. Biofilm formation *in vitro* was identified for strains causing recurrent pyelonephritis or kidney infections, but less biofilm was formed by strains causing cystitis (Tapiainen *et al.*, 2014). Efflux pumps can have various roles in biofilm formation: efflux of extracellular polymeric substances (EPSs) that can adhere to each other as well as surfaces; efflux quorum quenching (QQ) molecules to regulate quorum sensing (QS), which is important for coordinating bacterial behaviours/processes in response to cell population density; indirect regulation of genes involved in biofilm formation; efflux of toxic molecules; influence aggregation by controlling adhesion to surfaces/cells (Alav, Sutton and Rahman, 2018). Efflux pump inhibitors (EPIs) were shown to reduce biofilm formation of UPEC strains by up to 99% as well as block AMR of biofilms (Kvist, Hancock and Klemm, 2008).

1.5.3 Virulence

RND pumps can also play a role in virulence of the pathogen by contributing to the colonization processes and survival in the host as well as intracellular survival. In an acute pneumonia model in rats, it was found that *Pseudomonas aeruginosa* mutants overexpressing MexAB-OprM, MexCD-OprJ or MexEF-OprN pumps could be isolated in the presence and absence of antibiotic, suggesting that these mutants were favoured regardless of whether they had been exposed to antibiotic (Join-Lambert *et al.*, 2001).

Virulence of *Klebsiella pneumoniae* strains was measured using the *Caenorhabditis elegans* model. Clinical MDR isolates with several efflux systems were used. Overexpression of the AcrAB-TolC efflux pump was correlated with an increase in virulence index of *K. pneumoniae* (Bialek *et al.*, 2010). This result was supported by

another study which demonstrated that AcrB knockout strains of *K. pneumoniae* had a reduced capacity to cause pneumonia in mice than the wildtype strain (Padilla *et al.*, 2010). These findings imply that RND pumps are important for increasing virulence of the bacteria as well as AMR.

1.6 Major facilitator family (MFS) transporter protein

The MFS is a secondary active transporter (Yan, 2013), and its role is to transport molecules from the cytoplasm into the periplasm. These pumps work on the basis of an alternating access mechanism (Yan, 2013), where conformational changes cause a bound substrate to be pushed from one side of the inner membrane to the other. There are three main groups of MFS transporters: uniporters – transport a single substrate down the concentration gradient; symporters – transport a substrate in association with a coupling ion (typically protons) against the concentration gradient; and antiporters – transport a substrate and a co-substrate in opposite directions against the concentration gradient, i.e. the binding of one substrate is dependent on the release of the other (Quistgaard *et al.*, 2016). A proposed mechanism of MFS transporters is the rocker-switch alternating access mechanism, which involves the movements of two symmetrically related, 6 transmembrane segment bundles (referred to as N-terminal and C-terminal domains) around a central substrate-binding site. This mechanism enables the alternation of the protein between outward- and inward-facing states (Drew *et al.*, 2021).

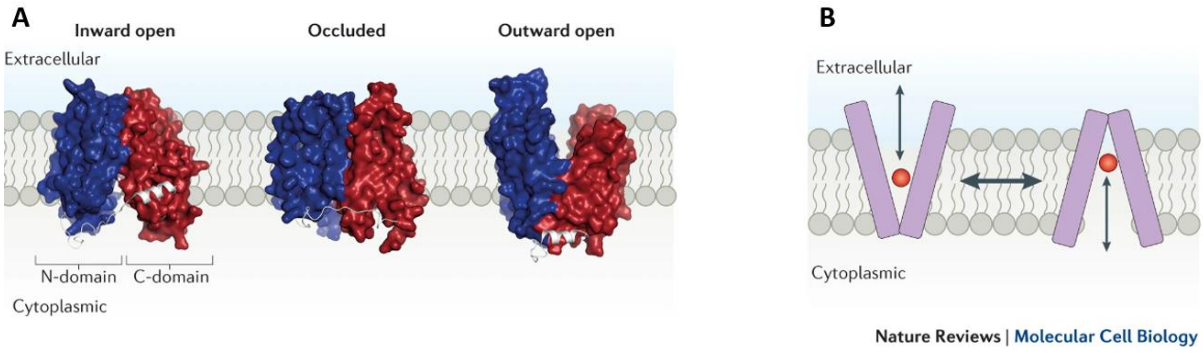

Figure 7. Major facilitator family (MFS) transporters transport substrates across biological membranes. Figure adapted from Quistgaard *et al.*, 2016. Panel A shows the structures representing inward open (based on LacY symporter), occluded (EmrD antiporter) and outward open (FucP symporter) conformations. Blue is the N-domain, red is the C-domain and grey is the linker between them. Each of these conformations must be made with every substrate that passes through the pump. Panel B shows the alternate access model, which assumes that when a substrate binds from one side of the membrane, the transporter undergoes a conformational change so that the binding site is inaccessible from that side of the membrane, but accessible on the opposite side to allow release (Quistgaard *et al.*, 2016).

MFS proteins are more commonly involved in the uptake of sugars, but have been known to transport drugs across the inner membrane, contributing to AMR (Pasqua *et al.*, 2019). MFS family proteins are responsible for the transport of substrates from the cytoplasm to the periplasm (Yan, 2013), but additional efflux pumps which are required to enable the transport of such periplasmic compounds across the outer membrane. An RND pump connected to an outer membrane TolC protein would allow this efflux (Pasqua *et al.*, 2019).

1.7 EefABC Efflux pump as characterised in *Klebsiella (Enterobacter) aerogenes*

A five-gene locus (*eefRABCD*) (figure 8) encodes a tripartite efflux pump (EefABC), belonging to the RND family, first characterised in *Klebsiella aerogenes* (Coudeyras *et al.*, 2008). This particular tripartite pump consists of EefB (inner membrane protein/ RND pump), EefA (adaptor protein), EefC (outer membrane protein) and EefR (regulatory protein) (Coudeyras *et al.*, 2008). Also encoded within the gene cluster is EefD, an MFS transporter protein (Fricke *et al.*, 2008).

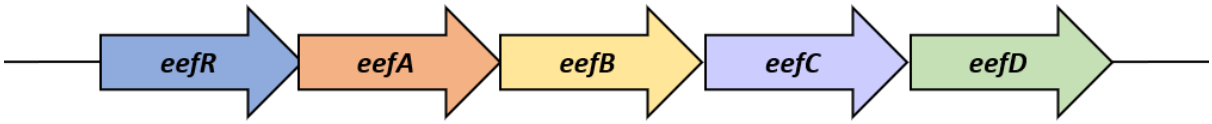

Figure 8. Genetic organisation of the five-gene operon encoding the EefABC tripartite efflux pump. Diagram created in Microsoft PowerPoint.

First identified in 2005, *eefABC* was discovered when an efflux pump from *E. aerogenes* (strain BW16627) was complemented with an *E. coli* (strain EP663) *tolC* mutant via bacteriophage for growth on plates with 0.05% deoxycholate. Recombinant plasmids were produced and the plasmid pEP770, which carried the shortest insert of overlapping DNA of 13.5 kb *E. coli* EP665 *acrAB tolC*, was constructed by P1 transduction of EP663 (*tolC*::Tn10) with a phage lysate prepared on EP661 (*ΔacrB*::Km^r). The product, EP665(pEP770), was able to grow on plates containing 0.1% sodium dodecyl sulfate, 0.05% deoxycholate, 3 µg/mL novobiocin, 5 µg/mL erythromycin, 200 µg/mL acriflavin or 10 µg/mL ethidium bromide (EtBr). The mutants grown lacked *acrAB-tolC*, so they should have been more susceptible to each of these compounds, however, they managed to grow. This experiment suggested that the DNA sequence taken from *K. aerogenes* must encode a complete tripartite efflux pump, which enabled the cells to grow in toxic conditions. The DNA region was analysed and open reading frames 3, 4 and 5 were found to be

homologous to efflux pump genes and named *eefABC*. The three genes were tightly linked, so the assumption that they were transcribed as an operon was made. Furthermore, EefC was found to contain a lipoprotein box (*C*VSL) which is characteristic of OprM and its homologues, which are acylated, thus implying that EefC is also acylated (Masi *et al.*, 2005).

The nucleoid binding protein, H-NS, is a repressor of the *eefABC* operon in *E. aerogenes*. Expression of *eefABC* is silent when grown in laboratory conditions but induced in an *E. coli hns* mutant and an *E. aerogenes* strain expressing a dominant negative H-NS protein. Strains which lacked AcrA and carried a dominant negative *hns* allele displayed increased resistance to antibiotics chloramphenicol and erythromycin. An experiment where inner membrane extracts were analysed by immunoblotting with antibodies found that expression of *eefA* was 75% higher in the strain which carried a dominant negative *hns* allele, suggesting that the expression of *hns* represses the expression of *eefA* (Masi *et al.*, 2005). The *eefABC* operon identified in *E. aerogenes* was cloned into *E. coli* to confirm whether H-NS acts as an *eefABC* repressor in *E. coli*. To do this, expression of *eef* on a P*eef*::*lacZ* reporter plasmid was monitored in different *E. coli* strains. The P*eef*::*lacZ* expression level increased threefold in the *hns* mutant in comparison to the parent strain, meaning *eef* genes were expressed more in the absence of H-NS. When the *hns* mutant was transformed with a plasmid which had the wild-type *E. coli hns* copy, P*eef*::*lacZ* expression level decreased. Results suggest that H-NS silences *eef* activity in the host *E. coli* (Masi *et al.*, 2005).

The pump was found to be functionally related to the AcrAB-TolC complex, which confers acriflavine resistance (Fricke *et al.*, 2008). AcrAB-TolC substrates are an extensive list, consisting of compounds belonging to various antibiotic classes such

as macrolides, β-lactams and fluoroquinolones, as well as dyes like ethidium bromide and rhodamine-6G (Jang, 2023). Sequence analysis of the *E. aerogenes eefABC* operon showed that EefA shared 49% sequence identity with the *E. aerogenes* AcrA periplasmic linker protein. EefB shared 57% sequence identity with the *E. aerogenes* AcrB inner membrane transporter, and EefC shared 24% sequence identity with the *E. aerogenes* TolC outer membrane protein (Masi *et al.*, 2005).

1.8 EefABC contributes to the antimicrobial resistant nature of *E. aerogenes*

The EefABC pump was initially found in *E. aerogenes* strains which were isolated from hospitals due to their multidrug-resistant behaviour (Mallea *et al.*, 1998). In a later study, four chloramphenicol resistant (CMR) mutants of *E. aerogenes* were isolated and tested for susceptibility to different antibiotics. Expression level of the *eefABC* promoter and the production of EefA and EefB proteins were analysed along with efflux activity. Four CMR mutants demonstrated increased resistance to antibiotics erythromycin and ticarcillin. In these mutants, the *eefABC* promoter was activated and two additional efflux proteins were detected (Masi, Pagès and Pradel, 2006).

EefABC was found to have a similar function to AcrAB-TolC, in terms of antimicrobial resistance, since when *eefABC* was overexpressed in an Δ*acrB* mutant strain of *E. cloacae*, the wildtype phenotype was partially restored. This information was discovered when minimum inhibitory concentrations (MICs) of *E. cloacae* using erythromycin compared the wildtype (encoding the *acrB* gene), a *ΔacrB* mutant and a *ΔacrB* mutant which overexpressed *eefB*. It was found that the *acrB* knockout strain was more susceptible to several antibiotics, including erythromycin, but when *eefB*

was overexpressed in the *acrB* knockout strain, the wildtype phenotype was restored, as in the MIC was the same as that of the wildtype (Guérin *et al.*, 2020).

1.9 EefABC is involved in acid tolerance in *Klebsiella pneumoniae*

In *K. pneumoniae*, the RND efflux complex, EefABC, is responsible for conferring resistance to inorganic acids to enable the pathogen to survive in the gastrointestinal tract (GI) of humans. This was confirmed by *in vivo* assays that showed that the Δ*eefA* mutant was expressed less in bacteria colonising the GI tract than the wild-type strain, which had a functioning efflux pump. From this result, it was inferred that bacteria which did not encode *eefA* were less able to colonise the GI tract (Coudeyras *et al.*, 2008). The acid tolerance assays compared the survival of a wildtype strain and an Δ*eefA* mutant version of the wildtype in a control of pH 7.0 nutrient broth and in an inorganic acid shock condition with HCL pH 4.0. At first, there was no statistical difference in survival percentage between the wildtype and mutant. However, the experiment was repeated, this time first preadapting cells to the different pH conditions, and the Δ*eefA* mutant showed a reduction in ability to adapt to an acidic environment in comparison to the wildtype in the inorganic acid shock condition. These findings suggest that the efflux pump is involved in the survival of *K. pneumoniae* cells in the acidic conditions of the GI tract in humans (Coudeyras *et al.*, 2008).

1.10 EefABC efflux pump identified in *E. coli*

E. coli K-12 (MG1655) was isolated from a diphtheria patient in 1922 and became the preferred model organism in genetics, molecular biology and biotechnology (Browning, Hobman and Busby, 2023), and so it was the earliest organism to be put forward for whole genome sequencing (Blattner *et al.*, 1997). This strain encodes 6 major RND systems (AcrB, AcrD, AcrF, CusA, MdtBC and MdtF) (Anes *et al.*, 2015) but lacks EefB. *E. coli* ATCC 25922 was isolated from a human clinical sample collected in Seattle (1946) and is commonly used as a quality control sample and encodes the RND pump EefB (Minogue *et al.*, 2014).

The large gene cluster that houses *eefABC* is absent in wildtype *E. coli* K-12, but has been identified in *E. coli* SMS-3-5, a strain isolated from an industrially polluted aquatic environment which is multidrug resistant. (Fricke *et al.*, 2008). EefR is a TetR-family transcriptional regulator (TFTR) that is encoded within the operon and is thought to be responsible for the regulation of efflux pump expression. In subsequent work, EefABC was detected in *E. coli* following a search for the presence of the TTFRs which resulted in the identification of *eefR*. The regulator was not identified in *E. coli* SMS-3-5, but in four other *E. coli* strains, indicating the presence of the *eefABC* complex in these strains (Colclough, Scadden and Blair, 2019). This was the first time the pump had been reported in *E. coli*.

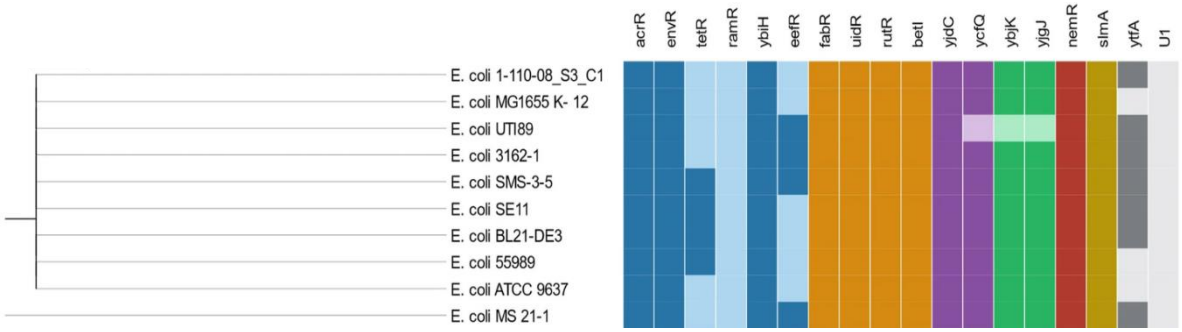

Figure 9. Patterns of TFTR presence/absence across *E. coli* strains. Figure taken from Colclough, Scadden and Blair, 2019. Darker coloured squares indicate the presence of the gene and lighter colours indicate absence (Colclough, Scadden and Blair, 2019).

In the NCBI database ('Escherichia coli ATCC 25922, complete genome', 2014), the complete genome of *E. coli* strain ATCC 25922 (CP009072.1) is broken up into genes and their proposed products (Table 1).

Table 1. The complete genome of *E. coli* ATCC 25922 broken up into genes and their proposed products. Data was taken from the NCBI database 'Escherichia coli ATCC 25922, complete genome', 2014.

Gene	Complement strand in CP009072.1	Product in CP009072.1	Locus tag in CP009072.1	Gene length (nucleotides) in CP009072.1
eefR	3742500..3743066	bacterial regulatory, tetR family protein	DR76_3503	567
eefA	3741230..3742351	efflux transporter, RND family, MFP subunit	DR76_350	1122
eefB	3738123..3741230	RND transporter, hydrophobe/amphiphile efflux-1 family protein	DR76_3501	3108
eefC	3736746..3738119	efflux transporter, outer membrane factor (OMF) lipo, NodT family protein	DR76_3500	1374
eefD	3735574..3736737	drug resistance transporter, Bcr/CflA subfamily protein	DR76_3499	1164

1.11 Previous work

This information comes from a PhD thesis (Pugh, 2022).

The Blair Lab studied >20,000 *E. coli* genomes and identified a 7th RND system involving EefB.

The presence of the *eefRABCD* operon in 19,247 assemblies (after duplicates were identified using MASH distances and removed) was determined using ABRicate. Findings confirmed that the *eefRABCD* operon was highly conserved in phylogroups B2, D, E, F and G (commonly associated with infection) to a similar level as the AcrAB-TolC RND system. The nucleotide identity of the *eefRABCD* operon was conserved in *E. coli* isolates to a similar level as *acrAB-tolC* as all genes (apart from *eefC* in ST354) were >97% identical to those in *E. coli* ATCC 25922. Findings are suggestive of a similar, critical biological function. Moreover, the *eefRABCD* operon was present in all sequence type (ST) groups of phylogroups B2, F and G, which are associated with human infection and MDR. The operon was also only absent in one ST group of phylogroups D and E (ST69 and ST182 respectively). The operon was absent in all ST groups belonging to phylogroups A, B1 and C, which are classed as environmental and commensal isolates. From this clear divide between phylogroups, a strong evolutionary relationship is apparent. In these commensal strains, conserved fragments of the operon were identified, suggesting that these strains did encode the pump, but it has since been lost.

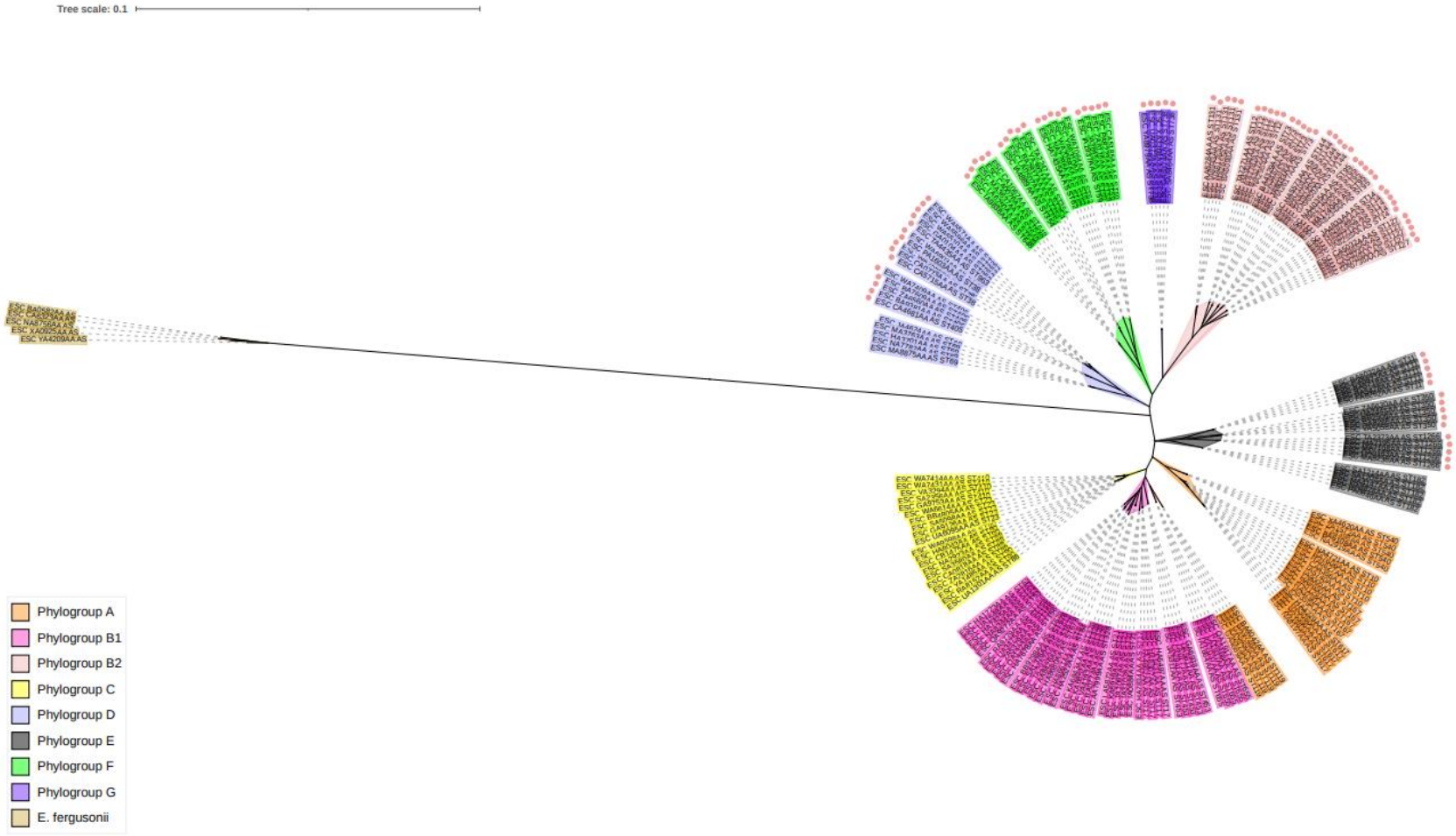

Figure 10. Phylogenetic structure of the assemblies used in the analysis of the distribution of the *eefRABCD* operon across *E. coli* ST groups within phylogroups. This diagram was taken from Pugh, 2022.

Five assemblies per ST (exception ST84=2) were chosen randomly. The tree was rooted using five *E. fergusonii* assemblies. Leaves are annotated with the ST group of the assembly and colour coded by phylogroup (see legend in bottom left corner of figure 10). STs positive for the *eefRABCD* operon are marked with ●. The tree was generated using RaXmL and visualised on iToL.

As part of this study the protein structure of the pump was modelled in collaboration with Prof V Bavro at the University of Essex. EefABC was predicted to have a broadly similar structure to the CusABC system, suggesting a role in metal ion tolerance. This idea came from MAFFT multiple sequence alignment of EefC with CusC, which is encoded on an operon with the RND metal ion pump CusBA, which has been linked to resistance of copper (I) and silver(I) ions.

1.12 Aims of the project

- To identify the biological function of the EefABC/D RND efflux system in *E. coli*.
- Identify potential substrates of the pump, including antibiotics, dyes and metals. Due to the similarities in gene sequence and comparable level of conservation to the AcrAB-TolC complex, and the structural similarities with CusABC, known substrates of these pumps should be tested for EefABC.
- Investigate the role of EefABC in the ability of *E. coli* to survive in a range of acidic environments in the human body, including inside the GI tract as well as urine.

2. MATERIALS AND METHODS

2.1 *E. coli* strains used in this study

The physiological role of EefABC was investigated in two ways, loss of function and gain of function. Loss of function was studied in *E. coli* ATCC 25922, a strain that naturally encodes the *eefRABCD* operon, and this operon was deleted. Gain of function was studied in *E. coli* MG1655, a strain which does not naturally encode the *eefRABCD* operon, and this operon was overexpressed.

Throughout this study, MG1655 was used as the wildtype for gain of EefABC function strains, which are strains derived from MG1655 with additional plasmids encoding the *eefABC* components. The *eefABC* operon was encoded on the plasmid pET21a, and the *eefD* gene onto pACYC177. The genes were encoded separately, because they were thought to encode 2 different classes of efflux pumps, and the use of different plasmids allowed for the transformation of a strain which carried both plasmids, and therefore expressed both pumps. Some of these strains were constructed to not have a functioning AcrB pump, due to previous work which showed that the conservation of *eefRABCD* was comparable to that of the *acrAB-tolC* RND system, hinting at a similar function. It was also known that presence of AcrB can mask other phenotypes, so in an *acrB* deleted environment, the functionality of EefB could be better examined. Additional MG1655 strains in which AcrB was still functional were used which had the pET21a vector, with or without *eefABC* or *eefD* encoded onto it.

ATCC 25922 was used as the wildtype for loss of EefABC function strains, which are *eefABC* or *eefD* knockout strains derived from ATCC 25922. This strain of *E. coli* also encoded *acrB*.

Strains were stored at -80˚C using protect conservation beads (Technical Service Consultants). When required, a bead was spread onto Luria Bertani (LB) agar (Sigma-Aldrich: L2897) containing 50 µg/mL antibiotic marker and incubated overnight at 37˚C. Overnight cultures were prepared by inoculating 5 mL LB broth (Sigma-Aldrich: L3022) with a single colony from a freshly streaked plate, with 50 µg/mL required antibiotic and incubated for 18 hours at 37˚C with aeration.

Table 2. *E. coli* strains used in the lab and the relevant antibiotic marker.

Culture collection number	Strain	Antibiotic marker	Reference
Loss of EefABC function strains			
EC112	ATCC 25922	N/A	Minogue *et al.*, 2014
EC196	ATCC 25922 Δ*eefABC*	N/A	Blair lab culture collection
EC227	ATCC 25922 Δ*eefD*	N/A	Blair lab culture collection
Gain of EefABC function strains (Δ*acrB* mutants)			
EC07	MG1655	N/A	Blattner *et al.*, 1997
EC99	MG1655 Δ*acrB* + pET21a	Carbenicillin	Blair lab culture collection
EC371	MG1655 Δ*acrB* +pET21a:*eefABC*	Carbenicillin	Blair lab culture collection
EC219	MG1655 Δ*acrB* + pACYC177	Kanamycin	Blair lab culture collection
EC220	MG1655 Δ*acrB* + pACYC177:*eefD*	Kanamycin	Blair lab culture collection
EC413	MG1655 Δ*acrB* +pET21a:*eefABC* + pACYC177:*eefD*	Kanamycin + Carbenicillin	Blair lab culture collection
Gain of EefABC function strains (with *acrB*)			
EC97	MG1655 + pET21a	Carbenicillin	Blair lab culture collection
EC369	MG1655 + pET21a:*eefABC*	Carbenicillin	Blair lab culture collection
EC414	MG1655 + pET21a:*eefABC* + pACYC177:*eefD*	Kanamycin + carbenicillin	Blair lab culture collection

2.2 Plasmids used in this study

The correct plasmid in the strain was maintained by incubating the plasmid on LB agar or in LB broth which contain 50 µg/mL of the antibiotic.

Table 3. Plasmids and their associated antibiotic marker.

Plasmid	**Antibiotic marker**	**Source**
pET21a	Carbenicillin	Novagen/ Thermo Fisher
pACYC177	Kanamycin + carbenicillin	Schottel, Bibb and Cohen, 1981

2.3 PCR amplification

PCR amplification was performed in an Eppendorf Nexus GX2 thermal cycler (Eppendorf, UK). DNA culture was prepared by adding a single colony of a strain to 100 µL distilled nuclease-free water and lysated for 5 minutes in a thermal cycler at 95°C. PCR reaction mixtures were made up of 12.9 µL MyTaq 2x Red (Meriden: BIO21109), 1 µL of 25 µM forward primer, 1 µL of 25 µM reverse primer, 9.1 µL nuclease free water and 1.5 µL lysate template DNA. Annealing temperature was calculated using NEB Tm Calculator (*NEB Tm Calculator*), (product group: Taq DNA polymerase, polymerase/kit: Taq 2X master mix). Primers used are listed in table 4.

Table 4. Oligonucleotide primers used in this study.

Laboratory code	Primer name	Sequence (5'-3')	GC content (%)	Tm (˚C)	supplier
P291	EC *eefA* internal check F	GAACAAACATTCCCGGTAAT	40	51	Sigma Aldrich
P292	EC *eefA* internal check R	CGCTTATTTAAGGAAGGTGA	40	51	Sigma Aldrich
P293	EC *eefB* internal check F	GATCACCAGAATGACCGAGA	50	55	Sigma Aldrich
P294	EC *eefB* internal check R	TTTACCGTTGATGGTTTCAG	40	51	Sigma Aldrich
P295	EC *eefC* internal check F	AATCGTCGGGAAAAAGTTAG	40	51	Sigma Aldrich
P296	EC *eefC* internal check R	AGGTAGTAACCATTGCACTG	45	53	Sigma Aldrich
P701	EC *eefD* internal check F	CATAAAGCTTTGAATCAGGC	40	50	Eurogentec
P702	EC *eefD* internal check R	TTCTATTGCTCGTGACAAAT	35	50	Eurogentec
P121	EC *acrB* internal check F	AATGGCGCTGTCGGTACT	56	59	Sigma Aldrich
P122	EC *acrB* internal check R	CCCAGAGTGGTGTTAATGTCG	52	57	Sigma Aldrich

PCR conditions are listed in table 4, annealing temperature is dependent on the primer used.

Table 5. PCR conditions.

Steps 2-4 were repeated 30 times

Step	**Temperature (˚C)**	**Time (min)**
1. Denaturation	95	1:00
2. Denaturation	95	0:15
3. Annealing	Variable	0:15
4. Extension	72	0:10
5. Extension	72	5:00

For analysis, PCR products were electrophoresed on a 1.0% agarose gel (100 mL 1XTAE buffer, 1 g agarose and 10 µL Midori green) in 1 X TAE buffer at 100V for 110 minutes, along with 5 µL of 100 bp hyper ladder (New England Biolabs).

2.4 Isolation of plasmid DNA

Plasmid DNA was isolated using the QIAprep mini prep kit (QIAgen: 27106) according to manufacturer's instructions.

2.5 Production of electrocompetent cells

Cells needed to be electroporated to allow entry of exogenous DNA to create the desired construct. In a 500 mL Duran bottle, 50 mL LB broth was inoculated with 3 mL overnight culture and cells were grown at 37˚C until OD_{600nm} = 0.6. Culture was transferred to a falcon tube and chilled on ice. Cells were harvested by centrifugation at 3000 x g for 10 minutes at 4˚C and the supernatant discarded. Cells were resuspended in 25 mL ice-cold 15% glycerol. Harvesting and resuspension steps

were repeated 2 more times. Cells were harvested again and resuspended in a final volume of 500 µL glycerol. The product, 60 µL culture, was aliquoted into microcentrifuge tubes and store at -80˚C.

2.6 Bacterial transformation

Competent cells and the plasmid DNA (no more than 10% of the total volume) were transferred to a pre-chilled 0.2 cm gap electroporation cuvette to a total volume of 50 µL and chilled on ice for up to 30 minutes. The Eppendorf Eporator (Eppendorf, UK) was set to 2.5kV voltage, 25 µF capacitance, 200Ω. Immediately after the pulse was applied, 950 µL LB was added to the electroporation cuvette. All cells were transferred out of the cuvette into a universal tube. The universal tube was incubated with aeration at 37˚C for 1 hour to allow the cells to recover without antibiotic. After incubation, 100 µL culture was spread onto an agar plate containing appropriate antibiotic markers. The rest of the culture was centrifuged at 14,000 x g for 1 minute, the supernatant discarded, and cells resuspended in 100 µL LB then spread onto another antibiotic plate. Plates were incubated overnight at 37˚C.

2.7 Measurement of antimicrobial susceptibility by Agar MIC

Minimal inhibitory concentration (MIC) is the lowest concentration of an antibiotic or dye that is required to inhibit the visible growth of bacteria (Wiegand, Hilpert and Hancock, 2008).

A series of Iso-Sensitest agar (20 mL) (Oxoid: CM0471) square plates were poured with ranging concentrations of various compounds. Plates were dried before use at 60°C.

Overnight cultures were diluted 1000-fold and 180 µL of the diluted culture was added to a round-bottom 96-well plate. For each strain, 3 wells were allocated to provide 3 technical replicates. The multipoint inoculator (Mass Uridot, Mast Group Ltd.) was set up with enough pins to dip into each well used on the 96-well plate. The Uri Dot inoculated each plate with 1 µL of every sample. An antibiotic free start agar plate was stamped first, and an antibiotic free agar end plate was stamped last to ensure viability of all cultures. Spots on each plate were allowed to dry before incubation overnight at 37˚C (Kowalska-Krochmal and Dudek-Wicher, 2021).

2.8 Measurement of antimicrobial susceptibility by broth dilution MIC

All wells of a round bottomed 96-well plate were inoculated with 50 µL iso-sensitest broth (except for the first column, A1-H1). Additional Iso-Sensitest broth was made up to be twice the maximum concentration of the compound required and 100 µL of this was added to all the wells in the first column. To perform a serial dilution, 50 µL was removed from the first column and added to the second column and so forth until the 10^{th} column, reducing the concentration of the previous column by half each time. Finally, 50 µL was removed from the 10^{th} column and discarded. The 11^{th} and 12^{th} control columns should contain no substrate. Overnight culture (approximately $1x10^9$ cfu/ml) was diluted 1:100 by adding 50 µL culture to 5 mL Iso-Sensitest broth to give $1x10^7$ cfu/mL. This was diluted further 1:20 by taking 250 µL bacteria into 4750 µL Iso-Sensitest broth to give $5x10^7$ cfu/mL. The first 11 wells in each row were inoculated with 50 µL of this cell suspension (1 row was allocated per strain, 8 strains can be tested on one 96-well plate). The plate was covered with a lid and incubated overnight at 37˚C. The next day, each well was examined for growth (Kowalska-

Krochmal and Dudek-Wicher, 2021). The lowest concentration that prevents visible growth of the bacteria is noted as the MIC for that strain.

Table 6. Compounds used in MICs.

Antibiotic	Supplier	Catalogue number	Solubility	Concentration range (µg/mL)
Ampicillin	Sigma	A9393	1M sodium bicarb	0.03 to1024
Azithromycin	Alfa Aesar	J66740	DMSO	0.5 to 1024
Chloramphenicol	Sigma	C0378-5G	70% Methanol	0.015 to 512
Ciprofloxacin	Acros	449620050	SDW + acetic acid	0.008 to 128
Cobalt (II) chloride	Sigma	232696-5G	SDW	8 to 1024
Erythromycin	Acros Organic	A0415457	70% Ethanol	0.5 to 1024
Ethidium bromide	Fisher	10042120	SDW	1 to 1024
Gentamicin Sulfate	Fisher	10224873	SDW	0.03 to 1024
Meropenem Trihydrate	TCI Chemicals	M2279-1G	SDW	0.015 to 1024
Moxifloxacin hydrochloride	Sigma	PHR1542-1G	60% DMSO	0.015 to 64
Novobiocin sodium salt	Alfa Aesar	J60928	SDW	1 to 512
Polymixin B sulfate	PhytoTech	P6809-1G	SDW	0.125 to 64
Tetracycline hydrochloride	Sigma	T7660-5G	SDW	0.015 to 1024
Ticarcillin disodium salt	Sigma	T5639	SDW	1 to 1024

2.9 Growth Kinetics

Overnight cultures were prepared, then 1 mL LB broth was inoculated with 10 µL culture. A 96-well plate containing 90 µL LB broth was inoculated with 10 µL of the diluted culture. The plate was covered with a “BreatheEasy” membrane and placed into the BMT LabTech Fluostar Omega plate reader. The programme covered 73 cycles in double orbital shaking mode, taking an OD_{600nm} measurement every 10 minutes, giving a total run time of 12 hours (Sprouffske and Wagner, 2016).

Data generated in the plate reader was used to calculate generation time using Microsoft Excel. The mean OD of LB alone was subtracted from the mean OD of the sample for each time point. From this, natural log (Ln(OD)) was calculated and a graph was drawn with a linear trendline. Points from the graph that were non-linear were removed, making the R^2 value closer to 1. Growth rate was calculated using the formula “=INDEX(LINEST(natural log, time))”. The natural log of 2 (Ln2) was divided by growth rate to calculate generation time in hours, then multiplied by 60 to get the time in minutes.

When measuring the growth rate in the presence of erythromycin, 2 µg/mL erythromycin stock was added to the LB in the 96-well plate instead of the antibiotic marker. If using EtBr or rhodamine-6G (R6G), 8 µg/mL stock was added to the LB in the 96-well plate instead of the antibiotic marker.

2.10 Ethidium Bromide accumulation

For the accumulation assay, 10 mL LB broth was inoculated with 400 µL overnight culture and incubated at 37˚C with aeration until OD_{600nm} = 0.4. Cultures were centrifuged at 3000 x g for 10 minutes at 23˚C, supernatant discarded. The pellet was resuspended in 10 mL fresh 20mM potassium phosphate buffer (PPB) buffer pH7 + 1mM $MgCl_2$ (3.08 mL 1M K_2HPO_4, 1.93 mL 1M KH_2PO_4, 245 mL sterile distilled water (SDW) and 250 µL 1M $MgCl_2$) and OD_{600nm} adjusted to 0.2. Culture (190 µL) was loaded into a black 96-well plate (including three technical replicates per strain). The last column contained 3 repeats of 200 µL of PPB as a control. The Fluostar was set up to add 10 µL of 500 mg/mL (25 mg/mL) EtBr to each well containing a sample during the run. EtBr was not added to the control wells (Viveiros *et al.*, 2008).

2.11 Ethidium Bromide efflux assay Fluostar

To measure efflux, conditions which favoured accumulation of EtBr must first be administered. The conditions included no glucose, incubation temperature at 25˚C and the presence of an efflux pump inhibitor (Viveiros *et al.*, 2008). The inhibitor used in this experiment was carbonyl cyanide m-chlorophenyl hydrazone (CCCP).

LB broth was inoculated with 400 µL overnight culture and grown at 37˚C until OD_{600nm} = 0.4. Cultures were centrifuged at 3000 x g for 10 minutes at 23˚C, supernatant discarded. The pellet was resuspended in 10 mL fresh 20mM PPB buffer pH7 and 1mM $MgCl_2$ (3.08 mL 1M K_2HPO_4, 1.93 mL 1M KH_2PO_4, 245 mL SDW and 250 µL 1M $MgCl_2$) the OD_{600nm} adjusted to 0.2. The suspension was transferred to a new tube. Cells were de-energised, and efflux inhibited by adding 100 µL of 10mM CCCP stock (0.01 g in 4 mL SDW and 1 mL DMSO), as well as 500 µL of a 1,000 µg/mL EtBr stock (0.01 g in 10 mL SDW). Culture was incubated at 23˚C for 1 hour.

Cultures were centrifuged at 3000 x g for 10 minutes at 23˚C and the supernatant discarded. The pellet was resuspended in 10 mL 20mM PPB and 1mM $MgCl_2$. A black 96-well plate was inoculated with 190 µL culture (due to time sensitivity, only 1 technical replicate was used). Once in the plate reader, 10 µL 20% glucose was added to each well to re-energise the RND efflux pump and begin efflux.

It was possible to use DNA-intercalating dyes such as EtBr to measure efflux and accumulation since it only fluoresces when it is bound to intracellular DNA, making it possible to quantify efflux and accumulation (Paixão *et al.*, 2009).

2.12 Measurement of virulence in the *Galleria mellonella* model

To achieve different concentrations of cells, OD_{600nm} of overnight cultures was adjusted to 0.1 or 1.0 using the formula:

(Desired OD_{600nm} /Measured OD_{600nm} of culture) x 1000 = volume of culture in µL up to 1 mL PBS

A Galleria grabber was prepared (a wet sponge in a bulldog clip) and one larva was placed into it so that its underside was facing upwards. The larvae were injected in the 3rd segment from the tail with 20 µL diluted culture. The needle was removed slowly, and the larvae placed in a petri dish. This was repeated using 10 larvae per strain. All larvae infected with the same strain of bacteria were kept in the same petri dish. Squares of white tissue as well as wood chippings filled the petri dishes as food and shelter for the worms. The dishes were kept in a secure box with some damp tissue to prevent the larvae from drying out in the 37˚C incubator. The larvae were checked every 24 hours over 5 days to count how many had survived. If the larvae did not wriggle when poked, then it was dead.

2.13 Measurement of biofilm formation using Crystal Violet

Overnight cultures were grown in 5 mL LB broth without salt (5g tryptone, 2.5g yeast extract and distilled water up to 500 mL) at 37˚C with aeration. Culture was diluted to OD_{600nm} of 0.1 in 5 mL LB broth with NaCl (475 mL SDW H_2O, 5g Tryptone (Oxoid: LP0042), 5g NaCl and 2.5g yeast extract (Oxoid: LP0021) using the formula:

$$(0.1/OD_{600nm} \text{ of culture}) \times 5000 = \text{volume of culture in µL up to 5 mL LB}$$

Diluted culture (200 µL) was aliquoted into wells of a 96-well plate, including 4 replicates per strain. The plate was incubated at 30˚C for 72 hours.

Biofilms needed to be washed to remove unattached cells. To do this, the plate was turned upside down into a tray of biocide to remove liquid and rinsed with tap water to remove any unattached cells. The wells were inoculated with 200 µL 01.% crystal violet solution stain the cells associated with biofilm and the plate was left to incubate at room temperature for 15 minutes. Crystal violet was removed from the wells by turning the plate upside down into a tray of biocide and washing with water, before 200 µL 70% ethanol was added to wells to solubilise the crystal violet solution associated with biofilm. OD_{600nm} of each well was measured using the Fluostar Omega to quantify the amount of biofilm produced (Baugh *et al.*, 2012).

2.14 Acid tolerance

Overnights were diluted to OD_{600nm} = 0.2 in 5 mL MOPS media, pH 7.0 or pH 5.0 (100 mL MOPS 10X buffer, 10 mL 0.132M K_2HPO_4, 10 mL 20% glucose and SDW up to 1L). Cultures diluted in pH 5 adjusted MOPS minimal media were incubated for 1 hour at 37˚C with aeration for preadaptation. All cultures were centrifuged at 3000 x

g for 12 minutes and the supernatants were discarded. The pellet was resuspended in 1 mL MOPS minimal media, either pH 7.0 or pH 4.0 (acid-shock). Viable counts were taken immediately after this point (T=0) and after 120 (T=120) and 240 (T=240) minutes of incubation at 37˚C with aeration. For viable counts, wells of the first column of a 96-well plate were inoculated with 100 µL culture. Wells in columns 2-8 had 90 µL PBS. 10 µL was taken from the first column into the second, and so forth, until column 8 where 10 µL was discarded, providing a 1:10 serial dilution. Then, 5 µL from all wells was spotted onto a square agar plate and after incubation overnight at 37˚C, CFU/mL was calculated (Coudeyras *et al.*, 2008).

2.15 Growth kinetics to measure acid tolerance with preadaptation

An overnight culture was split into 2 universal tubes and centrifuged at 3000 x g for 12 minutes, then resuspended in 2.5 mL either MOPS pH 7.0 or MOPS pH 5.0 then incubated for 1 hour at 37°C with aeration. The growth kinetics protocol and data analysis were the same as method 2.9, but instead of LB broth, the 96-well plate was inoculated with 90 µL MOPS minimal media adjusted to pH 7 or pH 4. In the plate reader, optical density at 600_{nm} was measured for 46 cycles, with 30 minutes between each cycle, running for a total of 23 hours.

2.16 Metabolomics using liquid chromatography – mass spectrometry (LC-MS) sample preparation

These experiments were performed in collaboration with Dr Gerald Larrouy-Maumus at Imperial College London.

Metabolomics refers to the study of metabolites within an organism and produces data about the mechanistic biochemistry of a cell which can be linked directly to the

molecular phenotype (Prosser, Larrouy-Maumus and Carvalho, 2014). In this study, an untargeted approach was taken to generate a global metabolomics profile using LC-MS. Metabolomics of prepared samples was carried out and analysed by collaborator Dr Gerald Larrouy-Maumus. Cells retrieved during the exponential and stationary growth phases were prepared as samples. Internal and external metabolites were analysed.

To prepare the samples for metabolomics, overnight cultures were diluted to OD_{600nm} = 0.2 in 100 mL pH 7 MOPS minimal media and incubated at 37˚C with aeration. Samples of 12 mL were taken when cells had reached the exponential growth phase and placed into a 15 mL falcon tube for 10 minutes of centrifugation at 3000 x g at 4˚C. The supernatant contained external metabolites and was filter sterilised and stored at -80˚C. This method was repeated once cells had reached stationary growth phase.

Pellets were washed three times with cold PBS and centrifuged at 3000 x g for 10 minutes at 4˚C before being resuspended with 1 mL ACN:MeOH:ddH_2O 40:40:20 v:v:v. Cells were placed into a 2 mL Fast Prep lysate tubes (115076200-CF, 1150680-CF, MPBio) which contained ~250 µL volume of 0.2 mm acid-washed beads (G1145, Sigma) and disrupted in a bead beater using 2 cycles of 30 seconds at setting 6.0. Tubes were rested on ice for 2 minutes in between cycles. Once beads had settled, the suspension was transferred to a Spin-X 0.2 µm filter column (Costar, 8160) and centrifuged at 15,000 x g for 20 minutes at 4˚C. The flow-through contained internal metabolites and was stored at -80˚C.

2.17 Liquid chromatography-mass spectrometry for untargeted metabolomic analysis

These experiments were carried out and provided by collaborator Dr Gerald Larrouy-Maumus.

Aqueous normal-phase liquid chromatography was performed using an Agilent 1290 Infinity II LC system equipped with a binary pump, temperature-controlled autosampler (set at 4°C) and a temperature-controlled column compartment (set at 25°C) containing a Cogent Diamond Hydride Type C silica column (150 mm x 2.1 mm; dead volume of 315 µL). A flow rate of 0.4 mL/min was used. The elution of metabolites was performed using solvent A which consisted of 0.2% deionised water (resistivity ~18 MΩ cm) and 0.2% acetic acid, and solvent B which consisted of 0.2% acetic acid in acetonitrile. The following gradient was applied at a flow rate of 0.4 mL/min: 0 minutes, 85% B; 0-2 minutes, 85% B; 3-5 minutes, 80% B, 6-7 minutes, 75% B; 8-9 minutes, 70% B; 10-11 minutes, 50% B; 11.1-14 minutes, 20% B; 14.1-25 minutes, 20% B; and 5 minutes of re-equilibration at 85% B. Accurate mass spectrometry was performed using an Agilent Accurate Mass 6545 QTOF apparatus. Dynamic mass axis calibration was achieved by continuous infusion after the chromatography of a reference mass solution using an isocratic pump connected to an ESI ionisation source operated in positive ion mode and negative ion mode. The nozzle and fragmentor voltages were set to 2000 V and 100 V respectively. The nebuliser pressure was set to 50 psig, and the nitrogen drying gas flow rate was set to 5 l/minute. The drying gas temperature was maintained at 300°C. The MS acquisition rate was 1.5 spectra/sec, and *m/z* data ranging from 50 to 1200 were stored. The instrument enabled accurate mass spectral measurements with an error of less than 5 parts per million (ppm), a mass resolution ranging from 10000 to 45000 over the *m/z* range of 121-955 atomic mass units, and a 100000-fold dynamic range

with picomolar sensitivity. The data were collected in centroid 4-GHz (extended dynamic range) mode. The detected *m/z* data were deemed to represent metabolites, which were identified based on unique accurate mass-retention times and MS/MS fragmentation identifiers for masses exhibiting the expected distribution of accompanying isotopomers. The typical variation in the abundance of most of the metabolites remained between 5 and 10% under these experimental conditions.

2.17 Liquid chromatography-mass spectrometry for untargeted metabolomic analysis for polar compounds

These experiments were carried out and provided by collaborator Dr Gerald Larrouy-Maumus.

The data were acquired with an Agilent 1290 Infinity II UHPLC coupled to a 6545 LC/Q-TOF system. Chromatographic separation was performed with an Agilent InfinityLab Poroshell 120 HILIC-Z (2.1 x 100 mm, 2.7 µm (p/n 675775-924) column. The HILIC-Z methodology was optimized for polar metabolites. For easy and consistent mobile-phase preparation, a concentrated 10x solution consisting of 100 mM ammonium acetate (pH 9.0) in water was prepared to produce mobile phases A and B. Mobile phase A consisted of 1.0 mM ammonium acetate in water (pH 9.0) with a 5-µM Agilent InfinityLab Deactivator Additive (p/n 5191-4506), and mobile phase B consisted of 1.0 mM ammonium acetate (pH 9.0) in 10:90 (v:v) water/acetonitrile with a 5-µM Agilent InfinityLab Deactivator Additive (p/n 5191-4506). The following gradient was applied at a flow rate of 0.5 ml/min: 0 minutes, 100% B; 0-11.5 minutes, 70% B; 11.5-15 minutes, 100% B; 12-15 minutes, 100% B; and 5 minutes of re-equilibration at 100% B. Accurate mass spectrometry was performed using an Agilent Accurate Mass 6545 QTOF apparatus. Dynamic mass axis calibration was achieved by continuous infusion after the chromatography of a reference mass

solution using an isocratic pump connected to an ESI ionization source operated in negative-ion mode. The following parameters were used: sheath gas temperature, 300°C; nebulizer pressure, 40 psig; sheath gas flow, 12 l min^{-1}; capillary voltage, 3000 V; nozzle voltage, 0 V; and fragmentor voltage, 115 V. The data was collected in centroid 4 GHz (extended dynamic range) mode.

2.18 Metabolites data analysis

Methodology was carried out and provided by collaborator Dr Gerald Larrouy-Maumus.

Metabolites were extracted using Agilent Profinder version B.8.0.00 service pack 3 and multivariate analysis performed using Mass Profiler Professional B.14.

CHAPTER 3. RESULTS - EEFABC IS NOT A DRUG TRANSPORTER, BUT CAN TRANSPORT THE DNA-INTERCALATING DYES ETHIDIUM BROMIDE AND RHODAMINE-6G

3.1 Background

The RND efflux pump, EefABC, is highly conserved in strains of *E. coli* commonly associated with infection. This chapter explores, through susceptibility testing, the hypothesis that the pump has a role in the antimicrobial resistant nature of such strains. Compounds from a range of different classes of antibiotics were selected because they had been mentioned previously in literature as substrates of either EefABC in *E. aerogenes*, or AcrB in *E. coli*. In previous studies, an *E. coli* strain with a plasmid containing the RND pump AcrAB demonstrated decreased susceptibility to DNA-intercalating dyes EtBr and R6G, as well as being responsible for the transport of a wide range of antibiotic classes including chloramphenicols, tetracyclines, quinolones, macrolides, and β-lactams (Nishino and Yamaguchi, 2001; Alav *et al.*, 2021). EefABC has been identified in strains of *E. aerogenes* that have developed resistance to quinolones (Mallea *et al.*, 1998) (ciprofloxacin and moxifloxacin were used in this study), chloramphenicol, erythromycin and ticarcillin (Masi, Pagès and Pradel, 2006). In *E. cloacae*, overexpression of *eefABC* was found to increase MICs of the compounds erythromycin and ethidium bromide (Guérin *et al.*, 2016).

Polymyxin B is a lipopeptide (polypeptide) antibiotic isolated from *Bacillus polymyxa* that interacts with and disrupts the LPS of the outer membrane of Gram-negative

bacteria, leading to cell death (Zavascki *et al.*, 2007). This was included in some experiments due to the difference in origin and mechanism from other antibiotics.

3.2 Aims

- Investigate susceptibility to a range of antimicrobials, dyes, and metals as potential substrates of the Eef complex to determine efflux substrates.
- To further investigate the proposed substrates identified through MIC data by measuring growth kinetics, to generate more sensitive data, before using an assay to measure active efflux.

3.3 Hypothesis

- EefABC can transport clinically relevant antimicrobial compounds in *E. coli*.

3.4 Initial characterisation of strains

All strains used in this study (table 2) (except for MG1655 + pET21a:*eefABC* + pACYC177:*eefD*) were taken from long-term storage at -80°C since they had been used in the lab previously. Strains containing an antibiotic marker were characterised by selective plating on agar containing the antibiotic to confirm resistance. Strain identity was checked using PCR followed by gel electrophoresis to ensure that they had the correct genetic modification (gene deletion/ overexpression).

3.4.1 Creation of an *E. coli* gain of EefABCD function strain

To create a strain of *E. coli* with a gain of function of the both the EefABC and EefD efflux pumps, *E. coli* MG1655 strain (which does not naturally encode the *eef* operon on the chromosome) was transformed with plasmids encoding the RND pump EefABC and the MFS pump EefD (MG1655 + pET21a:*eefABC* + pACYC177:*eefD*).

To do this, the pACYC177:*eefD* plasmid was isolated and transformed into electrocompetent MG1655 cells which already contained the pET21a:*eefABC* plasmid. The final product was plated onto LB agar containing carbenicillin and kanamycin to select for both plasmids. Colonies grown from this culture were checked using PCR to amplify the *eefABCD* genes. Amplified PCR products from the new strain are visible on the gel image (figure 11) and predicted PCR band sizes are shown in Table 7.

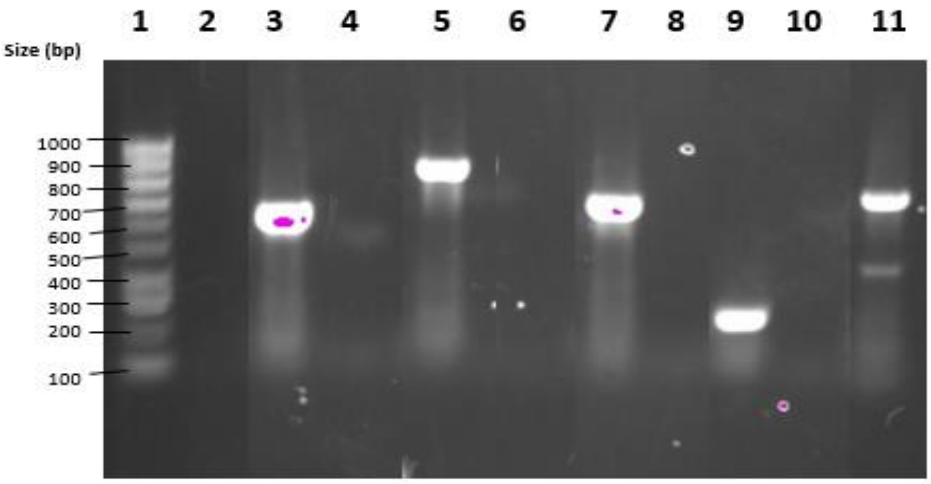

Figure 11. Gel electrophoresis of PCR results for the amplification of *eefA*, *eefB, eefC, eefD and acrB* on 1% agarose gel and 1XTAE, to show successful transformation. Lanes are as follows: 1) hyperladder 100bp, 2) *eefA* negative control, 3) *eefA* MG1655 + pET21a:*eefABC* + pACYC177:*eefD*, 4) *eefB* negative control, 5) *eefB* MG1655 + pET21a:*eefABC* + pACYC177:*eefD*, 6) *eefC* negative control, 7) *eefC* MG1655 + pET21a:*eefABC* + pACYC177:*eefD*, 8) *eefD* negative control, 9) *eefD* MG1655 + pET21a:*eefABC* + pACYC177:*eefD*, 10) *acrB* negative control, 11) *acrB* MG1655 + pET21a:*eefABC* + pACYC177:*eefD*.

Table 7. Predicted sizes (and position of the band) of the amplified gene products.

Gene product	Size of product (base pairs)
eefA	594
eefB	845
eefC	694
eefD	304
acrB	822

The strain produced the correct bands for all genes amplified confirming successful transformation of *E. coli* MG1655 with *eefABC* and *eefD*. Negative controls in lanes 2, 4, 6, 8 and 10 produced no bands. MG1655 + pET21a:*eefABC* + pACYC177:*eefD* produced an *eefA* band between 500-600 bp in lane 3, an *eefB* band at 800-900 bp in lane 5, and an *eefC* band at 600-700 bp in lane 7. There was a band at 300-400 bp in lane 9 for *eefD*, indicating that the transformation was successful. The band at 800-900 bp in lane 11 indicated the presence of *acrB*. This new strain was added to the culture collection.

3.4.2 Growth kinetics of *E. coli* strains in LB broth

The growth kinetics of all strains was measured to see if gain or loss of *eef* genes altered the growth rate of *E. coli* in LB broth. Loss of EefABC function strains and gain of EefABC function strains were incubated for 12 hours in LB broth and the OD_{600nm} was measured every 10 minutes and the generation time calculated (Materials and Methods 2.9). Data produced would be used throughout the project as the standard growth rate and generation time of each strain in LB media.

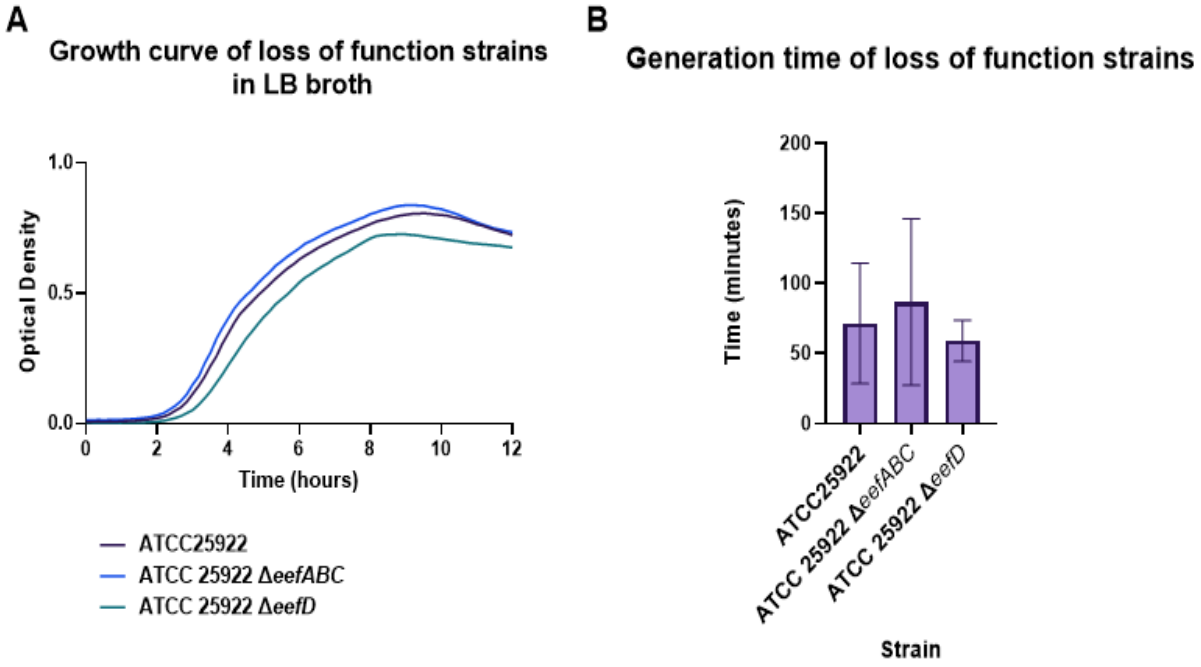

Figure 12. Growth kinetics of loss of function *E. coli* strains in LB broth.
Panel A) growth curves of loss of function *E. coli* strains (measure of optical density at 600 nm over a 12-hour period). Panel B) Generation time of loss of function strains. Each data point is an average of 3 biological repeats, error bars of standard deviation to show (3 technical repeats per biological repeat).

There was no statistically significant difference in growth between the wildtype ATCC 25922 and the loss of EefABCD function strains.

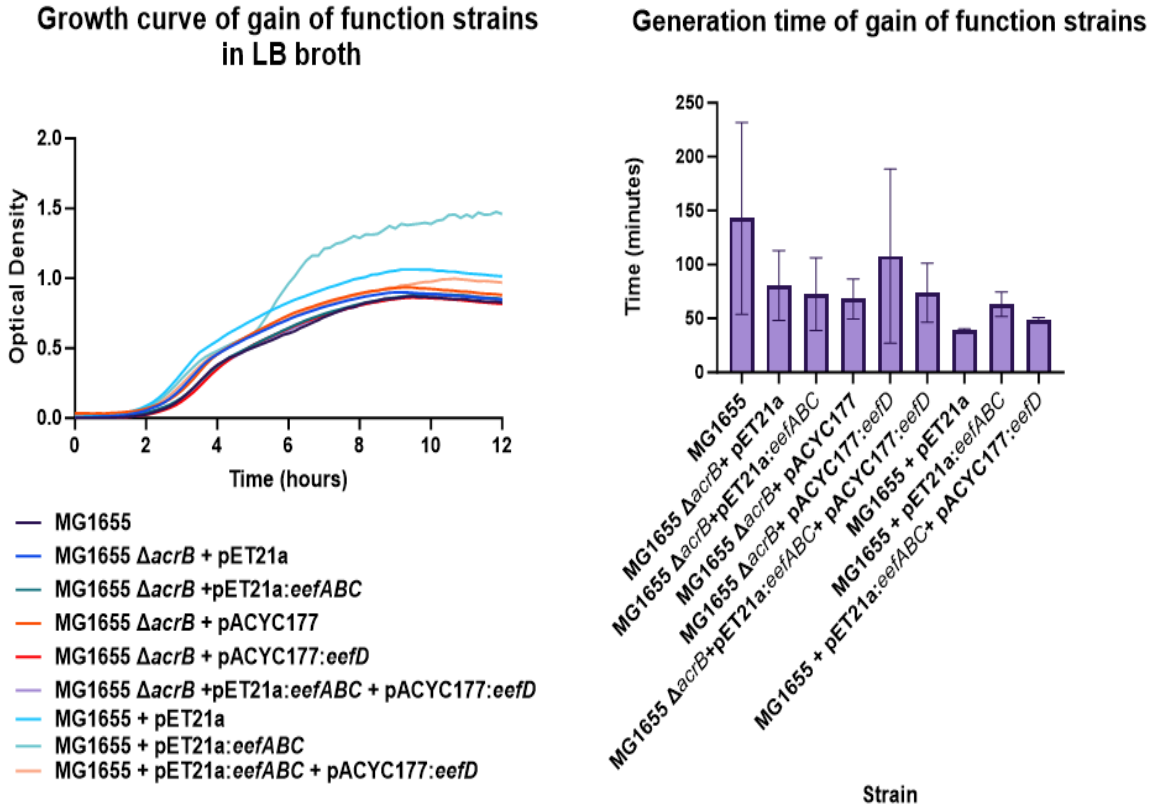

Figure 13. Growth kinetics of gain of function *E. coli* strains in LB broth. Panel A) growth curves of gain of function *E. coli* strains (measure of optical density at 600 nm over a 12-hour period). Panel B) Generation time of gain of function strains. Each data point is an average of 3 biological repeats, error bars of standard deviation to show (3 technical repeats per biological repeat).

There was no significant difference between the growth curves of knockout strains compared to the parent strains, or the wildtype MG1655 (Panel A), except for MG1655 + pET21a:*eefABC*, which appeared to enter a secondary log phase later than the other strains and grew to a higher optical density. The reason for this remains unclear but this surprising growth pattern was consistent over 3 biological

repeats, each performed on different days. Generation times of the strains were similar throughout.

3.5 Growth assays and susceptibility tests to identify potential substrates of EefABC

Many RND pumps transport antibiotics (see Introduction 1.5.1) so the ability of EefABC to transport clinically relevant antibiotics was tested. MICs of antibiotics of different classes were measured to see whether susceptibility to the drugs was affected by either gain or loss of EefABC/D function.

3.5.1 Agar dilution MIC results

For this agar MIC experiment, a range of antibiotics from different classes was selected, along with dyes and metals.

Table 8. Agar dilution MIC results.

MIC is the lowest concentration of an antibiotic or dye that is required to inhibit the visible growth of bacteria. MIC units are µg/mL.

Strain	CIP	ERY	ETBR	GEN	MER	MOX	TET	CHL	NOV	COB
ATCC 25922	0.03	64	256	0.5	0.03	0.06	1	4	512	512
ATCC 25922 Δ*eefABC*	0.03	64	256	0.5	0.03	0.03	1	4	256	512
ATCC 25922 Δ*eefD*	0.03	64	256	0.5	0.015	0.06	2	8	256	512
MG1655	0.03	64	512	0.25	0.03	0.06	2	8	>512	512
MG1655 Δ*acrB* + pET21a	0.03	2	8	0.12	0.03	0.015	0.5	1	16	512
MG1655 Δ*acrB* + pET21a:*eefABC*	0.03	**64**	**256**	0.5	0.03	0.06	1	2	32	512
MG1655 Δ*acrB* + pACYC177	0.03	4	8	0.12	0.03	0.015	0.5	1	32	512
MG1655 Δ*acrB* + pACYC177:*eefD*	0.03	4	8	0.12	0.03	0.015	0.5	1	32	512
MG1655 Δ*acrB* +pET21a:*eefABC* + pACYC177:*eefD*	0.03	**64**	**256**	0.5	0.03	0.06	1	2	32	512

CIP ciprofloxacin, ERY erythromycin, ETBR ethidium bromide, GEN gentamicin, MER meropenem, MOX moxifloxacin, TET tetracycline., CHL chloramphenicol, NOV novobiocin, COB cobalt.

A fold change greater than two is highlighted in grey.

Deletion of *eefABC* or *eefD* in *E. coli* strain ATCC 25922 did not alter susceptibility to any of the compounds tested. A reason for this might be that because AcrB is still functional in the loss of EefABC function strains, any EefB activity might have been masked.

Gain of EefABC/D function strains did not alter susceptibility to compounds ciprofloxacin, gentamicin, meropenem, moxifloxacin, tetracycline, chloramphenicol, novobiocin or cobalt, suggesting that they are not substrates of the efflux pump.

For reference, the Δ*acrB* knockout strains (EC99 and EC219) had lower MICs than the wildtype MG1655 (EC07) for nearly all the compounds tested. For a compound to be considered as a substrate of EefB, the MICs of gain of EefABC function strains should be higher than those of the Δ*acrB* knockout strains.

In the presence of erythromycin, the MICs for Δ*acrB* knockout strains (EC99 and EC219) were 2 µg/mL and 4 µg/mL respectively. With the overexpression of *eefABC* (EC371), or *eefABCD* (EC413), MICs increased to 64 µg/mL. This suggests that overexpression of *eefABC*, with and without overexpression of *eefD*, was able to reduce susceptibility of *E. coli* to the antimicrobial erythromycin.

In the presence of EtBr, the MICs for Δ*acrB* knockout strains (EC99 and EC219) were both 8 µg/mL. With the addition of *eefABC*, or *eefABC* and *eefD*, MICs increased to 256 µg/mL. This suggests that overexpression of *eefABC*, with and without overexpression of *eefD*, could reduce susceptibility of *E. coli* to the toxic dye EtBr.

Gain of EefD function did not alter MIC results for any of the compounds tested and no additional MIC change increase was observed when *eefD* was overexpressed

with *eefABC*, compared to when just *eefABC* was overexpressed. This suggests that the MFS (EefD) pump was not involved in the transportation of these compounds.

MIC data concluded that gain of EefABC function decreased susceptibility of *E. coli* to the antibiotic erythromycin, and the dye EtBr suggesting these are substrates of the pump.

3.5.2 Broth dilution MIC results

The broth dilution method was used to gather MIC data for individual compounds, since this was much faster than using the agar dilution method. Polymyxin B is from a class of antibiotics called “polypeptides” (Zavascki *et al.*, 2007) and these have different mechanisms of action to the other antimicrobials tested previously, so it was interesting to see whether deletion or expression of *eefABC* affected susceptibility.

Table 9. Broth dilution MIC results for the polypeptide antibiotic Polymixin B.

MIC is the lowest concentration of an antibiotic or dye that is required to inhibit the visible growth of bacteria. MIC units are µg/mL.

Strain	Polymixin B
ATCC25922	0.5
ATCC 25922 Δ*eefABC*	0.5
ATCC 25922 Δ*eefD*	0.5
MG1655	0.5
MG1655 Δ*acrB* + pET21a	1
MG1655 Δ*acrB* +pET21a:*eefABC*	0.5
MG1655 Δ*acrB* + pACYC177	0.5
MG1655 Δ*acrB* + pACYC177:*eefD*	0.5
MG1655 Δ*acrB* +pET21a:*eefABC* + pACYC177:*eefD*	0.5

There was no difference in MICs for loss of EefABC function or gain of EefABC function strains of the antimicrobial peptide polymyxin B, suggesting that polymyxin B is not a substrate of the efflux pump.

3.5.3 EefABC does not transport the antibiotic erythromycin

The MIC results showed that susceptibility of *E. coli* to the macrolide antibiotic erythromycin decreased when EefABC was expressed (Table 8), suggesting that erythromycin could be a substrate of the pump. To further investigate whether erythromycin was a substrate of the pump, growth kinetics in the presence of 2

µg/mL erythromycin were measured to determine whether there was a difference in growth rate of *E. coli* in loss of EefABC function strains and gain of EefABC function strains. This concentration was chosen because this was the MIC of erythromycin for the *acrB* knockout strain. For this experiment, it was hypothesised that gain of EefABC function strains would be able to grow better in this concentration than the *acrB* knockout strains, if EefB was able to transport erythromycin, thus producing a similar growth pattern to the wildtype (MG1655), which encodes AcrB.

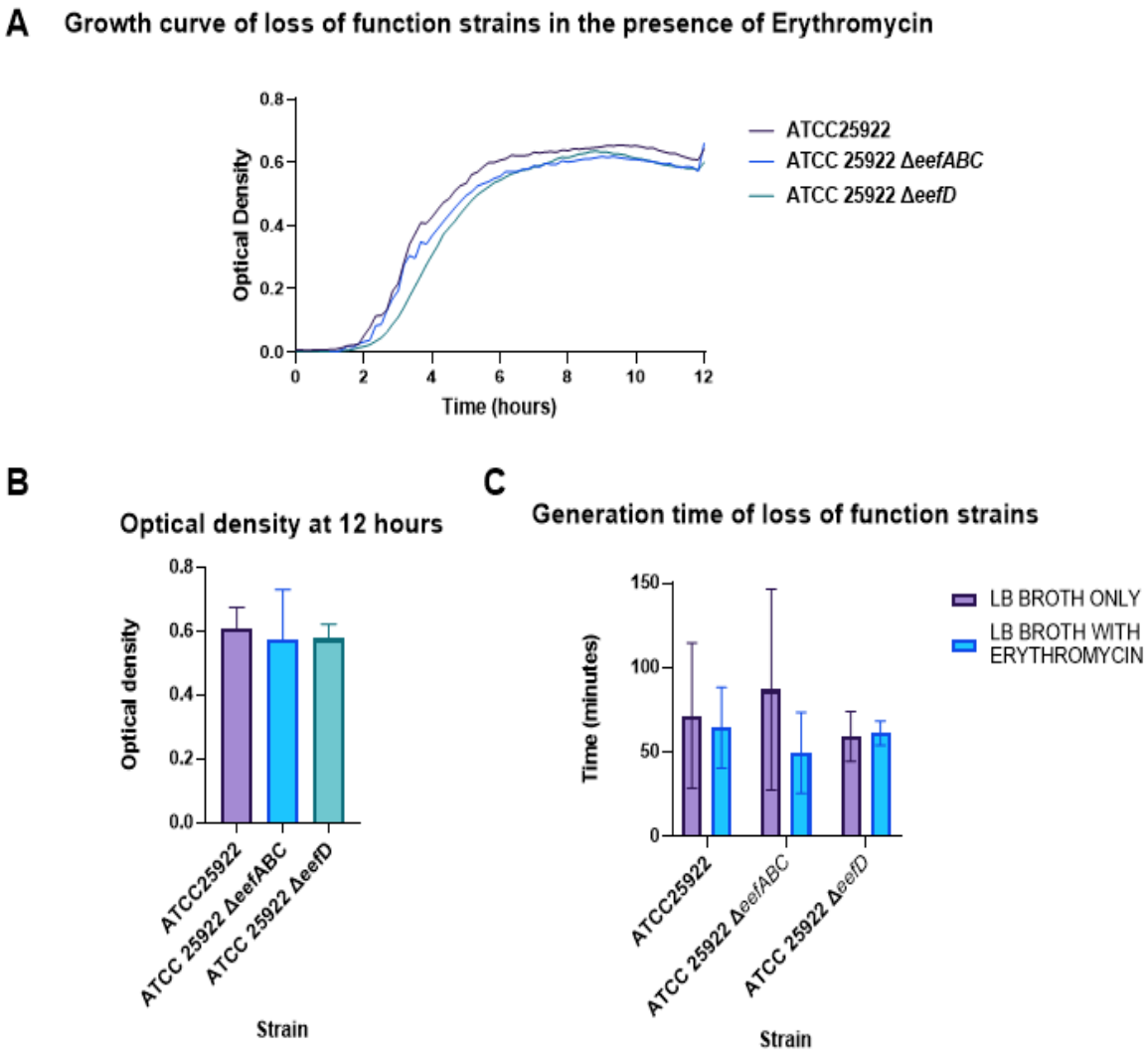

Figure 14. Growth kinetics of loss of function *E. coli* strains in the presence of 2 µg/mL erythromycin. Panel A) growth curves of loss of function *E. coli* strains (measure of optical density at 600 nm over a 12-hour period). Panel B) Comparison of optical density after 12 hours between loss of function strains. This is the final OD measurement taken at 12 hours. Panel C) mean generation time of loss of function *E. coli* strains. Each data point is an average of 3 biological repeats, error bars of standard deviation to show (3 technical repeats per biological repeat). Level of significance between end points has been calculated using the one-way-anova

analysis. Level of significance between generation time has been calculated using the two-way-anova analysis. Significance at $P \leq 0.05$ marked with an asterisk.

There was no observable difference in growth curves, or a significant difference in generation time between the *eefABC* and *eefD* knockout strains and the wildtype, ATCC 25922 (Figure 14. Panels A and C). Panel B shows that there was no significant difference between the end points of each strain, showing that the loss of EefABC/D strains both grew to the same optical density as the wildtype. Loss of EefABC/D function strains did not alter growth of *E. coli* in the presence of erythromycin.

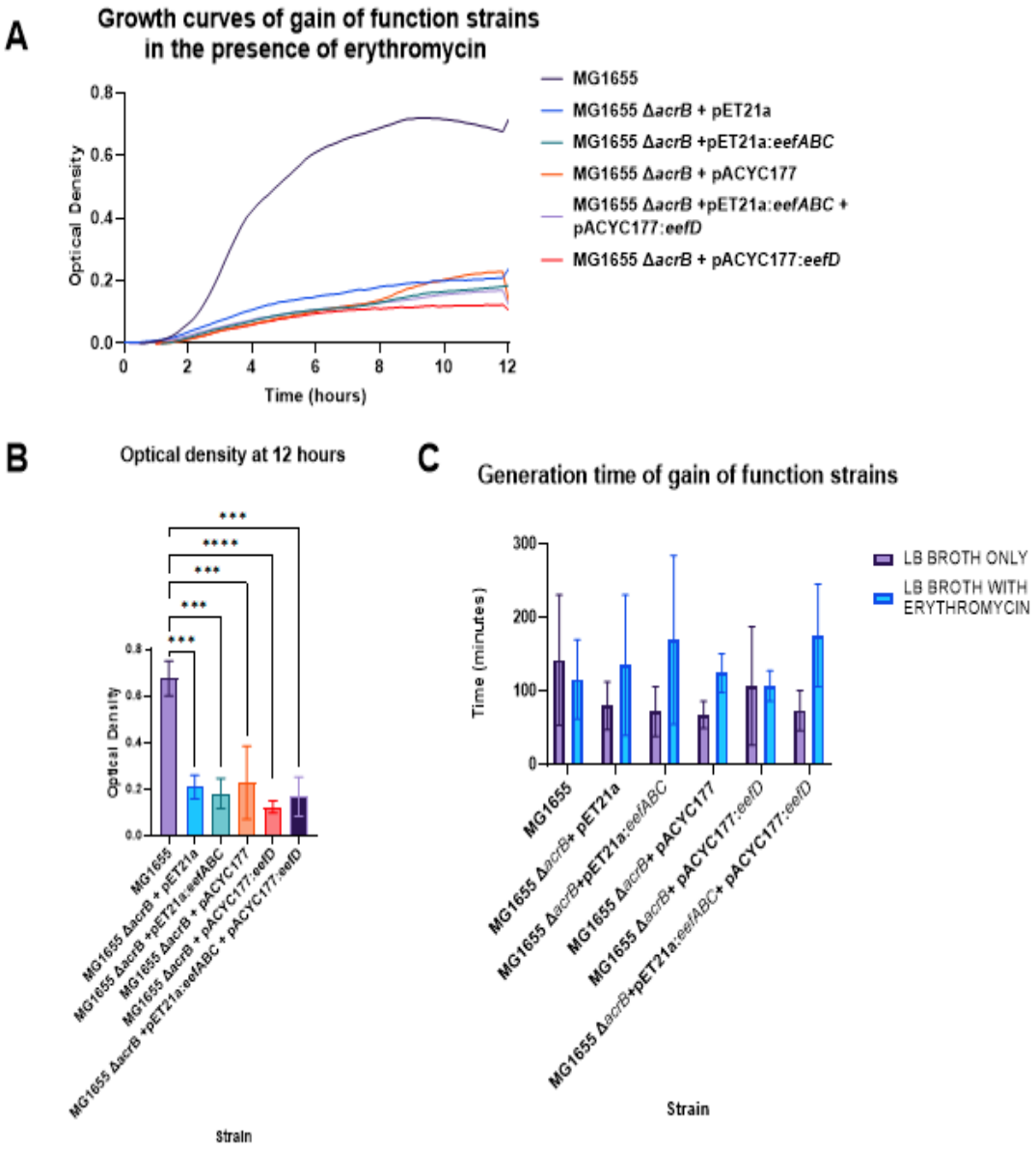

Figure 15. Growth kinetics of gain of function *E. coli* strains in the presence of 2 µg/mL erythromycin. Panel A) growth curves of gain of function *E. coli* strains (measure of optical density at 600 nm over a 12-hour period). Panel B) Comparison of optical density after 12 hours between gain of function strains. This is the final OD measurement taken at 12 hours. Panel C) mean generation time of gain of function *E. coli* strains. Each data point is an average of 3 biological repeats, error bars of

standard deviation to show (3 technical repeats per biological repeat). Level of significance between end points has been calculated using the one-way-anova analysis. Level of significance between generation time has been calculated using the two-way-anova analysis. Significance at $P \leq 0.05$ is marked with an asterisk.

Growth of all *ΔacrB* mutant strains was slower than the wildtype in the presence of erythromycin, which makes sense because erythromycin is a substrate of AcrB, and therefore removing this pump should lead to an increase in intracellular accumulation of the antibiotic, therefore limiting growth. Overexpression of *eefABC/D* in the absence of *acrB* did not compensate for the loss of AcrB. The optical density at 600 nm measured after 12 hours, is displayed in Panel B. This figure shows that there was a significant decrease in the end point measurements from the wildtype to all strains lacking AcrB and shows that expression of Eef proteins did not help the strains lacking AcrB reach a higher end point in the presence of erythromycin. Panel C shows that in *ΔacrB* mutants, regardless of whether *eefABC* or *eefD* were overexpressed, generation time of *E. coli* cells increased, though this was not statistically significant. Gain of EefABC/D function strains did not grow better in the presence of erythromycin.

3.5.4 Agar MIC to confirm previous erythromycin MIC data

Another agar dilution MIC was carried out to see whether the pattern for erythromycin could be repeated. Azithromycin was also tested because it is a member of the macrolide class of antibiotics, like erythromycin.

Table 10. Agar dilution MIC results of macrolide antibiotics erythromycin and azithromycin.

MIC is the lowest concentration of an antibiotic or dye that is required to inhibit the visible growth of bacteria. MIC units are µg/mL.

Strain	Erythromycin	Azithromycin
ATCC25922	64	8
ATCC 25922 Δ*eefABC*	64	8
ATCC 25922 Δ*eefD*	128	8
MG1655	64	4
MG1655 Δ*acrB* + pET21a	16	1
MG1655 Δ*acrB* +pET21a:*eefABC*	8	1
MG1655 Δ*acrB* + pACYC177	32	2
MG1655 Δ*acrB* + pACYC177:*eefD*	16	1
MG1655 Δ*acrB* +pET21a:*eefABC* + pACYC177:*eefD*	8	1

Deletion of *eefABC* or *eefD* did not alter susceptibility to either of the compounds tested, perhaps because AcrB is still functional in these strains and masking EefB activity.

With regards to analysing gain of EefABC function data: the Δ*acrB* knockout strains had lower MICs than the wildtype MG1655 for nearly all the compounds tested. For a compound to be considered as a substrate of EefB, the MICs of gain of EefABC function strains should be higher than those of the Δ*acrB* knockout strains.

When *eefABC* or *eefABC* and *eefD* were overexpressed, MICs did not increase in comparison of the Δ*acrB* knockout strains, in the presence of either erythromycin or azithromycin, suggesting that neither are substrates of the pump.
The reason behind the obvious difference in previous MIC results remains unclear, but together with these MIC results and growth kinetics in erythromycin, it was concluded that this antimicrobial compound is not a substrate of EefABC.
At this point, during this project and other projects in the Blair lab, no antibiotics have been identified as substrates of the EefB RND pump in *E. coli*.

3.6 EefABC can transport ethidium bromide

3.6.1 Growth of cells in the presence of ethidium bromide

From MIC results (table 8), it was concluded that susceptibility of *E. coli* to the DNA-intercalating dye EtBr decreased when EefABC was overexpressed. Growth kinetics were measured to determine whether there was a difference in growth of *E. coli* in the presence of 8 µg/mL EtBr in loss of EefABC function strains and gain of EefABC function strains. This concentration was chosen because this was the MIC of EtBr for

the *acrB* knockout strain, which should theoretically grow worse under these conditions than the AcrB encoding wildtype (MG1655) and gain of EefABC function strains. Restoration of the phenotype by gain of EefABC function strains would then support the hypothesis that EtBr is a substrate of EefB.

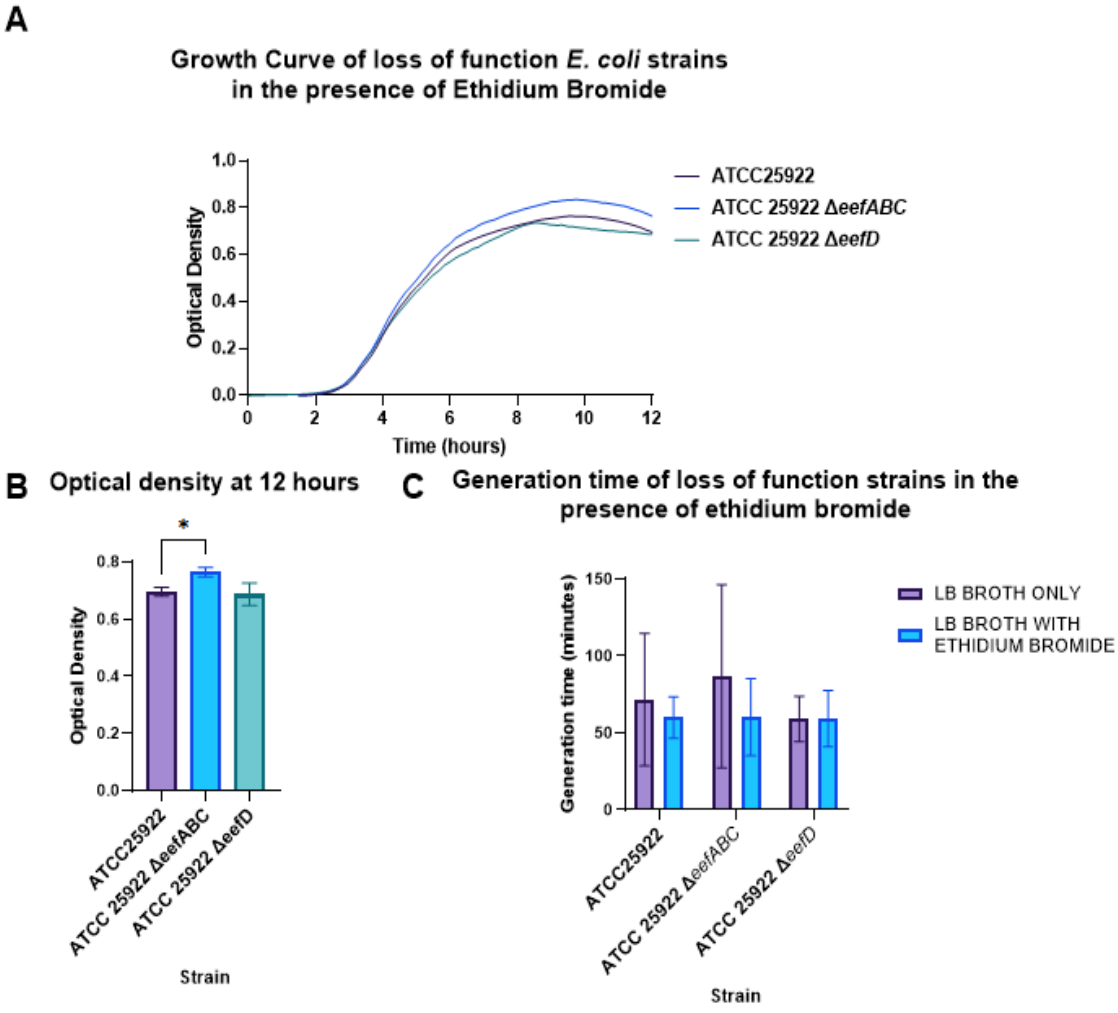

Figure 16. Growth kinetics of loss of function *E. coli* strains in the presence of 8 µg/mL ethidium bromide. Panel A) growth curves of loss of function *E. coli* strains (measure of optical density at 600 nm over a 12-hour period). Panel B) Comparison of optical density after 12 hours between loss of function strains. This is the final OD measurement taken at 12 hours. Panel C) mean generation time of loss of function *E. coli* strains. Each data point is an average of 3 biological repeats, error bars of

standard deviation. Level of significance between end points has been calculated using the one-way-anova analysis. Level of significance between generation time has been calculated using the two-way-anova analysis. Significance at $P \leq 0.05$ is marked with an asterisk.

The growth curves for the *eefABC* and *eefD* deleted strains and the wildtype were similar (Panel A). There was a significant difference between the end point of the wildtype and the loss of EefABC function strain (Panel B), however, the final OD for the knockout strain was higher than the wildtype. This was an unexpected difference because if EefABC could assist with efflux of EtBr, and therefore increase survival of the bug in the presence of EtBr, the loss of EefABC function strain should grow worse than the other strains.

In the wildtype ATCC 25922, the generation time of cells in the presence of EtBr was the same as cells grown in LB broth without EtBr (Panel C). The generation times of the loss of EefABC function strain and loss of EefD function strain were not significantly different from wildtype, suggesting that the absence of the EefABC or EefD pumps did not affect growth.

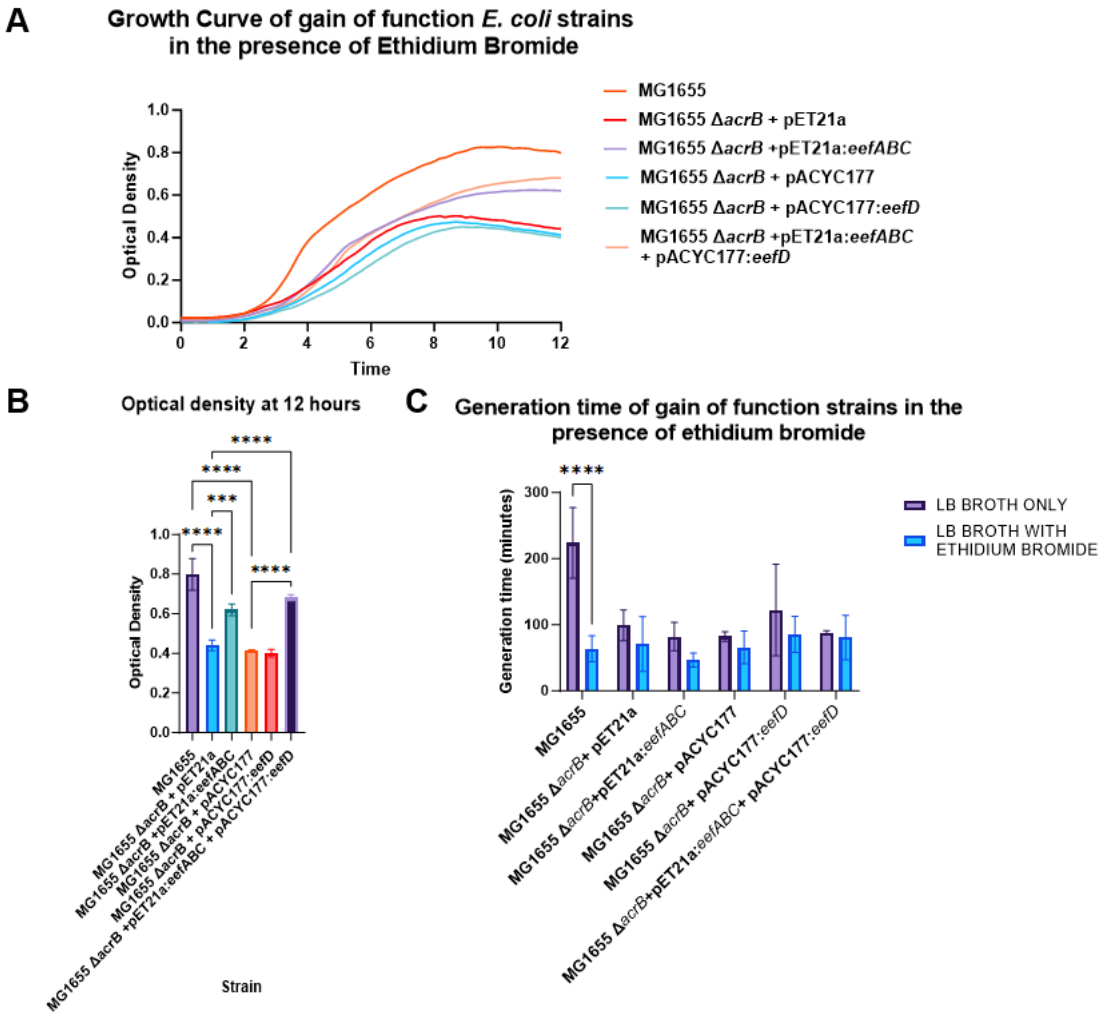

Figure 17. Growth kinetics of gain of function *E. coli* strains in the presence of 8 µg/mL ethidium bromide. Panel A) growth curves of gain of function *E. coli* strains (measure of optical density at 600 nm over a 12-hour period). Panel B) Comparison of optical density after 12 hours between gain of function strains. This is the final OD measurement taken at 12 hours. Panel C) mean generation time of gain of function *E. coli* strains. Each data point is an average of 3 biological repeats, error bars of standard deviation to show (3 technical repeats per biological repeat). Level of significance between end points has been calculated using the one-way-anova analysis. Level of significance between generation time has been calculated using the two-way-anova analysis. Significance at P ≤ 0.05 is marked with an asterisk.

Deletion of *acrB* in MG1655 decreased growth in the presence of EtBr (figure 17 panel A). Gain of EefABC function strains grew significantly better in the presence of EtBr than the *acrB* knockout strains, reaching a higher optical density after 12 hours of growth (figure 17 panel B). Gain of EefABC function strains grew significantly worse than the wildtype strain, suggesting only a partial restoration of phenotype. There was a stronger significant increase in optical density at 12 hours for the gain of EefABC and EefD function strain, than for the gain of EefABC function strain. This suggested that cooperation of EefABC and EefD allows cells to grow better in ethidium bromide than when they work alone.

Generation time (panel C) of the gain of EefABC function strain was quicker than strains which didn't encode the protein. Strains transformed with a pACYC177 plasmid had longer generation times than strains with a pET21a plasmid when grown in ethidium bromide, and the reason for this is unknown.

When only *eefD* was overexpressed, growth was the same as the *acrB* deleted strains, with no significant difference in optical density after 12 hours (panel B) between the gain of EefD function strain and the *acrB* knockout strains. Generation time (panel C) of this strain was the slowest, suggesting that EefD does not increase growth in EtBr.

3.6.2 Accumulation of intracellular ethidium bromide

The MIC and growth kinetics data put forward EtBr as a potential substrate of the EefB RND pump. Therefore, the level of intracellular EtBr was measured over time to determine whether strains with a functioning EefABC efflux system would accumulate less intracellular EtBr than strains without the pump.

Cells were incubated with EtBr for 1 hour and the level of intracellular EtBr was measured continually to produce a curve of fluorescence, where the level of fluorescence is directly related to the amount of intracellular EtBr. If EefABC transported EtBr out of the cell, the final amount (or fluorescence) of intracellular EtBr in gain of EefABC function strains should be significantly less than that of *acrB* knockout strains which have no active efflux system. To measure this, fold-change was calculated which compares the end point of all strains to the wildtype (the wildtype MG1655 therefore had a fold-change of 1.0)

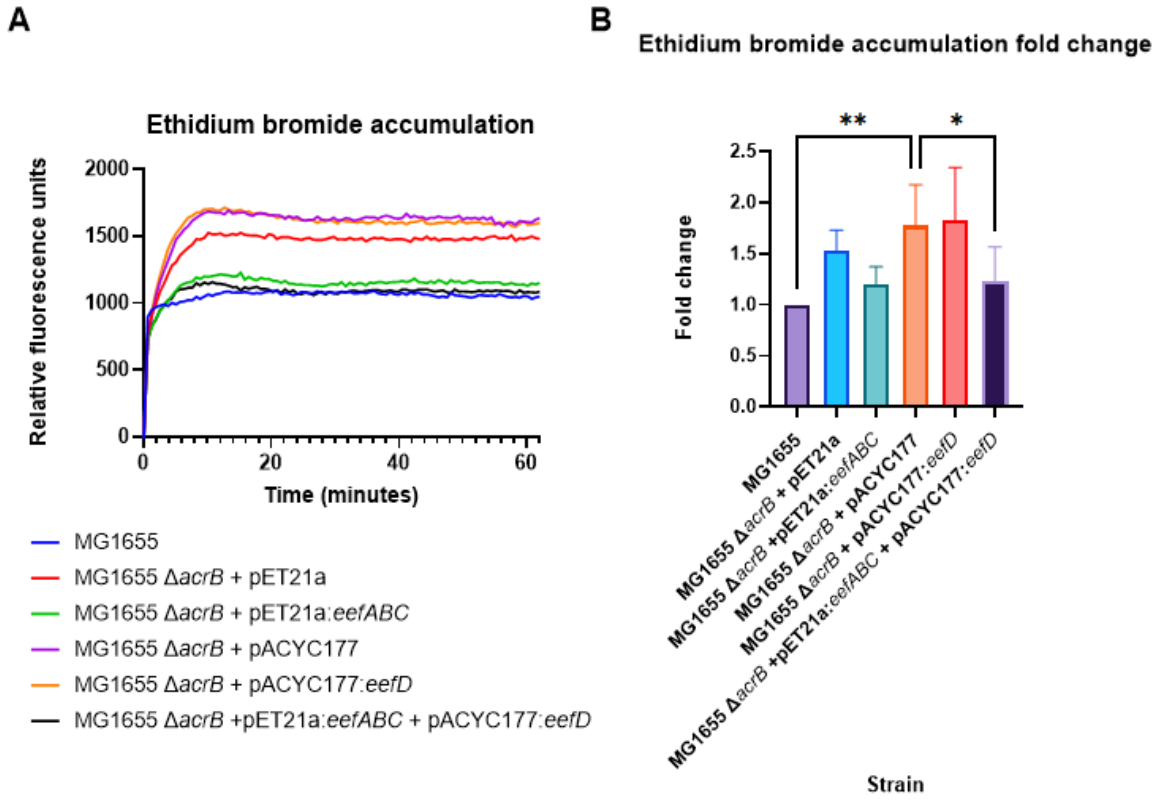

Figure 18. Ethidium bromide accumulation assay for gain of function *E. coli* strains. Panel A) Accumulation of ethidium bromide inside cells over time. Panel B) Fold-change which compares the end point of all strains to the wildtype. Level of significance has been calculated using one-way-Anova analysis. Each data point is an average of 3 biological repeats, error bars of standard deviation to show (3

technical repeats per biological repeat). Significance at $P \leq 0.05$ is marked with an asterisk.

Panel A displays curves which represent the accumulation of intracellular EtBr over time, with a higher level of fluorescence relating to a higher internal concentration of EtBr. Most of the accumulation occurred within the first 10 minutes. Deletion of *acrB* in MG1655 resulted in more accumulation of intracellular EtBr over time. The fluorescence curve in panel A shows that the gain of EefABC function strain accumulated less EtBr than the *acrB* knockout strain, though this was not found to be significant. The gain of EefABC and EefD function strain accumulated significantly less intracellular EtBr than the *acrB* knockout strain, which suggests that the RND pump, EefB, is better able to prevent accumulation of EtBr when EefD is also encoded for. The gain of EefD function strain did not accumulate less EtBr than the *acrB* knockout strain, suggesting that overexpression of this pump could not compensate for the loss of AcrB. Overexpression of *eefABC* was linked to decreased intracellular accumulation of the toxic dye, EtBr, inside *E. coli* cells suggesting that EtBr is transported by the pump.

3.6.3 Efflux of EtBr out of cells

The evidence up to this point suggested that EtBr is a substrate of the EefABC efflux pump. While this is clearly not a natural substrate of the system, it is useful as it allows us to directly measure rate of efflux. An efflux assay was carried out to prove that the pump was active. Cells were incubated with CCCP to inhibit efflux and EtBr to allow for accumulation. Following washing to remove extracellular EtBr, glucose was injected into the culture to reenergise and restart the pumps. The amount of intracellular EtBr was measured over 2 hours.

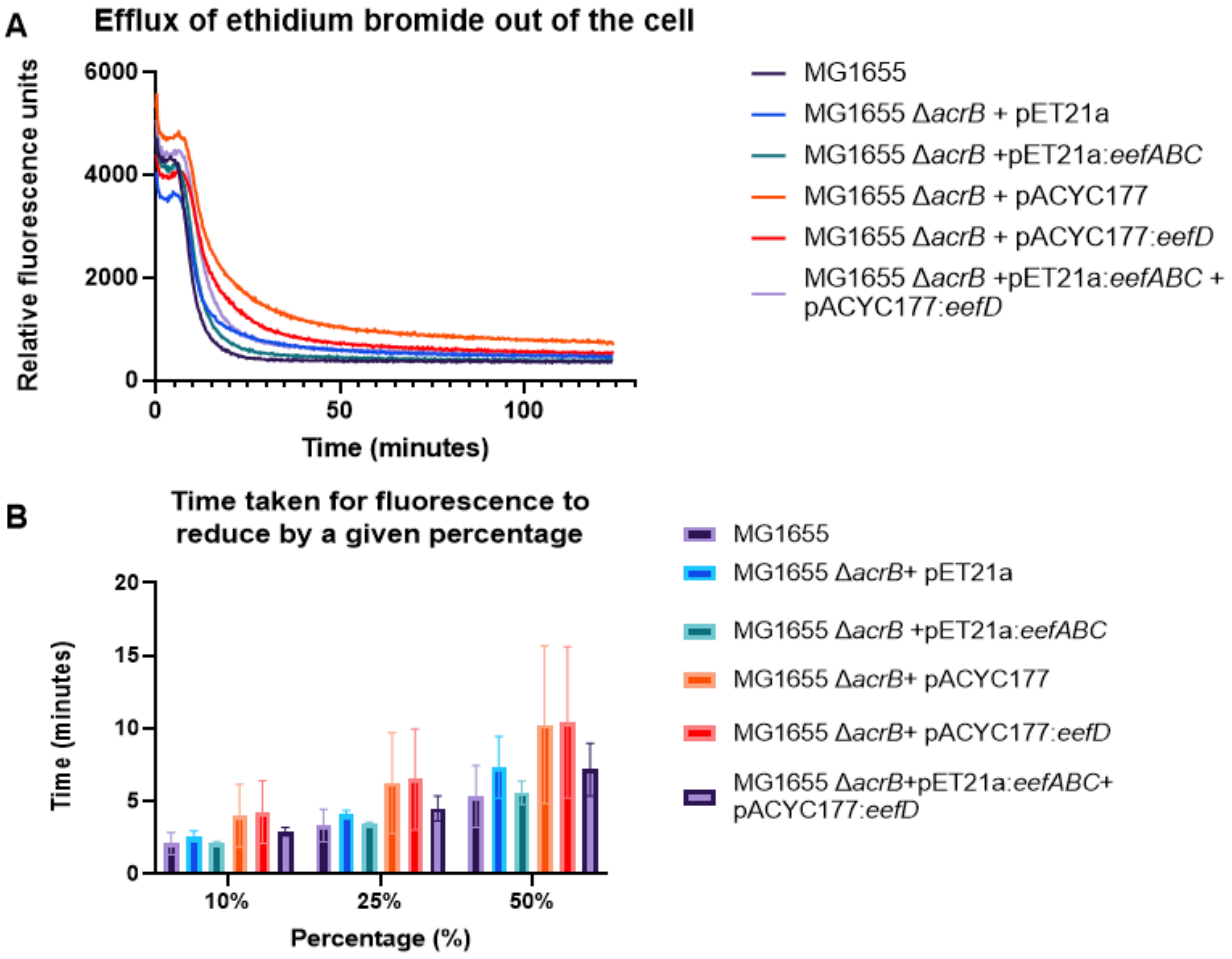

Figure 19. Ethidium Bromide efflux assay for gain of EefABC function *E. coli* strains. Panel A) fluorescence measured over time relating to the amount of ethidium bromide inside the cell. Panel B) The time taken for the volume of ethidium bromide inside the cell to decrease by 10%, 25% and 50%. Level of significance was calculated using 2-way-anova analysis. Data points are the average of 3 biological repeats, error bars of standard deviation to show. Significance at $P \leq 0.05$ is marked with an asterisk, however, none of the results were statistically significant.

The graph in Panel A shows decreasing fluorescence as EtBr is pumped out of the cell. Curves of the strains MG1655 Δ*acrB* +pET21a:*eefABC* and MG1655 Δ*acrB* +pET21a:*eefABC* + pACYC177:*eefD* appeared to be closest to that of MG1655

wildtype. The strains shown to have a higher end point were MG1655 Δ*acrB* + pET21a, MG1655 Δ*acrB* + pACYC177 and MG1655 Δ*acrB* + pACYC177:*eefD,* which all lacked *eefABC*.

Panel B shows the time taken for EtBr to be transported out of the cell. The most notable differences were in the time it took for EtBr levels to be reduced by 50%. It took less than 6 minutes for the wildtype MG1655 strain to reduce internal EtBr levels by 50%. When AcrB wasn't present, this time increased to 7 minutes for the pET21a vector and to 10 minutes for the pACYC177 vector. When the pET21a vector had a gene which expressed *eefABC* production, the time to get to 50% was reduced to 6 minutes, similar to the wildtype which encoded AcrB. The strain with both plasmids which expressed *eefABC* and *eefD* decreased EtBr levels by 50% in less than 8 minutes, which isn't as low as wildtype phenotype but was lower than its parent strains. When *eefD* alone was expressed, it took longer for EtBr levels to drop by 50%. These differences were not statistically significant, though slight differences were notable and linked expression of EefABC with increased efflux of intracellular EtBr. Calculation of percentage reduction of internal EtBr showed that the strains which overexpressed *eefABC* or *eefABCD* were able to transport EtBr out of the cell more quickly than the strains which didn't encode any of the proteins, or the MFS transporter alone.

Efflux data combined with accumulation data provided evidence that the pump was active in transporting intracellular EtBr.

3.7 EefABC can transport rhodamine-6G

3.7.1 Growth of cells in the presence of R6G

R6G is a fluorescent dye which binds to DNA, similarly to EtBr (Al Masum *et al.*, 2016). Because of this similarity, growth kinetics were measured to determine whether there was a difference in growth of *E. coli* in the presence of 8 µg/mL R6G in loss of EefABC function strains and gain of EefABC function strains.

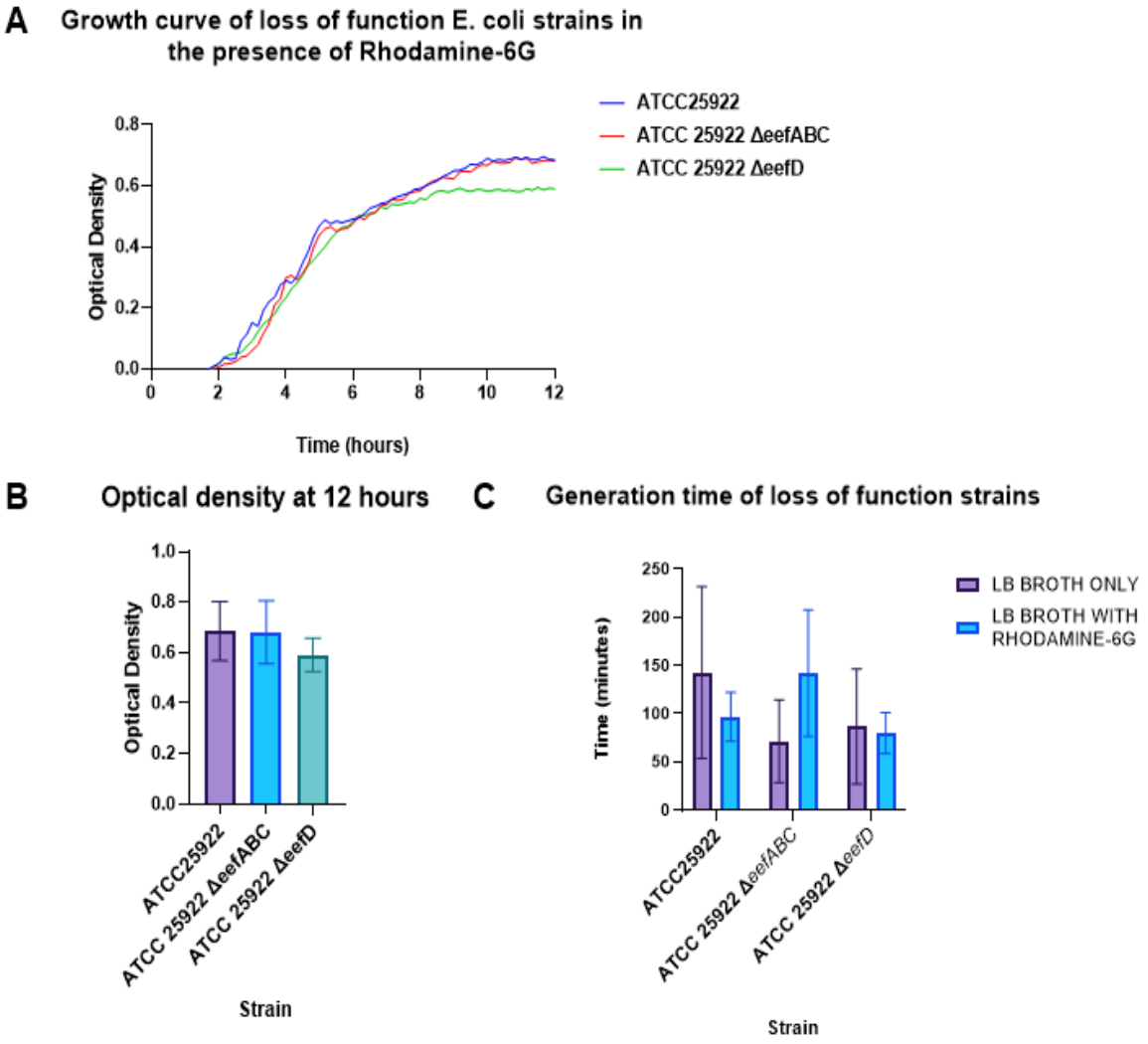

Figure 20. Growth kinetics of loss of function *E. coli* strains in the presence of 8 µg/mL rhodamine-6G. Panel A) growth curves of loss of function *E. coli* strains (measure of optical density at 600 nm over a 12-hour period). Panel B) Comparison of optical density after 12 hours between loss of function strains. This is the final OD measurement taken at 12 hours. Panel C) mean generation time of loss of function *E. coli* strains. Each data point is an average of 3 biological repeats, error bars of standard deviation to show (3 technical repeats per biological repeat). Level of significance between end points has been calculated using the one-way-anova analysis. Level of significance between generation time has been calculated using

the two-way-anova analysis. Significance at $P \leq 0.05$ is marked with an asterisk, however, none of the results were statistically significant.

Growth curves of ATCC 25922 Δ*eefABC and* ATCC 25922 Δ*eefD* were similar to those of ATCC 25922 (figure 20 Panel A), which is the parent strain for the loss of EefABC function strains. There was no significant difference between the final optical density measured after 12 hours of any strains meaning that the loss of EefABC function strain did not grow less than the wildtype in the presence of R6G (figure 20 Panel B). Generation time of ATCC 25922 Δ*eefABC* was slower than the other strains, though this was not a significant difference. Generation time did not increase for the loss of EefD function strain (Panel C). No conclusions can be drawn about the ability of EefABC to transport R6G using loss of EefABC function strains.

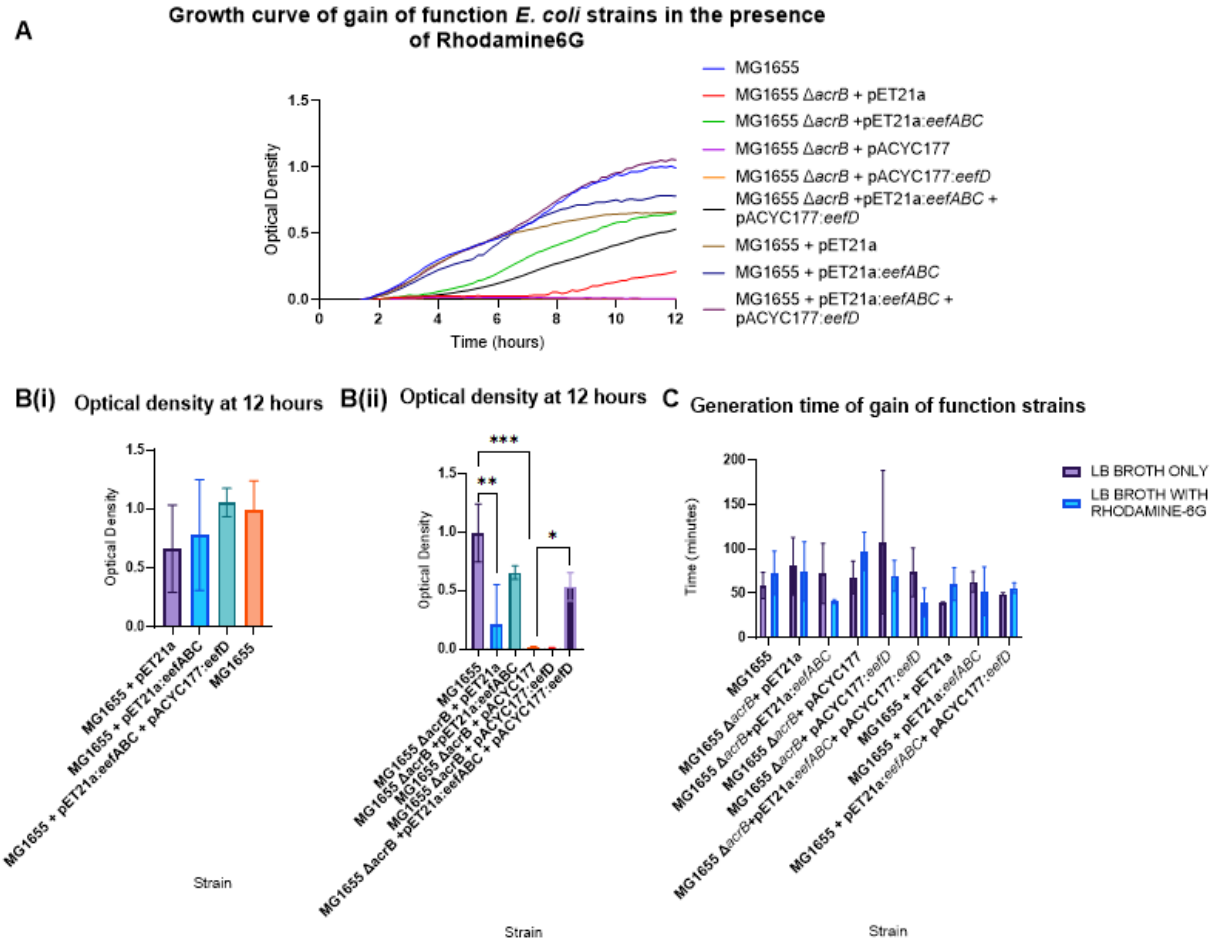

Figure 21. Growth kinetics of gain of function *E. coli* strains in the presence of 8 µg/mL rhodamine-6G. Panel A) growth curves of gain of function *E. coli* strains (measure of optical density at 600 nm over a 12-hour period). Panel B) Comparison of optical density after 12 hours between gain of function strains (i) without *acrB* and (ii) with *acrB*. This is the final OD measurement taken at 12 hours. Panel C) mean generation time of gain of function *E. coli* strains. Each data point is an average of 3 biological repeats, error bars of standard deviation to show (3 technical repeats per biological repeat). Level of significance between end points has been calculated using the one-way-anova analysis. Level of significance between generation time has been calculated using the two-way-anova analysis. Significance at $P \leq 0.05$ is marked with an asterisk.

Deletion of *acrB* in MG1655 decreased cell growth in the presence of R6G (figure 21 panel A) and increased generation time (panel C). Gain of EefABC function strains grew to a higher optical density after 12 hours than the *acrB* deleted strains (panel B), though this was only a significant increase for the gain of EefABCD function strain in the absence of *acrB*. Gain of EefABC function strains had the fastest generation times, though not significant. This might suggest that expression of the genes encoding both pumps, EefABC and EefD, is required to improve growth of cells in R6G.

The strain which grew to the highest optical density after 12 hours in R6G (also higher than wildtype) was the gain of EefABCD function strain which still had a functioning AcrB pump (panel B(i)). Although this was not a significant difference, it is still interesting to see that EefABCD might be used in synergy with AcrB, producing the most cell growth.

Overexpression of *eefD* alone did not increase growth, with no significant difference in optical density after 12 hours (panel B) between the gain of EefD function strain and the *acrB* knockout strains. Generation times (panel C) of gain of EefD function strains were slower than gain of EefABC function strains. This suggests that EefD did not increase growth of *E. coli* cells in the presence of R6G.

3.8 Discussion and future work

Results gathered from experiments which measured the growth kinetics and MICs of loss of EefABC/D function strains in the presence of antimicrobials or dyes did not reveal the natural function of the pump. The reason for this might have been because the gene encoding the RND pump AcrB was active in these strains and could

therefore mask the phenotype of the EefB pump. It is known that AcrB is responsible for the transport of a wide variety of classes of antibiotics (Alav *et al.*, 2021) so this is certainly a possibility.

Significant differences were observed when *acrB* had been deleted from MG1655 and compared to gain of EefABC function strains, because any interference caused by AcrB was eliminated. By using a Δ*acrB* knockout strain, any increase in growth and efflux, or decrease in susceptibility and accumulation observed could be assumed to be a result of overexpression of *eefABC.* The aim of this chapter was to identify substrates of the RND pump EefB, but unlike the highly prevalent AcrB, no antimicrobial compounds were recognized as substrates. There were no differences in MIC data for any antimicrobial compounds tested for loss of EefABC function strains or gain of EefABC function strains.

The EefABC efflux complex in *E. coli* differs to the EefABC tripartite efflux pump in *K. aerogenes,* which is thought to transport an extensive list of antimicrobial compounds including chloramphenicol, erythromycin, novobiocin, etc (Masi *et al.*, 2005; Masi, Pagès and Pradel, 2006). There is no evidence to support the hypothesis that EefABC is involved in the efflux of antimicrobial compounds, and therefore there is expected to have an involvement in AMR of *E. coli*. This statement contradicts the notion that RND efflux pumps are one of the main contributors to AMR, particularly MDR, in Gram-negative clinical pathogens (Zwama and Nishino, 2021) due to their capabilities in the expulsion of antimicrobial compounds. The reasoning behind this could be as simple as the *E. coli* EefB substrate not being tested for susceptibility within this study. However, this is unlikely because susceptibility profiles of the selected antibiotics could be generalised to other compounds from the same class,

and so there is no evidence to suggest that the pump can transport any other compounds.

MIC data highlighted the dye, EtBr, as a potential substrate of EefB and subsequent testing provided further evidence to support this. Dyes are not considered to be natural substrates, and therefore efflux of EtBr could not be the natural function of the pump. However, this data was important as it provided evidence that the pump is functional and validates the MIC data gathered for all other compounds. This information was key to motivate the progression of research into EefABC. EtBr is also a known substrate many RND efflux pumps including *Helicobacter pylori* HefABC, *E. coli* AcrAB-TolC, *Serratia marcescens* SdeAB, etc (Mardanova *et al.*, 2013; Alav *et al.*, 2021; Raj *et al.*, 2021). Referring to growth kinetics in the presence of EtBr, cells which overexpressed both *eefABC* and *eefD* grew to a significantly higher optical density than the other strains. This might suggest that EefABC is better able to transport some substrates with the assistance of the MFS transporter, EefD. An explanation for this is that when EtBr penetrates through the outer membrane, it quickly enters the cytoplasm and from there can be transported back into the periplasm by EefD for expulsion by EefABC (Miki and Hardt, 2013).

Though there was evidence of EefABC being active in *E. coli*, the natural function of the pump had not been established, since MIC data rejected the hypothesis that the pump is involved in AMR. The reasoning behind the evolutionary conservation of the pump remains unknown.

Moving on from the attempt to characterise the substrates of the Eef complex, the physiological roles of EefABC in *E. coli* were explored. Since functional RND pumps existed even before antibiotics were used in clinical settings (Zwama and Nishino,

2021), they must have physical roles in the survival and fitness of microbes, promoting colonization and persistence within hosts, and overall virulence of pathogens. This notion was later explored in chapter 4.

3.9 Key Findings

- Deletion/overexpression of *eefABC* did not affect susceptibility of *E. coli* strains MG1655 or ATCC 25922 to antimicrobial compounds or metals tested.
- Overexpression of *eefABC* decreased susceptibility of *E. coli* strain MG1655 to EtBr.
- In the absence of AcrB (*ΔacrB), E. coli* strains which overexpressed *eefABC* grew better in media containing 8 µg/mL EtBr or 8 µg/mL R6G than strains which didn't.
- In the absence of AcrB, overexpression of *eefABC* conferred lower accumulation of EtBr, and more rapid efflux of EtBr.

CHAPTER 4. RESULTS - INVESTIGATION OF THE PHYSIOLOGICAL ROLES OF EEFABC

4.1 Background

EefABC is an RND efflux complex that is highly conserved in *E. coli* strains associated with infection. Expression of several efflux pumps have been linked increased virulence and the ability of the pathogen to cause infection (Guérin *et al.*, 2016). Efflux pumps have been found to be involved in various physiological roles including biofilm production and acid tolerance. This chapter attempts to characterise the physiological roles of EefABC in *E. coli*, particularly biofilm formation, acid tolerance and the ability to cause infection in the host.

Biofilm is an important factor when it comes to infection, since this allows the bacterial cells to aggregate and adhere to surfaces and tissues (Høiby, 2017), resulting in a prolonged infection. Testing acid tolerance is relevant because *E. coli* needs to be able to survive the variable pHs throughout the gastrointestinal tract of humans, in which it often resides. Deletion of EefABC has previously been linked to decreased survival in acidic pH in *K. pneumoniae* as less *eefA* knockout cells survived in acidic conditions than strains expressing *eefA* (Coudeyras *et al.*, 2008). Furthermore, studies using the *Galleria mellonella* model of infection have correlated overexpression of some efflux pumps with an increase in insect death (Bialek *et al.*, 2010).

The largest differences observed in chapter 3 occurred when EefABC was expressed in a Δ*acrB* mutant background. Therefore, this chapter focussed on gain of function experiments using the test strain MG1655 Δ*acrB* + pET21a:*eefABC,* and its

behaviour was compared to the wildtype, MG1655, and an MG1655 *acrB* knockout strain.

4.2 Aims

- Characterise the physiological functions of EefABC, by comparing biofilm formation, acid tolerance, and virulence of strains with and without EefABC in the absence of AcrB.
- Develop a method which will provide insight into how well the bacteria can adapt to a lower pH.

4.3 Hypotheses

- Biofilm formation will be higher for strains encoding a plasmid containing the genes for *eefABC* than the *acrB* knockout strain.
- Survival in acidic pH conditions will be lower than at a neutral pH, but survival of a strain harbouring a plasmid encoding the genes for *eefABC* will be increased in acidic conditions than the *acrB* knockout strain.
- *Galleria mellonella* will have a lower probability of survival when infected with *E. coli* strains encoding a plasmid containing the genes for *eefABC* than without.

4.4 Expression of EefABC does not affect biofilm formation

Biofilm formation was quantified by solubilising crystal violet staining the cells associated with biofilm with ethanol and measuring optical density at 600nm. Both wildtype strains, ATCC 25922 and MG1655, were used in this experiment for comparison because MG1655 is typically a poor biofilm producer (Beloin, Roux and

Ghigo, 2008), so it was useful to see how well the laboratory strain ATCC 25922 formed biofilm.

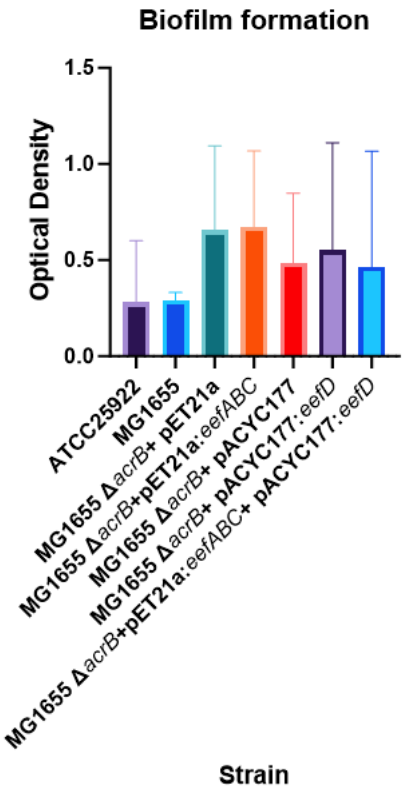

Figure 22. Measuring biofilm formation using crystal violet. Optical density (measured at 600nm) is directly proportional to the amount of biofilm formation in each well. Data points are the average of 3 biological repeats and 4 technical repeats, with error bars of standard deviation. Significance at P≤0.05 between gain of EefABC function strains and the *ΔacrB* strains was determined using the two-way-anova statistical test. Significance at P ≤ 0.05 is marked with an asterisk.

There were no statistically significant differences in biofilm formation between any of the gain of EefABC function strains and the Δ*acrB* strains. Biofilm formation was low in wildtype strains ATCC 25922 and MG1655 in comparison to *ΔacrB* mutant strains which didn't encode EefABC, though this was not significant. The optical density of

the *ΔacrB* mutant strains was the same as that of gain of EefABC/D function strains. The reason for the increase in biofilm formation in *ΔacrB* mutant strains is unknown, but this data was consistent for all repeats and might be an effect of the plasmid itself, and nothing to do with the knockout of acrB.

The data suggests that unlike other efflux pumps present in *E. coli*, EefABC does not have a prominent role in biofilm formation under these conditions.

4.5 Acid tolerance assay to measure survival of cells

Tolerance to acidic conditions was measured by calculating the CFU/mL of cells after exposure to acidic conditions after 0 hours, 1 hour, 2 hours and 4 hours of incubation and comparing the percentage change in CFU/mL of each strain after each time point. Each strain was grown at 37°C for a total of 4 hours at pH 7 MOPS minimal media and in pH 4 MOPS minimal media (acid-shock). In a previous study which performed acid tolerance assays with *K. pneumoniae*, the only significant difference was observed when strains were allowed a period of time to preadapt to a lower pH (Coudeyras *et al.*, 2008). Therefore, a pre-adaptation step was included where strains were first incubated for 1 hour in MOPS minimal media at a slightly lower pH (pH 5), before subsequent incubation at pH 4. For acid tolerance experiments, the wildtype MG1655, an MG1655 *acrB* knockout strain and the gain of EefABC function in an *acrB* deleted background were used. This was to test whether overexpression of *eefABC* could improve survival of the *acrB* knockout strain in acidic conditions. Eliminating the major RND pump AcrB could make the survival of *E. coli* worse in acidic conditions, so it would be interesting to see whether overexpression of *eefABC* could better equip the cells for survival.

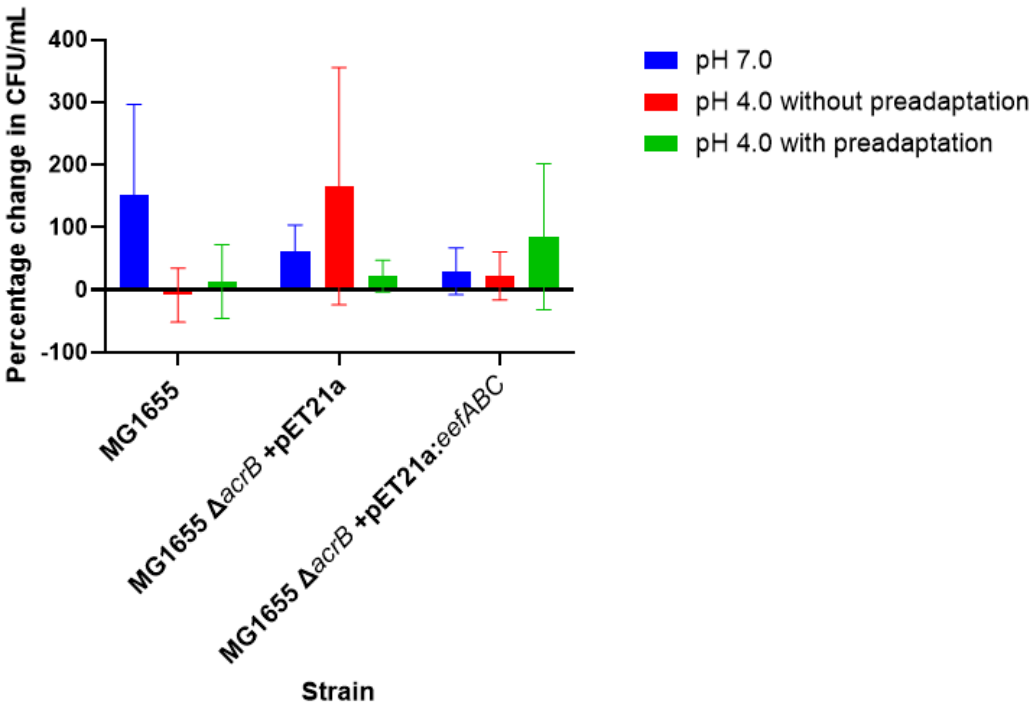

Figure 23. Percentage change in survival (CFU/mL) of cells grown at pH 7 or pH 4 MOPS minimal media. Preadapted cells were incubated at 37°C in MOPS minimal media adjusted to pH 5 for 1 hour before being incubated in MOPS minimal media adjusted to pH 4. Cells were grown in MOPS minimal media at either pH 7 or pH 4 for a total of 4 hours. CFU/mL counts were calculated after 0 hours and then at 4 hours and the percentage change in growth after 4 hours was plotted. Data points are the average of 3 biological repeats and 1 technical repeat, with error bars of standard deviation. Level of significance was determined using the two-way-anova statistical test. Significance at level $P \leq 0.05$ is marked with an asterisk.

No significant difference was observed when the perecentage change of CFU/mL for each strain grown in neutral conditions was compared to the percentage change of CFU/mL of the same strains grown in acidic conditions.

CFU/mL for strains under each condition was calculated at various time points, but the largest difference in CFU/mL counts was observed after 4 hours, so the percentage increase between 0 hours and 4 hours was calculated and plotted onto figure 23.

Less MG1655 cells survived after 4 hours of incubation in acidic conditions, without preadaptation. Survival of MG1655 cells increased slightly when the preadaptation step was added, though this was not significant.

More cells belonging to the *acrB* knockout strain survived at pH 4 without preadaptation than at pH 7, and the reason for this is unknown. However, there was some variation in results because 2 out of 3 biological repeats displayed this large percentage increase in survival after 4 hours, whereas the third repeat only showed a small increase. Less *acrB* knockout cells survived in pH 4 after preadaptation than at pH 7 and pH 4 without preadaptation.

After growth in pH 4 without preadaptation, survival of the gain of EefABC function strain was very similar to survival in pH 7. More cells belonging to the gain of EefABC function *E. coli* strain survived at pH 4 with preadaptation, than at pH 4 without preadaptation, though this is not a significant increase.

Data from this experiment did not provide evidence to suggest that overexpression of EefABC improves acid tolerance of *E. coli.* However, the data collected was inconsistent between repeats.

4.6 Measuring growth kinetics of gain of EefABC function strains in neutral and acidic conditions

To get a better understanding of growth of gain of EefABC function *E. coli* strains in acidic conditions, optical density (600nm) of cells incubated at 37˚C for 23 hours was

measured at 30-minute intervals in a plate reader to generate a growth curve. This was done to test the hypothesis that overexpression of *eefABC* would increase growth of *E. coli* cells in acidic conditions.

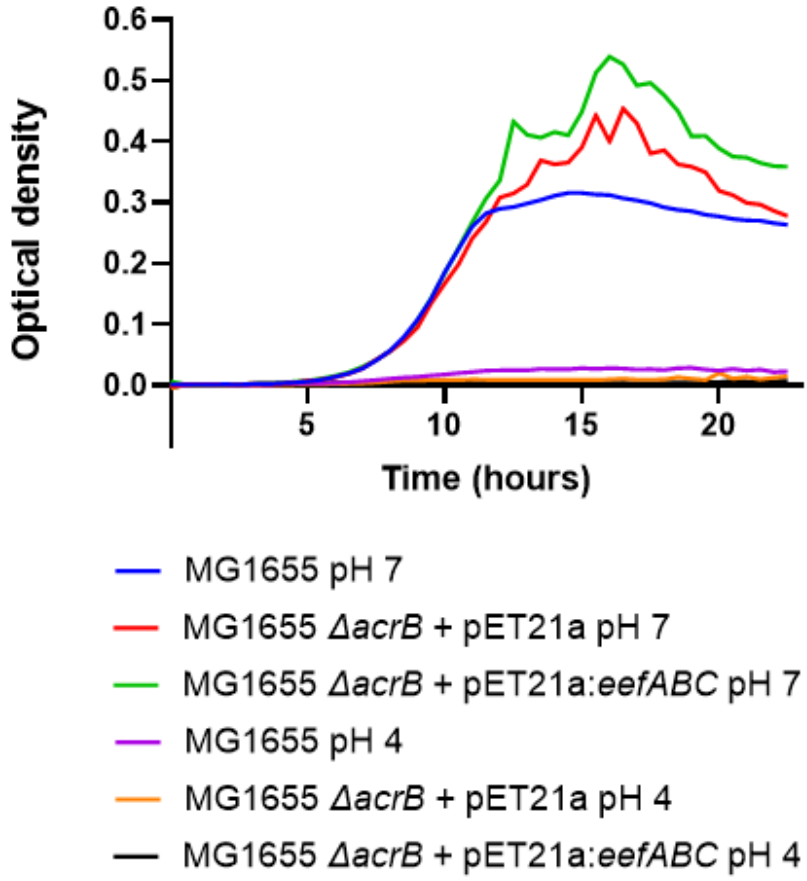

Figure 24. Growth kinetics analysis of gain of EefABC function *E. coli* strains in MOPS media adjusted to either pH 7.0 or pH 4.0. Optical density was measured at 600nm every 30 minutes for 23 hours to produce a growth curve. Each data point is an average of 3 biological repeats (3 technical repeats per biological repeat).

For all strains, cells grew better in pH 7 adjusted MOPS minimal media than in pH 4 adjusted MOPS minimal media. Growth of strains in pH 4 did not reach exponential

growth phase, therefore it was not possible to calculate and compare generation times. Overexpressing *eefABC* did not increase growth of *acrB* deleted MG1655 *E. coli* cells in acidic conditions. This experiment provided no data to support the hypothesis that the RND complex, EefABC, is involved in acid tolerance in *E. coli.*

Later experiments involved the preadaptation of cells to a lower pH by lowering the pH of MOPS minimal media to pH 5 prior to incubation in pH 4 MOPS minimal media.

4.7 Measuring growth kinetics of gain of EefABC function strains in neutral and acidic conditions, with preadaptation

In a previous study (Coudeyras *et al.*, 2008), a difference in acid tolerance between the wildtype and the loss of EefABC function strain was observed when strains were first incubated for 1 hour in slightly less acidic conditions than the final pH used in the experiment (i.e. the sample was incubated for 1 hour in pH 5.0 adjusted MOPS minimal media then resuspended in pH 4 adjusted MOPS minimal media for further incubation and measurement).

Growth kinetics of gain of EefABC function strains were measured again, but this time a preadaptation step was included. For this experiment, acid shocked cells were preadapted by incubation at 37˚C for 1 hour in pH 5 MOPS minimal media then resuspended in pH 4 MOPS minimal media before being incubated in a plate reader at 37˚C for 23 hours with optical density (600_{nm}) measured every 30 minutes.

This experiment looked for evidence to suggest that overexpression of *eefABC* would increase growth of an *acrB* knockout MG1655 *E. coli* strain in acidic conditions. This data would also confirm whether strains which were previously unable to grow in acidic conditions could become preadapted to these conditions through gradual exposure.

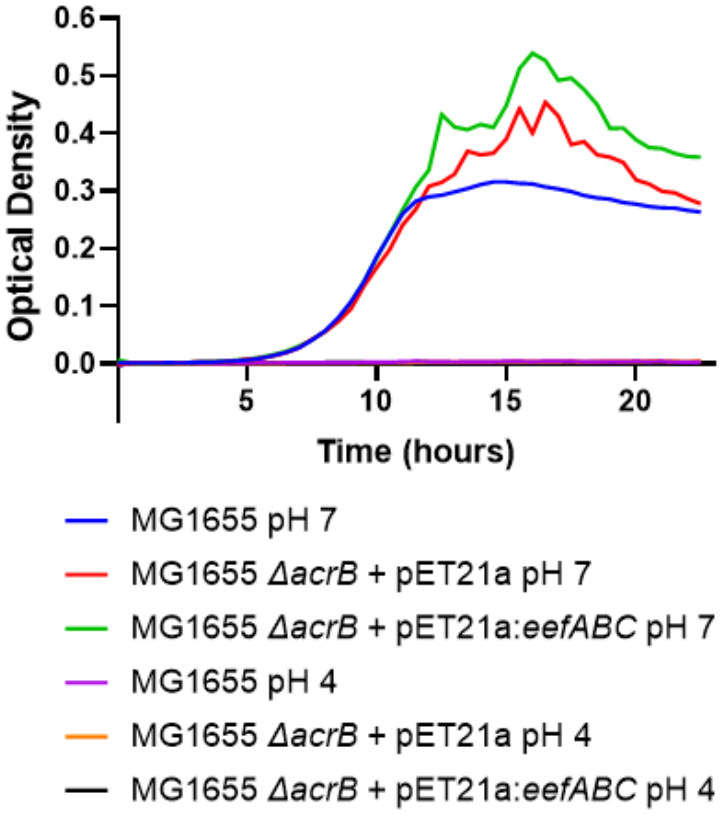

Figure 25. Growth kinetics analysis of gain of EefABC function *E. coli* strains in either MOPS minimal media adjusted to pH 7.0 or pH 4.0. Strains incubated in pH 4 had been incubated at pH 5 for 1 hour prior to measurement of growth kinetics (preadapted). Growth curves of gain of EefABC function *E. coli* strains are shown in figure 25. Optical density was measured at 600nm every 30 minutes for 23 hours to produce a growth curve. Each data point is an average of 3 biological repeats (3 technical repeats per biological repeat).

For all strains, cells grew better in pH 7 adjusted MOPS minimal media than in pH 4 adjusted MOPS minimal media. Growth of strains in pH 4 did not reach exponential growth phase, therefore it was not possible to calculate and compare generation times.

Overexpressing *eefABC* did not increase growth of *acrB* deleted MG1655 *E. coli* cells in acidic conditions, even after a preadaptation step was included.

Growth kinetics did not provide any data to support the hypothesis that EefABC is involved in acid tolerance in *E. coli.*

4.8 Survival of *Galleria mellonella* is reduced by overproduction of EefABC

Galleria mellonella larvae were injected with $1x10^6$ cells of either MG1655 or MG1655 *ΔacrB* + pET21a:*eefABC* and survival of the larvae was measured every 24 hours for 5 days. MG1655 (or K-12) is a non-pathogenic strain of *E. coli*, which does not cause infection (Kaper, 2002). This experiment was conducted to test whether overexpression of *eefABC* was able to make MG1655 *E. coli* cells better able to cause fatal infection in *Galleria mellonella*. Controls were included to eliminate causes of death including PBS contaminated with external microorganisms used to dilute bacterial culture (PBS control); trauma inflicted by inserting the needle (stab control); and poor quality of larvae i.e. prior infection/end of life cycle/poor living conditions (control).

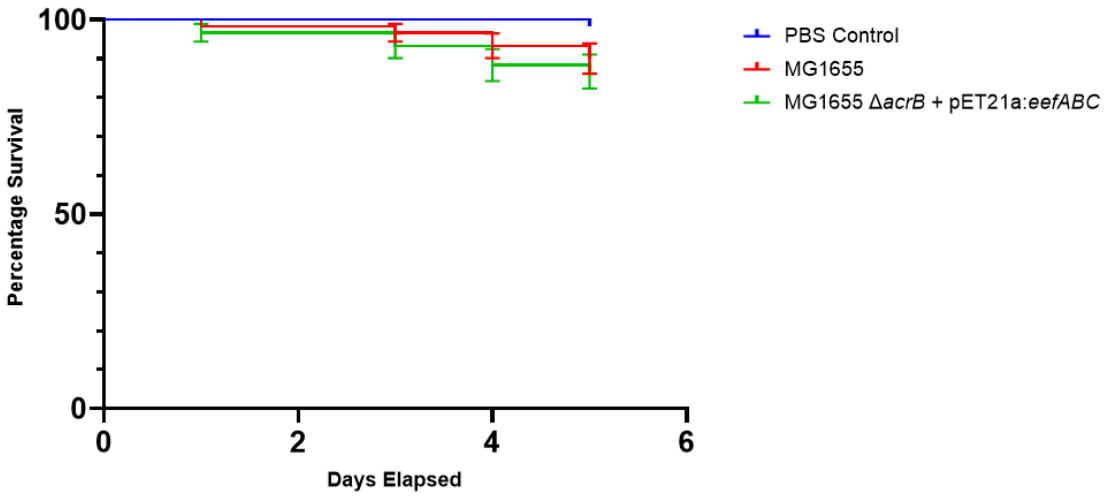

Figure 26. Time-dependent survival of *Galleria mellonella* after infection with *E. coli* over a period of 5 days. Data is a collation of 4 biological repeats in which each condition had 15 larvae pre replicate. Error bars show standard error. PBS control larvae were injected with 20 µL PBS solution, whilst larvae in the other 2 conditions were injected with $1x10^6$ cells of either MG1655 or its gain of EefABC function counterpart MG1655 *ΔacrB* + pET21a:*eefABC*. Significance at $P \leq 0.05$ was tested using the log-rank (Mantel-Cox) statistical test.

For display purposes, control and stab control results were not included in the data set. Most of the infected larvae survived for the full 5-day period, equivalent to the PBS control data shown in the graph, indicating that the larvae used in this study were healthy and could survive the insertion of a needle.

The graph in figure 26 shows that PBS control larvae had a 100% chance of survival for 5 days, which indicated that there were no factors which could have compromised survival such as: quality of larvae, incubation conditions, contaminated PBS dilutant or insertion of the needle. This meant that death of larvae which had been injected

with *E. coli* was related to infection. Percentage survival of infected larvae, for both conditions, was lower than the PBS control, which confirmed that both strains used were appropriate because they had the ability to cause fatality due to infection.

Whilst the graph shows that percentage survival was lower in the strain which overexpressed *eefABC* than the wildtype, this was not a significant difference. This data does not provide enough evidence to suggest that expression of EefABC does increase the probability of fatality due to infection. Under all conditions, the number of larvae deaths was low - percentage of survival was never below 80% - and this could have been a result of injecting the larvae with too few *E. coli* cells. To assess this, the *Galleria mellonella* infection model was repeated, but larvae were injected with a higher concentration of cells.

Further *Galleria mellonella* infection experiments involved the dilution of MG1655, MG1655 *ΔacrB* + pET21a and MG1655 *ΔacrB* + pET21a:*eefABC E. coli* cultures to $1x10^7$ cells per 20 µL injected. Controls remained the same.

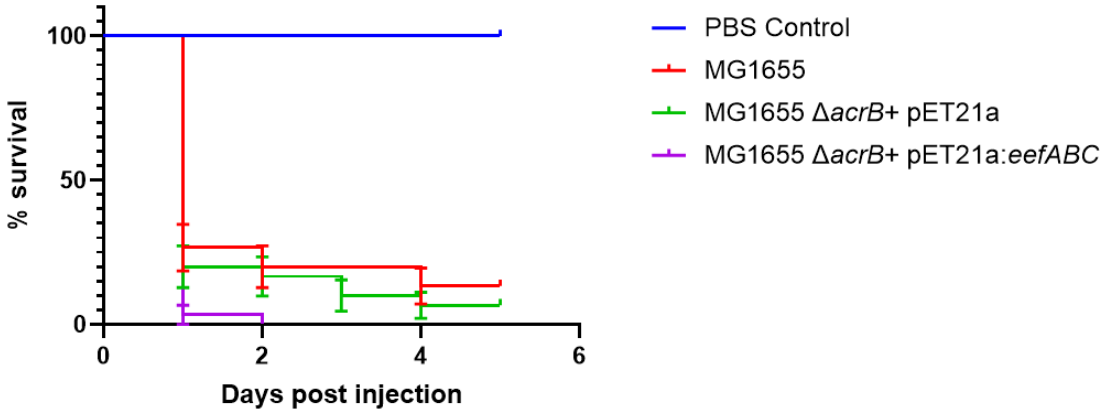

Figure 27. Time-dependent survival of *Galleria mellonella* after infection with *E. coli* over a period of 5 days. Data is a collation of three biological repeats and each

condition had ten larvae for each replicate. Error bars show standard error. PBS control larvae were injected with 20 µL PBS solution, whilst larvae in the other 2 conditions were injected with $1x10^7$ cells of either MG1655, MG1655 Δ*acrB* + pET21a or its gain of EefABC function counterpart MG1655 *ΔacrB* + pET21a:*eefABC.* Significance at level $P \leq 0.05$ was tested using the log-rank (Mantel-Cox) statistical test.

All control larvae (which had not been stabbed with a needle), stabbed larvae and larvae injected with PBS survived for the full 5 days, indicating that the larvae used in this study were healthy and could survive the insertion of a needle. Only results from the PBS control are displayed in figure 27.

The deletion of *acrB* in MG1655 did not significantly reduce or increase survival of *Galleria mellonella* larvae in comparison to the wildtype MG1655. However, overexpression of *eefABC* did significantly lower the percentage of larvae which survived in comparison to the *ΔacrB* deleted strain. All the larvae inoculated with $1x10^7$ of this strain of *E. coli* died within the first 2 days after infection.

These results suggest that overexpression of the EefABC efflux pump increased virulence in the *Galleria mellonella* model of infection.

4.9 Discussion and future work

The aim of this chapter was to identify potential physiological roles of EefABC. To ensure that the presence of AcrB did not mask any effects, experiments were carried out using a gain of EefABC function strain overexpressed in an *acrB* deleted environment and comparing this against an *acrB* knockout strain. Data relating to the *acrB* knockout strain were compared to the wildtype, MG1655. Data gathered from

experiments which measured biofilm production as well as survival and growth of cells in the presence of a lower pH did not support the hypotheses that overexpression of EefABC is involved in increased biofilm formation or acid tolerance. Findings did, however, correlate infection by a gain of EefABC function strain with increased death of *Galleria mellonella*, supporting the hypothesis that *eefABC* does increase virulence.

There was no evidence that EefABC was involved in biofilm formation in *E. coli*. This differs from previous work with other efflux pumps or other species. For example, the expression of RND systems AcrAB-TolC of *E. coli*, MexAB-OprM of *Pseudomonas aeruginosa*, and AdeFGH of *Acinetobacter baumannii* have all been shown to increase biofilm production (Gillis *et al.*, 2005; He *et al.*, 2015; Wan *et al.*, 2022) . However, not all RND pumps have been shown to enhance biofilm production when expressed, such as MexGHI-OpmD and MexEF-OprN of *P. aeruginosa* (Gillis *et al.*, 2005). Further contradictory research showed that the addition of PaβN, (an inhibitor of AcrAB), significantly reduced biofilm formation by up to 80% (Kvist, Hancock and Klemm, 2008). It was concluded that overexpression of eefABC did not increase biofilm production, therefore, it could be inferred that deletion or inhibition of *eefABC* would not decrease biofilm production.

No significant increase in survival or growth of *E. coli* was observed in the gain of EefABC function strain when incubated under acidic conditions, suggesting that overexpression of the pump did not increase acid tolerance. This result was unexpected because a study (Coudeyras *et al.*, 2008) showed that Δ*eefA* deletion in *K. pneumoniae* showed a reduction in its ability to adapt to an inorganic acidic environment in terms of survival, but after 1 hour of preadaptation, the strain encoding *eefA* better survived in the same acidic environment.

Gram-negative pathogens, particularly those belonging to groups Enterobacteriaceae and the non-fermenters, are responsible for most clinical infections (Oliveira and Reygaert, 2023), and those expressing RND pumps appear to be better able to cause infection (Bialek *et al.*, 2010). A significant increase in death of *Galleria mellonella* larvae was observed when they were infected with a greater concentration of gain of EefABC function *E. coli* cells, providing evidence to suggest that expression of the pump increased fatality upon infection. This observation was useful because it provided insight into why the pump may have been so highly conserved in *E. coli* phylogroups commonly associated with infection (Pugh, 2022) and provides evidence that the pump does have a natural function and is of use to infectious bacteria. A similar observation was made for the AcrAB-TolC complex where 100% of *Galleria mellonella* larvae infected with an *acrB* knockout strain survived over the course of the experiment (3 days), whereas only 40% of larvae survived when infected with the wildtype strain (Guérin *et al.*, 2016). Again, not all RND pumps have been shown to increase virulence using the *G. mellonella* model, including the MexAB-OprM efflux pump of *P. aeruginosa* (Adamson, Krikstopaityte and Coote, 2015). But now there is evidence linking expression of the EefABC efflux pump of *E. coli*, as well as the AcrAB-TolC complex, with increased virulence in *Galleria mellonella*. The reasoning for increased virulence of Gram-negative bacteria due to expression of some efflux pumps might be that some efflux pumps are able to export virulence determinants, such as toxins, adhesins and other proteins important for colonisation and infection of hosts (Piddock, 2006), as shown when *Salmonella typhimurium* lacking the AcrAB-TolC efflux pump was less able to adhere to, invade and survive in both mouse macrophages and human embryonic intestinal cells. For *S. typhimurium*, it was established that the removal of AcrAB-TolC disrupts the work

of Type III secretion systems which includes altering the cell membranes of hosts cells to allow for bacterial adhesion.

Despite now being linked to infection, the actual function of the efflux pump remains unknown, since common roles of other pumps, including drug transport and biofilm formation, have been ruled out for EefABC in *E. coli*. So far, no compounds have been identified as substrates of EefB. However, there is now evidence to suggest that the pump is functional *in vivo,* and this now provides insight into why the pump has been conserved across infectious phylogroups of *E. coli*.

It was decided that metabolomics could be useful in a final attempt to clarify the function of EefABC as this could potentially produce a list of substrates by comparing the internal and external metabolites of *E. coli* MG1655 and the gain of EefABC function strain at different growth phases.

4.10 Key findings

- Overexpression of *eefABC* did not increase biofilm formation of *E. coli*.
- Overexpression of *eefABC* did not increase survival or growth of *E. coli* in acidic conditions.
- Overexpression of *eefABC* significantly reduced survival of *Galleria mellonella* larvae upon infection with *E. coli*.

5. RESULTS – INVESTIGATING THE DIFFERENCES IN INTERNAL AND EXTERNAL METABOLITES IN A GAIN OF EEFABC FUNCTION STRAIN

5.1 Background

Metabolomics uses extraction, chromatographic separation and mass spectrometry techniques to generate a profile of small molecules that are derived from cellular metabolism (Liu and Locasale, 2017) to provide insights into biochemical reactions. Results from this chapter are based on data provided and analysed by collaborator Dr Gerald Larrouy-Maumus upon receiving extractions from samples of *E. coli* MG1655 and MG1655 + pET21a:*eefABC*. It was thought that comparing intracellular and extracellular metabolites of both strains at log and stationary growth phases could provide an insight into the biochemical reactions occurring in those strains, and therefore identify substrates of EefABC.

5.2 Aims

- To provide a list of metabolites, using metabolomics, which are either more abundant or less abundant in MG1655 and MG1655 + pET21a:*eefABC* strains.
- To identify molecules which are transported by EefABC.

5.3 Hypotheses

EefABC is functional and is transporting intracellular substrates out of the cell, therefore:

- The intracellular metabolites of MG1655 will differ from the intracellular metabolites of MG1655 + pET21a:*eefABC.*
- The extracellular metabolites of MG1655 will differ from the extracellular metabolites of MG1655 + pET21a:*eefABC.*

5.4 Using the HILIC-Z column to identify polar metabolites

Samples used in this set of experiments were taken from the supernatant (extracellular metabolites) and the pellets (intracellular metabolites) prepared for each strain, whilst the cells were at log and stationary growth phases.

Upon running samples on a column named HILIC_Z, no difference in metabolites were observed in samples obtained from pellets. However, a difference of 3 metabolites was identified in the supernatant at the LOG phase of growth, namely acetylene, ornaline and camoensine. These metabolites were more abundant in the supernatant produced by gain of EefABC function cells, suggesting that these had been exported by the pump.

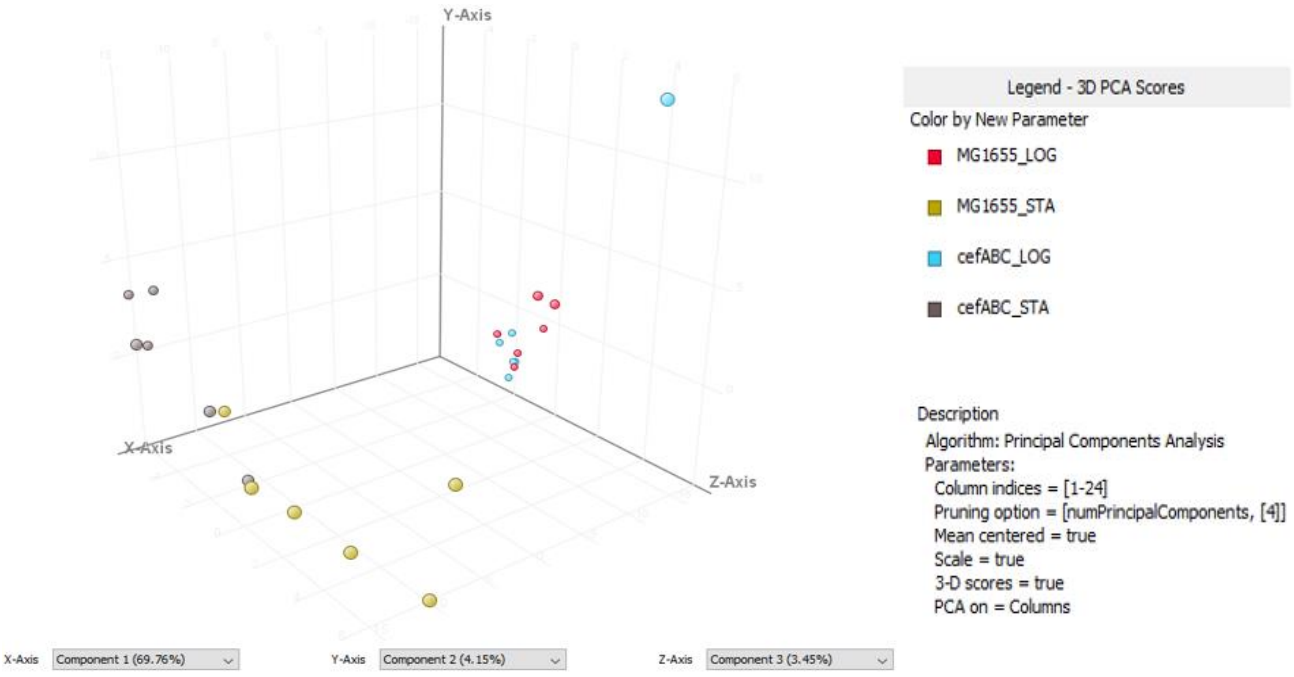

Figure 28 Principal component analysis (PCA).

PCA scores of each sample confirm that each biological and technical repeat belong to the correct strain, at each growth phase, by closely linking them together on the 3D graph. The purpose of this graph is to show that there is little variance between samples and since the parameters of the 2 strains. Plots for MG1655 and MG1655 + pET21a:*eefABC* are separated from each other, so it can be concluded that no cross-contamination occurred during sample preparation.

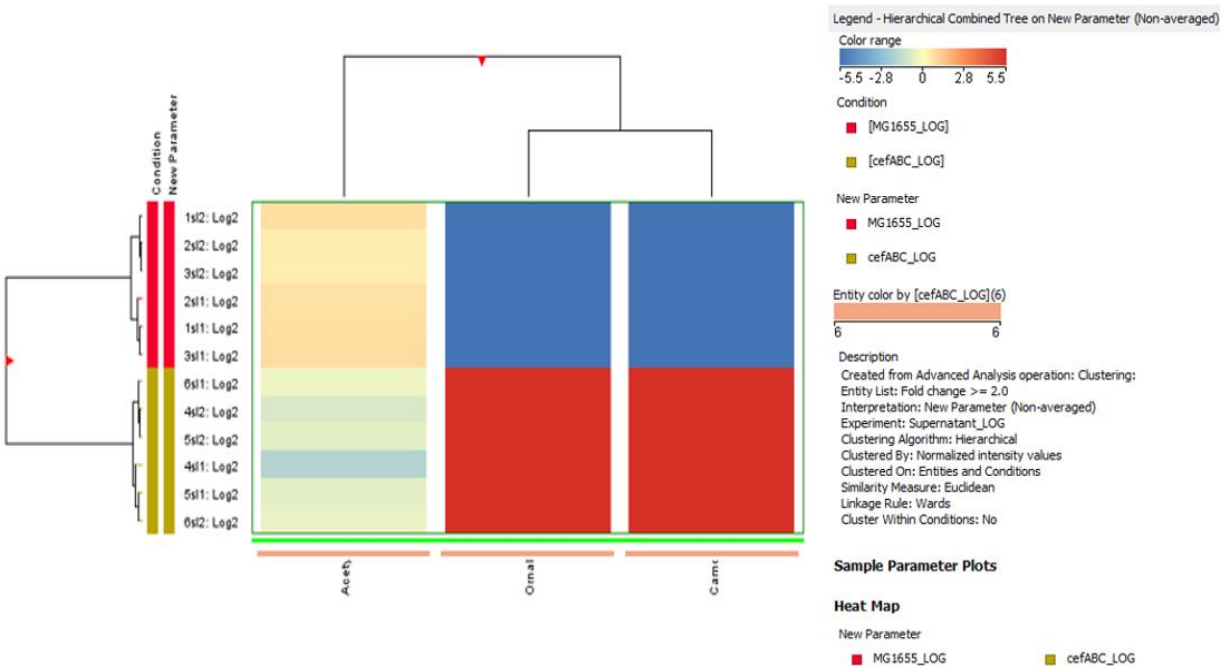

Figure 29 Hierarchical combined tree on new parameters (non-averaged).

Numbers 1-3 refer to 3 biological repeats of *E. coli* MG1655. Numbers 4-6 refer to 3 biological repeats of *E. coli* MG1655 + pET21a:*eefABC*. All the samples were taken from the supernatant during the exponential growth phase. Numbers 1 and 2 refer to technical replicates of each sample. For example, 1sl2 means: 1 biological repeat of *E. coli* MG1655; supernatant; log growth phase; technical repeat 2. The colour range in the top right-hand corner is the heat map gradient, with blue meaning that the compound was less abundant and red meaning the compound was more abundant.

The heat map in figure 29 shows an obvious distinction between MG1655 and MG1655 + pET21a:*eefABC* in terms of external metabolites. Acetylene was more prevalent in the supernatants of MG1655 than the gain of EefABC function strain. Ornaline and camoensine were more prevalent in the supernatants of the gain of EefABC function strain than in MG1655, however the identification of these compounds is not certain at this point. This data was consistent across all biological

and technical repeats, giving confidence that there is a difference in metabolites between strains. To be certain of the metabolites, further analysis must occur.

5.5 Using the Diamond Hydride column to identify metabolites

Further analysis was conducted for samples collected from pellets and supernatants by running them in positive and negative ion mode using a Diamond Hydride column.

No change in metabolites were observed for samples taken from pellets at log or stationary growth phases.

A difference in metabolites was observed between the wildtype and gain of EefABC function strains both in positive and negative ion mode. Again, the metabolites were conserved across all biological and technical repeats.

When run on positive ion mode, a metabolite with the mass 396.0998 was more abundant in the supernatant of the gain of EefABC function strain than in the supernatant of the wildtype strain during both the log and stationary phases, across all repeats.

When analysed in negative ion mode, a metabolite with the mass 230.1421 was present in the supernatant of the gain of EefABC function strain during the log growth phase, and a metabolite with the mass 308.1196 in the supernatant of the gain of EefABC function strain during the stationary growth phase. Again, these results were consistent across all repeats.

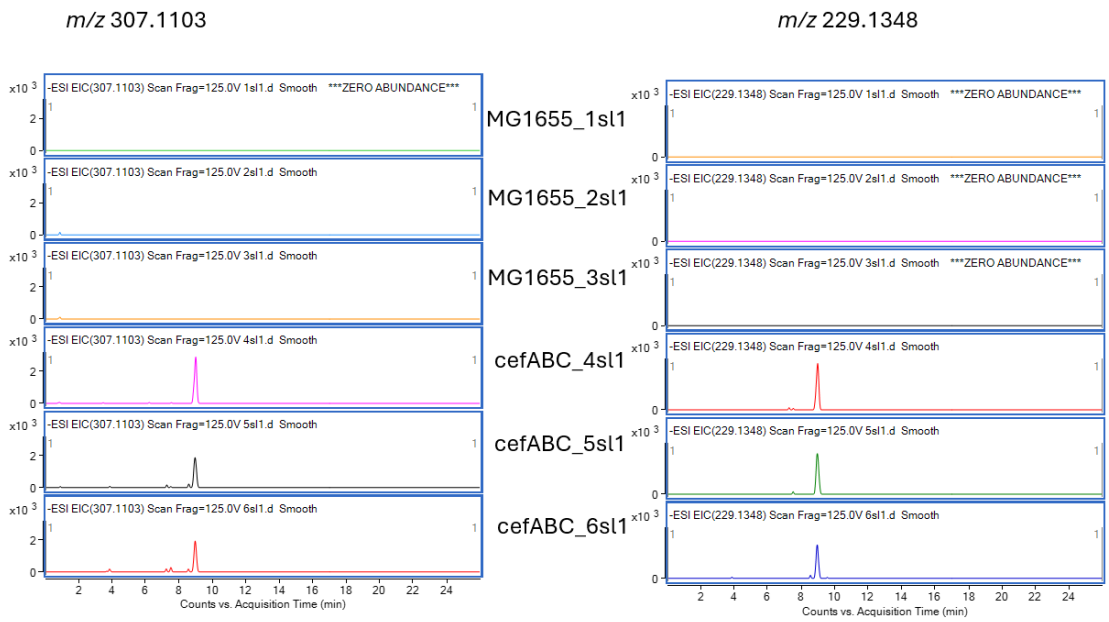

Figure 30. Mass-to-charge ratio (*m/z*) peaks observed when samples taken from the supernatant during log growth phase were run in negative ion mode using a Diamond hydride column.

Peaks for molecules with *m/z* 307.1103 and *m/z* 229.1348 were observed across all 3 technical repeats in the gain of EefABC function strain, but not in the wildtype.

Further analysis was required to assign an identity to the metabolites of interest, and this was done using tandem mass spectrometry (MS/MS) of those peaks.

5.6 Tandem mass spectrometry (MS/MS)

MS/MS was used to measure the mass-to-charge ratio (*m/z*) of the compounds identified in chapter 5.5, as well as their intermediates. The molecules with *m/z* 229.1348 (figure S.1) and *m/z* 307.1103 (figure S.2) were analysed using MS/MS to match the fragments to known compounds.

None of the fragments could be identified using the *E. coli* database ECMDB.

The compound with *m/z* 307.2201, which was equivalent to mass 308.1181, was entered into the *E. coli* BioCYC database (*BioCyc Pathway/Genome Database Collection*).

Table 11 Compound identified using the *E. coli* BioCYC database, ECOCYC, based on the mass provided by the MS/MS spectra.

Search Mass	Monoisotopic MW	Compound Name	Chemical Formula
308.1181	308.1219656292	*N*-(1-deoxy-D-fructose-1-yl)-L-glutamine	C11H20N2O8

The compound identified in table 11 is likely to be the metabolite of interest, however this was not confirmed.

The compound with *m/z* 229.1348, equivalent to mass 230.1426, had no hits using the BioCYC database.

5.7 Discussion

Ornaline and camoensine are compounds which were putatively identified in chapter 5.4. Ornaline is a glutamic acid derivative produced in plants during a metabolic reaction (*ornaline (CHEBI:133921)*), which makes it unlikely that this an exact identification of the compound purified in the HILIC-Z column, since *E. coli* is not a plant. The same goes for camoensine, which is also a compound naturally found in plant species (PubChem).

One compound which was putatively identified in the supernatant of the gain of EefABC function strain was *N*-(1-deoxy-D-fructose-1-yl)-L-glutamine, otherwise known as deoxyfructosyl glutamine (DGF), which is a naturally occurring Amadori compound found in rotting fruits and vegetables (Baek *et al.*, 2003). There is no

evidence to suggest that this compound is involved in infection and therefore has no clinical relevance, so the presence of DFG in the supernatant, assuming that it has been exported by *E. coli*, remains a mystery. Furthermore, DFG is only a putative identification and so this might not be the right compound. Whilst it is likely that DGF is a compound that is present in the supernatant of the gain of EefABC function strain, there needs to be extensive evidence to support this. After a conversation with Dr Gerald Larrouy-Maumus, it was determined that to validate this assumption, the next step would be to purchase DGF and inject this into the samples and calculate MS/MS retention times.

One limitation of this study was that it was not possible to annotate some of the metabolites because they were not readily available on the *E. coli* databases used. Given more time, it would be possible to purify each of the metabolite compounds and use nuclear magnetic resonance (NMR) to separate them into fragments which can be assigned to chemical groups to determine the chemical structure of the compound. The structures provided can then be synthesised for further validation work that does not rely on the use of commercially available molecules. This work is likely to be completed in the near future by the Blair Lab in collaboration with Dr Gerald Larrouy-Maumus.

Overall, metabolomic analysis has provided strong evidence to suggest that there is a difference in metabolites, where *E. coli* cells which overexpress *eefABC* have an abundance of 3 metabolites in the supernatant, in contrast to the wildtype. This statement was authenticated by the fact that the phenotype was highly conserved across biological and technical repeats. Whilst the chemical structures of these metabolites remain unknown at this moment in time, this is clear evidence to suggest that the efflux pump is functional and can transport some compounds out of the cell.

From the highly promising information provided in chapter 5, it is likely that further metabolomics analysis will be carried out in the future to identify the substrate of EefABC. The next step would be to conduct NMR to separate purified metabolites to provide a clearer and more accurate identification of the compounds. The direction of this project could be agreed upon with collaborator Dr Gerald Larrouy-Maumus.

5.8 Key findings

- There was no difference in internal metabolites for either strain during log or stationary growth phase.
- Acetylene, ornaline and camoensine were identified as external metabolites consistently across all repeats. Supernatants from gain of EefABC function strains were positive for ornaline and camoensine, unlike the wildtype.
- The compound named *N*-(1-deoxy-D-fructose-1-yl)-L-glutamine was identified using MS/MS spectrometry.

6. DISCUSSION

The aim of the study was to characterise the functional role of the novel efflux pump, EefABC, commonly found in *E. coli* isolates associated with infection. RND efflux pumps are most known for their ability to confer antimicrobial resistance, but some have been characterised for their physiological roles.

The 7th RND pump of *E. coli*, *eefB*, which is encoded on a five gene operon with a TetR regulator, a PAP, OMF and an MFS pump, is not a drug transporter, but its ability to transport EtBr provides evidence that the pump is functional.

Data collected about loss of EefABC function strains did not reveal very much about the function of the pump, probably because the gene encoding the RND pump AcrB was active. Previous work showed that the conservation of *eefRABCD* was comparable to that of the *acrAB-tolC* RND system (Pugh, 2022), proposing that the two systems have a similar important biological function. More varied results were obtained when *eefABC* was overexpressed in an *acrB* deleted MG1655 background, otherwise known as gain of EefABC function. Interference of AcrB was eliminated, and it was clearer to see the effects of *eefABC* expression. By using an *acrB* knockout strain, it can be assumed that any change in patterns of results was because of *eefABC* and not *acrB*.

There is no clear evidence to suggest that EefABC in *E coli* transports antimicrobial drugs, which differs from EefABC in *E. aerogenes* (Masi *et al.*, 2005; Masi, Pagès and Pradel, 2006). This finding also distinguishes EefABC in *E. coli* from AcrAB-TolC in *E. coli*, which is able to transport a vast number of antibiotics (Jang, 2023). However, EefABC was shown to transport dyes EtBr and R6G, which is common for

many efflux pumps, including, but not limited to AcrAB-TolC (Jang, 2023), SdeXY (Chen *et al.*, 2003), AdeABC (Krishnamoorthy *et al.*, 2015).

Survival of *Galleria mellonella* larvae was reduced significantly when infected with gain of EefABC function *E. coli* strains, but the mechanism behind this remains unknown. This finding confirmed that expression of *eefABC* is important for *E. coli* to cause infection within hosts, which is concurrent with previous findings that showed that EefABC is highly conserved across pathogenic phylogroups of *E. coli* (Pugh, 2022), highlighting the clinical importance of the pump. The pump has not been effective in increasing means of infection through biofilm formation or through persistence of the pathogen in the potential acidic conditions it might encounter in the human GI tract.

Metabolomics data provided strong, consistent evidence to suggest a clear difference in metabolites in the supernatant produced by *E. coli* which overexpressed *eefABC*. This information was crucial to the understanding of the role EefABC since it suggested that the pump does have a natural function. Time limitations meant that the molecules thought to have been exported by the pump could not be assigned to known compounds, however, this is a highly promising work in progress which is expected to generate data to help to elucidate the role of the efflux pump. Metabolomics has only been used in very few cases to study the substrate profile of efflux pumps, so this is exciting new information. One study in particular (Cauilan *et al.*, 2019) used untargeted metabolomics to collect data about intracellular and extracellular metabolites which were either more or less abundant in loss of AcrB function *E. coli* strains in comparison to the wildtype, identifying potential substrates of the pump. These findings highlighted the major role of AcrAB-TolC in *E. coli*. Another study (Wang-Kan *et al.*, 2021) used untargeted metabolomics to putatively

identify potential substrates of AcrB in *E. coli* and *Salmonella typhmurium*, finding that metabolites differed between species, despite genetic similarities of the pump.

Efflux pump inhibitors (EPIs) are small molecules with potential therapeutic effects due to their ability to inhibit efflux pumps, thus increasing the effectiveness of antibiotics (Alenazy, 2022). Whilst EefABC from *E. coli* is not able to export antibiotics, expression of the pump is capable of increasing fatality in *Galleria mellonella* larvae, meaning that the unknown substrate being exported by EefABC might be a virulence factor. If this is the case, administration of EPIs might weaken the ability of *E. coli* to colonise the host, making eradication easier. Therefore, the use of EPIs alongside antibiotic treatment could be a good place to start in terms of treatment of clinically relevant *E. coli* strains which express the pump. Extensive research into the structural biology of the EefABC efflux pump could be useful in the development of a structural prototype for an EPI.

7. APPENDICES

7.1 Metabolomics data

Tandem mass spectrometry analysis (MS/MS) provided a breakdown of fragments of the molecules identified by chromatography using a Diamond Hydride column. Supplementary figures 1 and 2 show the MS and MS/MS scans of the molecules with *m/z* 229.1348 and *m/z* 307.1103.

m/z 229.1348

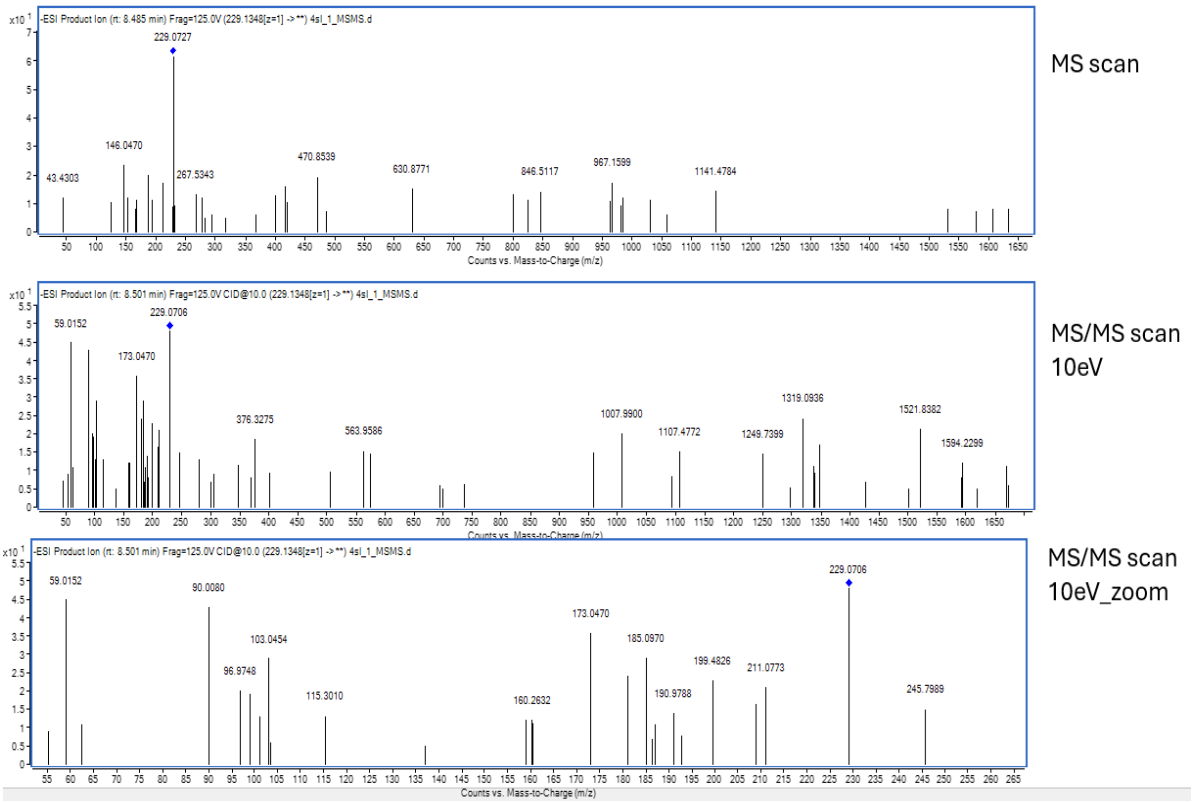

S.1. Tandem mass spectrometry scans of the compound identified in the supernatant of the gain of EefABC function strain during the log growth phase. The compound with *m/z* 229.1348 (equivalent to mass 230.1426) is marked with a blue diamond on the graph, and this is considered the parent strain to each of the fragments.

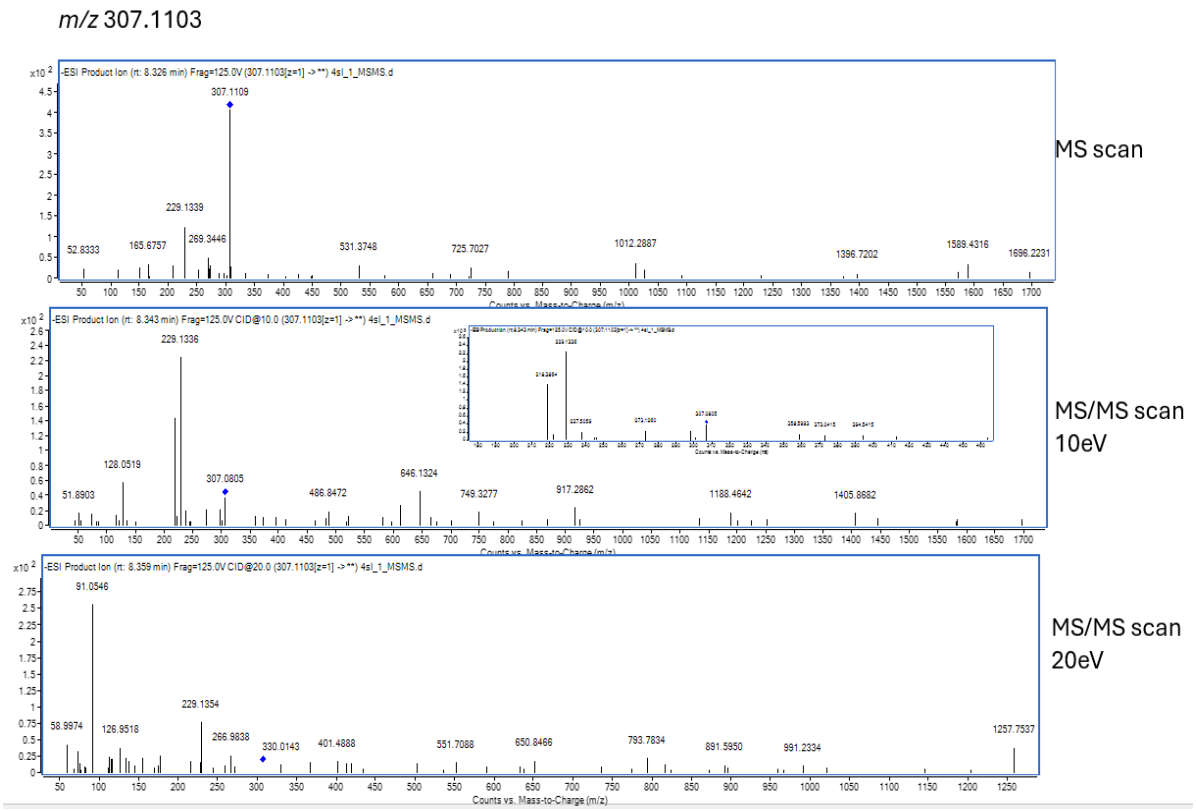

S.3. Tandem mass spectrometry scans of the compound identified in the supernatant of the gain of EefABC function strain during the log growth phase. The compound with *m/z* 307.1103 (equivalent to mass 308.1181) is marked with a blue diamond on the graph, and this is considered the parent strain to each of the fragments.

7. REFERENCES

Adamson, D.H., Krikstopaityte, V. and Coote, P.J. (2015) 'Enhanced efficacy of putative efflux pump inhibitor/antibiotic combination treatments versus MDR strains of Pseudomonas aeruginosa in a Galleria mellonella in vivo infection model', *Journal of Antimicrobial Chemotherapy*, 70(8), pp. 2271–2278. Available at: https://doi.org/10.1093/jac/dkv111.

Al Masum, A. *et al.* (2016) 'Biochemical activity of a fluorescent dye rhodamine 6G: Molecular modeling, electrochemical, spectroscopic and thermodynamic studies', *Journal of Photochemistry and Photobiology B: Biology*, 164, pp. 369–379. Available at: https://doi.org/10.1016/j.jphotobiol.2016.10.002.

Alav, I. *et al.* (2021) 'Structure, Assembly, and Function of Tripartite Efflux and Type 1 Secretion Systems in Gram-Negative Bacteria', *Chemical Reviews*, 121(9), pp. 5479–5596. Available at: https://doi.org/10.1021/acs.chemrev.1c00055.

Alav, I., Sutton, J.M. and Rahman, K.M. (2018) 'Role of bacterial efflux pumps in biofilm formation', *Journal of Antimicrobial Chemotherapy*, 73(8), pp. 2003–2020. Available at: https://doi.org/10.1093/jac/dky042.

Alenazy, R. (2022) 'Drug Efflux Pump Inhibitors: A Promising Approach to Counter Multidrug Resistance in Gram-Negative Pathogens by Targeting AcrB Protein from AcrAB-TolC Multidrug Efflux Pump from Escherichia coli', *Biology*, 11(9), p. 1328. Available at: https://doi.org/10.3390/biology11091328.

Anderson, M. *et al.* (2019) *Averting the AMR crisis: What are the avenues for policy action for countries in Europe?* Copenhagen (Denmark): European Observatory on Health Systems and Policies (European Observatory Policy Briefs). Available at: http://www.ncbi.nlm.nih.gov/books/NBK543406/ (Accessed: 21 July 2023).

Anes, J. *et al.* (2015) 'The ins and outs of RND efflux pumps in Escherichia coli', *Frontiers in Microbiology*, 6, p. 587. Available at: https://doi.org/10.3389/fmicb.2015.00587.

Baek, C.-H. *et al.* (2003) 'Convergent Evolution of Amadori Opine Catabolic Systems in Plasmids of Agrobacterium tumefaciens', *Journal of Bacteriology*, 185(2), pp. 513–524. Available at: https://doi.org/10.1128/JB.185.2.513-524.2003.

Bailey, J. *et al.* (2010) 'Distribution of Human Commensal Escherichia coli Phylogenetic Groups', *Journal of clinical microbiology*, 48, pp. 3455–6. Available at: https://doi.org/10.1128/JCM.00760-10.

Baugh, S. *et al.* (2012) 'Loss of or inhibition of all multidrug resistance efflux pumps of Salmonella enterica serovar Typhimurium results in impaired ability to form a biofilm', *Journal of Antimicrobial Chemotherapy*, 67(10), pp. 2409–2417. Available at: https://doi.org/10.1093/jac/dks228.

Beloin, C., Roux, A. and Ghigo, J.-M. (2008) 'Escherichia coli biofilms', *Current Topics in Microbiology and Immunology*, 322, pp. 249–289.

Bhandol, H.J. *et al.* (2020) 'Review: Structure and regulation of the Acr efflux pumps and their role in antibiotic resistance in Escherichia coli', *Undergraduate Journal of Experimental Microbiology and Immunology*, 6, pp. 1–16. Available at: https://doi.org/10.14288/ujemi.v6i.193259.

Bialek, S. *et al.* (2010) 'Membrane Efflux and Influx Modulate both Multidrug Resistance and Virulence of Klebsiella pneumoniae in a Caenorhabditis elegans Model', *Antimicrobial Agents and Chemotherapy*, 54(10), pp. 4373–4378. Available at: https://doi.org/10.1128/aac.01607-09.

BioCyc Pathway/Genome Database Collection (no date). Available at: https://biocyc.org/?sid=biocyc17-3927271793 (Accessed: 13 June 2024).

Blair, J.M.A. and Piddock, L.J.V. (2009) 'Structure, function and inhibition of RND efflux pumps in Gram-negative bacteria: an update', *Current Opinion in Microbiology*, 12(5), pp. 512–519. Available at: https://doi.org/10.1016/j.mib.2009.07.003.

Blattner, F.R. *et al.* (1997) 'The Complete Genome Sequence of Escherichia coli K-12', *Science*, 277(5331), pp. 1453–1462. Available at: https://doi.org/10.1126/science.277.5331.1453.

Browning, D.F., Hobman, J.L. and Busby, S.J.W. (2023) 'Laboratory strains of Escherichia coli K-12: things are seldom what they seem', *Microbial Genomics*, 9(2), p. mgen000922. Available at: https://doi.org/10.1099/mgen.0.000922.

Cauilan, A. *et al.* (2019) 'Global effect of the AcrAB–TolC multidrug efflux pump of Escherichia coli in cell metabolism revealed by untargeted metabolomics', *International Journal of Antimicrobial Agents*, 54(1), pp. 105–107. Available at: https://doi.org/10.1016/j.ijantimicag.2019.05.015.

Chaudhuri, R.R. and Henderson, I.R. (2012) 'The evolution of the Escherichia coli phylogeny', *Infection, Genetics and Evolution: Journal of Molecular Epidemiology and Evolutionary Genetics in Infectious Diseases*, 12(2), pp. 214–226. Available at: https://doi.org/10.1016/j.meegid.2012.01.005.

Chen, J. *et al.* (2003) 'An RND-type multidrug efflux pump SdeXY from Serratia marcescens', *Journal of Antimicrobial Chemotherapy*, 52(2), pp. 176–179. Available at: https://doi.org/10.1093/jac/dkg308.

Chitsaz, M. and Brown, M.H. (2017) 'The role played by drug efflux pumps in bacterial multidrug resistance', *Essays in Biochemistry*, 61(1), pp. 127–139. Available at: https://doi.org/10.1042/EBC20160064.

Colclough, A.L., Scadden, J. and Blair, J.M.A. (2019) 'TetR-family transcription factors in Gram-negative bacteria: conservation, variation and implications for efflux-mediated antimicrobial resistance', *BMC Genomics*, 20, p. 731. Available at: https://doi.org/10.1186/s12864-019-6075-5.

Coudeyras, S. *et al.* (2008) 'A tripartite efflux pump involved in gastrointestinal colonization by Klebsiella pneumoniae confers a tolerance response to inorganic acid', *Infection and Immunity*, 76(10), pp. 4633–4641. Available at: https://doi.org/10.1128/IAI.00356-08.

Dadgostar, P. (2019) 'Antimicrobial Resistance: Implications and Costs', *Infection and Drug Resistance*, 12, pp. 3903–3910. Available at: https://doi.org/10.2147/IDR.S234610.

Darby, E.M. *et al.* (2022) 'Molecular mechanisms of antibiotic resistance revisited', *Nature Reviews Microbiology*, (21), pp. 280–295.

De Pascale, G. and Wright, G.D. (2010) 'Antibiotic Resistance by Enzyme Inactivation: From Mechanisms to Solutions', *ChemBioChem*, 11(10), pp. 1325–1334. Available at: https://doi.org/10.1002/cbic.201000067.

Denamur, E. *et al.* (2021) 'The population genetics of pathogenic Escherichia coli', *Nature Reviews Microbiology*, 19(1), pp. 37–54. Available at: https://doi.org/10.1038/s41579-020-0416-x.

Drew, D. *et al.* (2021) 'Structures and General Transport Mechanisms by the Major Facilitator Superfamily (MFS)', *Chemical Reviews*, 121(9), pp. 5289–5335. Available at: https://doi.org/10.1021/acs.chemrev.0c00983.

'Escherichia coli ATCC 25922, complete genome' (2014). Available at: http://www.ncbi.nlm.nih.gov/nuccore/CP009072.1 (Accessed: 18 April 2024).

Fernández, L. and Hancock, R.E.W. (2012) 'Adaptive and Mutational Resistance: Role of Porins and Efflux Pumps in Drug Resistance', *Clinical Microbiology Reviews*, 25(4), pp. 661–681. Available at: https://doi.org/10.1128/cmr.00043-12.

Fernando, D.M. and Kumar, A. (2013) 'Resistance-Nodulation-Division Multidrug Efflux Pumps in Gram-Negative Bacteria: Role in Virulence', *Antibiotics*, 2(1), pp. 163–181. Available at: https://doi.org/10.3390/antibiotics2010163.

Flemming, H.-C. and Wingender, J. (2010) 'The biofilm matrix', *Nature Reviews Microbiology*, 8(9), pp. 623–633. Available at: https://doi.org/10.1038/nrmicro2415.

Fricke, W.F. *et al.* (2008) 'Insights into the environmental resistance gene pool from the genome sequence of the multidrug-resistant environmental isolate Escherichia coli SMS-3-5', *Journal of Bacteriology*, 190(20), pp. 6779–6794. Available at: https://doi.org/10.1128/JB.00661-08.

Giedraitienė, A. *et al.* (2011) 'Antibiotic Resistance Mechanisms of Clinically Important Bacteria', *Medicina*, 47(3), p. 19. Available at: https://doi.org/10.3390/medicina47030019.

Gillis, R.J. *et al.* (2005) 'Molecular basis of azithromycin-resistant Pseudomonas aeruginosa biofilms', *Antimicrobial Agents and Chemotherapy*, 49(9), pp. 3858–3867. Available at: https://doi.org/10.1128/AAC.49.9.3858-3867.2005.

Guérin, F. *et al.* (2016) 'Landscape of Resistance-Nodulation-Cell Division (RND)-Type Efflux Pumps in Enterobacter cloacae Complex', *Antimicrobial Agents and Chemotherapy*, 60(4), pp. 2373–2382. Available at: https://doi.org/10.1128/AAC.02840-15.

Guérin, F. *et al.* (2020) 'Landscape of in vivo Fitness-Associated Genes of Enterobacter cloacae Complex', *Frontiers in Microbiology*, 11. Available at: https://www.frontiersin.org/articles/10.3389/fmicb.2020.01609 (Accessed: 21 July 2023).

Haque, M. *et al.* (2018) 'Health care-associated infections – an overview', *Infection and Drug Resistance*, 11, pp. 2321–2333. Available at: https://doi.org/10.2147/IDR.S177247.

He, X. *et al.* (2015) 'Biofilm Formation Caused by Clinical Acinetobacter baumannii Isolates Is Associated with Overexpression of the AdeFGH Efflux Pump', *Antimicrobial Agents and Chemotherapy*, 59(8), pp. 4817–4825. Available at: https://doi.org/10.1128/AAC.00877-15.

Henderson, P.J.F. *et al.* (2021) 'Physiological Functions of Bacterial "Multidrug" Efflux Pumps', *Chemical Reviews*, 121(9), pp. 5417–5478. Available at: https://doi.org/10.1021/acs.chemrev.0c01226.

Hernando-Amado, S. *et al.* (2016) 'Multidrug efflux pumps as main players in intrinsic and acquired resistance to antimicrobials', *Drug Resistance Updates: Reviews and Commentaries in Antimicrobial and Anticancer Chemotherapy*, 28, pp. 13–27. Available at: https://doi.org/10.1016/j.drup.2016.06.007.

Høiby, N. (2017) 'A short history of microbial biofilms and biofilm infections', *APMIS*, 125(4), pp. 272–275. Available at: https://doi.org/10.1111/apm.12686.

Ibrahim, M., Bilal, N. and Hamid, M. (2012) 'Increased multi-drug resistant Escherichia coli from hospitals in Khartoum state, Sudan', *African Health Sciences*, 12(3), pp. 368–375.

Jaffe, A., Chabbert, Y.A. and Semonin, O. (1982) 'Role of porin proteins OmpF and OmpC in the permeation of beta-lactams', *Antimicrobial Agents and Chemotherapy*, 22(6), pp. 942–948. Available at: https://doi.org/10.1128/AAC.22.6.942.

Jang, S. (2023) 'AcrAB−TolC, a major efflux pump in Gram negative bacteria: toward understanding its operation mechanism', *BMB Reports*, 56(6), pp. 326–334. Available at: https://doi.org/10.5483/BMBRep.2023-0070.

Jesser, K.J. and Levy, K. (2020) 'Updates on defining and detecting diarrheagenic Escherichia coli pathotypes', *Current opinion in infectious diseases*, 33(5), pp. 372–380. Available at: https://doi.org/10.1097/QCO.0000000000000665.

Join-Lambert, O.F. *et al.* (2001) 'Differential Selection of Multidrug Efflux Mutants by Trovafloxacin and Ciprofloxacin in an Experimental Model ofPseudomonas aeruginosa Acute Pneumonia in Rats', *Antimicrobial Agents and Chemotherapy*, 45(2), pp. 571–576. Available at: https://doi.org/10.1128/aac.45.2.571-576.2001.

Kaper, J.B. (2002) 'Pathogenic Escherichia coli', *Nature Reviews Microbiology*, 2(2), pp. 123–40.

Kowalska-Krochmal, B. and Dudek-Wicher, R. (2021) 'The Minimum Inhibitory Concentration of Antibiotics: Methods, Interpretation, Clinical Relevance', *Pathogens*, 10(2), p. 165. Available at: https://doi.org/10.3390/pathogens10020165.

Krishnamoorthy, S. *et al.* (2015) 'Microbicides Alter the Expression and Function of RND-Type Efflux Pump AdeABC in Biofilm-Associated Cells of Acinetobacter baumannii Clinical Isolates', *Antimicrobial Agents and Chemotherapy*, 60(1), pp. 57–63. Available at: https://doi.org/10.1128/aac.01045-15.

Kvist, M., Hancock, V. and Klemm, P. (2008) 'Inactivation of Efflux Pumps Abolishes Bacterial Biofilm Formation', *Applied and Environmental Microbiology*, 74(23), pp. 7376–7382. Available at: https://doi.org/10.1128/AEM.01310-08.

Liu, X. and Locasale, J.W. (2017) 'Metabolomics: A Primer', *Trends in Biochemical Sciences*, 42(4), pp. 274–284. Available at: https://doi.org/10.1016/j.tibs.2017.01.004.

Mallea, M. *et al.* (1998) 'Porin alteration and active efflux: two in vivo drug resistance strategies used by Enterobacter aerogenes', *Microbiology (Reading, England)*, 144 (Pt 11), pp. 3003–3009. Available at: https://doi.org/10.1099/00221287-144-11-3003.

Mardanova, A.M. *et al.* (2013) 'Efflux systems in Serratia marcescens', *Microbiology*, 82(6), pp. 668–679. Available at: https://doi.org/10.1134/S0026261714010093.

Masi, M. *et al.* (2005) 'The eefABC Multidrug Efflux Pump Operon Is Repressed by H-NS in Enterobacter aerogenes', *Journal of Bacteriology*, 187(11), pp. 3894–3897. Available at: https://doi.org/10.1128/JB.187.11.3894-3897.2005.

Masi, M., Pagès, J.-M. and Pradel, E. (2006) 'Production of the cryptic EefABC efflux pump in Enterobacter aerogenes chloramphenicol-resistant mutants', *The Journal of Antimicrobial Chemotherapy*, 57(6), pp. 1223–1226. Available at: https://doi.org/10.1093/jac/dkl139.

Micenková, L. *et al.* (2016) 'Human extraintestinal pathogenic Escherichia coli strains differ in prevalence of virulence factors, phylogroups, and bacteriocin determinants', *BMC Microbiology*, 16(1), p. 218. Available at: https://doi.org/10.1186/s12866-016-0835-z.

Miki, T. and Hardt, W.-D. (2013) 'Outer Membrane Permeabilization Is an Essential Step in the Killing of Gram-Negative Bacteria by the Lectin RegIIIβ', *PLoS ONE*, 8(7), p. e69901. Available at: https://doi.org/10.1371/journal.pone.0069901.

Minogue, T.D. *et al.* (2014) 'Complete Genome Assembly of Escherichia coli ATCC 25922, a Serotype O6 Reference Strain', *Genome Announcements*, 2(5), pp. e00969-14. Available at: https://doi.org/10.1128/genomeA.00969-14.

Murakami, S. (2008) 'Multidrug efflux transporter, AcrB--the pumping mechanism', *Current Opinion in Structural Biology*, 18(4), pp. 459–465. Available at: https://doi.org/10.1016/j.sbi.2008.06.007.

Murray, C.J.L. *et al.* (2022) 'Global burden of bacterial antimicrobial resistance in 2019: a systematic analysis', *The Lancet*, 399(10325), pp. 629–655. Available at: https://doi.org/10.1016/S0140-6736(21)02724-0.

Naren, N. and Zhang, X.-X. (2020) 'Global Regulatory Roles of the Histidine-Responsive Transcriptional Repressor HutC in Pseudomonas fluorescens SBW25', *Journal of Bacteriology*, 202(13), p. 10.1128/jb.00792-19. Available at: https://doi.org/10.1128/jb.00792-19.

Nataro, J.P. and Kaper, J.B. (1998) 'Diarrheagenic Escherichia coli', *Clinical Microbiology Reviews*, 11(1), pp. 142–201. Available at: https://doi.org/10.1128/CMR.11.1.142.

NEB Tm Calculator (no date). Available at: https://tmcalculator.neb.com/#!/main (Accessed: 21 August 2023).

Nishino, K. and Yamaguchi, A. (2001) 'Analysis of a Complete Library of Putative Drug Transporter Genes in Escherichia coli', *Journal of Bacteriology*, 183(20), pp. 5803–5812. Available at: https://doi.org/10.1128/jb.183.20.5803-5812.2001.

Oliveira, J. and Reygaert, W.C. (2023) 'Gram-Negative Bacteria', in *StatPearls*. Treasure Island (FL): StatPearls Publishing. Available at: http://www.ncbi.nlm.nih.gov/books/NBK538213/ (Accessed: 15 January 2024).

ornaline (CHEBI:133921) (no date). Available at: https://www.ebi.ac.uk/chebi/searchId.do?chebiId=CHEBI:133921 (Accessed: 1 August 2024).

Padilla, E. *et al.* (2010) 'Klebsiella pneumoniae AcrAB Efflux Pump Contributes to Antimicrobial Resistance and Virulence', *Antimicrobial Agents and Chemotherapy*, 54(1), pp. 177–183. Available at: https://doi.org/10.1128/aac.00715-09.

Paixão, L. *et al.* (2009) 'Fluorometric determination of ethidium bromide efflux kinetics in Escherichia coli', *Journal of Biological Engineering*, 3, p. 18. Available at: https://doi.org/10.1186/1754-1611-3-18.

Pasqua, M. *et al.* (2019) 'The Varied Role of Efflux Pumps of the MFS Family in the Interplay of Bacteria with Animal and Plant Cells', *Microorganisms*, 7(9), p. 285. Available at: https://doi.org/10.3390/microorganisms7090285.

Perestrelo, S. *et al.* (2023) 'Building an International One Health Strain Level Database to Characterise the Epidemiology of AMR Threats: ESBL—AmpC Producing E. coli as An Example—Challenges and Perspectives', *Antibiotics*, 12(3), p. 552. Available at: https://doi.org/10.3390/antibiotics12030552.

Piddock, L.J.V. (2006) 'Multidrug-resistance efflux pumps ? not just for resistance', *Nature Reviews Microbiology*, 4(8), pp. 629–636. Available at: https://doi.org/10.1038/nrmicro1464.

Prosser, G.A., Larrouy-Maumus, G. and Carvalho, L.P.S. de (2014) 'Metabolomic strategies for the identification of new enzyme functions and metabolic pathways', *EMBO reports*, 15(6), pp. 657–669. Available at: https://doi.org/10.15252/embr.201338283.

PubChem (no date) *Camoensine*. Available at: https://pubchem.ncbi.nlm.nih.gov/compound/442946 (Accessed: 1 August 2024).

Pugh, H. (2022) *Diversity and conservation of RND efflux pumps across Escherichia coli*. d_ph. University of Birmingham. Available at: https://etheses.bham.ac.uk/id/eprint/12366/ (Accessed: 18 April 2024).

Quistgaard, E.M. *et al.* (2016) 'Understanding transport by the major facilitator superfamily (MFS): structures pave the way', *Nature Reviews Molecular Cell Biology*, 17(2), pp. 123–132. Available at: https://doi.org/10.1038/nrm.2015.25.

Raj, D.S. *et al.* (2021) 'Efflux pumps potential drug targets to circumvent drug Resistance – Multi drug efflux pumps of *Helicobacter pylori*', *Materials Today: Proceedings*, 45, pp. 2976–2981. Available at: https://doi.org/10.1016/j.matpr.2020.11.955.

Salipante, S.J. *et al.* (2015) 'Large-scale genomic sequencing of extraintestinal pathogenic Escherichia coli strains', *Genome Research*, 25(1), pp. 119–128. Available at: https://doi.org/10.1101/gr.180190.114.

Schaenzer, A.J. and Wright, G.D. (2020) 'Antibiotic Resistance by Enzymatic Modification of Antibiotic Targets', *Trends in Molecular Medicine*, 26(8), pp. 768–782. Available at: https://doi.org/10.1016/j.molmed.2020.05.001.

Schottel, J.L., Bibb, M.J. and Cohen, S.N. (1981) 'Cloning and expression in streptomyces lividans of antibiotic resistance genes derived from Escherichia coli.', *Journal of Bacteriology*, 146(1), pp. 360–368.

Shi, X. *et al.* (2019) 'In situ structure and assembly of the multidrug efflux pump AcrAB-TolC', *Nature Communications*, 10(1), p. 2635. Available at: https://doi.org/10.1038/s41467-019-10512-6.

Spellberg, B., B., M. (2011) 'Combating antimicrobial resistance: policy recommendations to save lives', *PubMed* [Preprint], (52). Available at: https://pubmed.ncbi.nlm.nih.gov/21474585/ (Accessed: 21 July 2023).

Sprouffske, K. and Wagner, A. (2016) 'Growthcurver: an R package for obtaining interpretable metrics from microbial growth curves', *BMC Bioinformatics*, 17(1), p. 172. Available at: https://doi.org/10.1186/s12859-016-1016-7.

Symmons, M.F. *et al.* (2009) 'The assembled structure of a complete tripartite bacterial multidrug efflux pump', *Proceedings of the National Academy of Sciences of the United States of America*, 106(17), pp. 7173–7178. Available at: https://doi.org/10.1073/pnas.0900693106.

Tacconelli, E. *et al.* (2018) 'Discovery, research, and development of new antibiotics: the WHO priority list of antibiotic-resistant bacteria and tuberculosis', *The Lancet. Infectious Diseases*, 18(3), pp. 318–327. Available at: https://doi.org/10.1016/S1473-3099(17)30753-3.

Tapiainen, T. *et al.* (2014) 'Escherichia coli biofilm formation and recurrences of urinary tract infections in children', *European Journal of Clinical Microbiology & Infectious Diseases*, 33(1), pp. 111–115. Available at: https://doi.org/10.1007/s10096-013-1935-4.

Viveiros, M. *et al.* (2008) 'Demonstration of intrinsic efflux activity of Escherichia coli K-12 AG100 by an automated ethidium bromide method', *International Journal of Antimicrobial Agents*, 31(5), pp. 458–462. Available at: https://doi.org/10.1016/j.ijantimicag.2007.12.015.

Wan, X. *et al.* (2022) 'Engineering a CRISPR interference system targeting AcrAB-TolC efflux pump to prevent multidrug resistance development in Escherichia coli', *Journal of Antimicrobial Chemotherapy*, 77(8), pp. 2158–2166. Available at: https://doi.org/10.1093/jac/dkac166.

Wang-Kan, X. *et al.* (2021) 'Metabolomics Reveal Potential Natural Substrates of AcrB in Escherichia coli and Salmonella enterica Serovar Typhimurium', *mBio*, 12(2), p. 10.1128/mbio.00109-21. Available at: https://doi.org/10.1128/mbio.00109-21.

Wiegand, I., Hilpert, K. and Hancock, R.E.W. (2008) 'Agar and broth dilution methods to determine the minimal inhibitory concentration (MIC) of antimicrobial substances', *Nature Protocols*, 3(2), pp. 163–175. Available at: https://doi.org/10.1038/nprot.2007.521.

Wilson, D.N. *et al.* (2020) 'Target protection as a key antibiotic resistance mechanism', *Nature Reviews Microbiology*, 18(11), pp. 637–648. Available at: https://doi.org/10.1038/s41579-020-0386-z.

Yan, N. (2013) 'Structural advances for the major facilitator superfamily (MFS) transporters', *Trends in Biochemical Sciences*, 38(3), pp. 151–159. Available at: https://doi.org/10.1016/j.tibs.2013.01.003.

Zavascki, A.P. *et al.* (2007) 'Polymyxin B for the treatment of multidrug-resistant pathogens: a critical review', *Journal of Antimicrobial Chemotherapy*, 60(6), pp. 1206–1215. Available at: https://doi.org/10.1093/jac/dkm357.

Zgurskaya, H.I. *et al.* (2018) 'Trans-envelope multidrug efflux pumps of Gram-negative bacteria and their synergism with the outer membrane barrier', *Research in microbiology*, 169(7–8), pp. 351–356. Available at: https://doi.org/10.1016/j.resmic.2018.02.002.

Zhang, gMin and Hao, Q. (2011) 'Crystal structure of NDM-1 reveals a common β-lactam hydrolysis mechanism', *The FASEB Journal*, 25(8), pp. 2574–2582. Available at: https://doi.org/10.1096/fj.11-184036.

Zwama, M. and Nishino, K. (2021) 'Ever-Adapting RND Efflux Pumps in Gram-Negative Multidrug-Resistant Pathogens: A Race against Time', *Antibiotics*, 10(7), p. 774. Available at: https://doi.org/10.3390/antibiotics10070774.